Selection of Modelling Level of Detail for Incorporating Stress Analysis into Evolutionary Robotics Simulations of Extinct and Extant Vertebrates

A thesis submitted to The University of Manchester for the degree of Ph.D in the Faculty of Engineering and Physical Sciences.

2015

Zartasha Mustansar

Interdisciplinary School for Ancient Life

School of Earth, Atmospheric and Environmental Sciences

Contents

LIST OF FIGURES

LIST OF TABLES

ABSTRACT

ABSTRACT OF THESIS submitted by **Zartasha Mustansar** for the degree of **Doctor of Philosophy** and entitled: *Selection of modelling level of detail for incorporating stress analysis into evolutionary robotics simulations of extinct and extant vertebrates.* Date of Submission: **10th April 2015**

This thesis concerns the simulation of locomotion in vertebrates. The state-of-the-art uses genetic algorithms together with solid body kinematics to generate possible solutions for stable gaits. In recent work, this methodology led to a hopping gait in a dinosaur and the researchers wondered if this was realistic. The purpose of the research carried out in this thesis was to examine whether quick and simple finite element analyses could be added to the simulator, to evaluate a simple "break" or "not break" failure criterion. A "break" would rule out gaits that might damage the owner's skeleton. Linear elastic analysis was considered as a possible approach as it would add little overhead to the simulations.

The author used X-ray computed tomography and the finite element method to examine the axial loading of a barnacle goose femur. The study considered four levels of detail for a linear elastic simulation, finding that all the analyses carried out overestimated the strength of the bone, when considering safety factors. The conclusion is that to incorporate stress-strain analysis into the gait simulation requires more realistic models of bone behaviour that incorporate the nonlinear response of bone to applied loading. A new study focusing on the use of novel techniques such as model order reduction is recommended for future work.

The outputs of this research include chapters written up as journal papers covering a 4D tomography experiment; a level of detail study; an analysis of a purported tendon avulsion injury in *Tyrannosaurus rex* and a review of the elastic properties of bone.

DECLARATION

No portion of the work referred to in this thesis has been submitted in support of an application for another degree or qualification of this or any other university or other institution of learning.

Zartasha Mustansar

COPYRIGHT STATEMENT

ABBREVIATIONS & ACRONYMS

FEM	Finite Element Modelling/Method
FEA	Finite Element Analysis
STL	Stereo lithography (file format)
DICOM	Digital Imaging and Communications in Medicine
IP	Image Processing
DVC/DIC	Digital Volume Correlation/Digital Image Correlation
FE	Finite Element
CAD	Computer Aided Design
CAE	Computer Aided Engineering
ParaFEM	Parallel Finite Element Modelling
INP	Input file for Abaqus
CPU	Central Processing Unit
T. Rex	*Tyrannosaurus rex*
CT	Computed Tomography
XCT	X-Ray Computed Tomography
MRI	Magnetic Resonance Imaging
MCD	Mechanical compression device
RAM	Random Access Memory
EPB	Extant Phylogenetic Bracketing
HA	Hydroxyapatite

3D	Three-Dimensional
2D	Two-Dimensional
MM	Mathematical Modelling
DEISA	Distributed European Infrastructure for Supercomputing applications
C3D4	A tetrahedron with four nodes
C3D10	A tetrahedron with ten nodes
C3D8	A hexahedral with eight nodes
C3D20	A hexahedral with twenty nodes
SRC	Student Research Competition

To my beloved parents and brother

Acknowledgements

"Making a big life change is scary. But you know, what's more scarier... 'Regret'. Remember that your thoughts are the primary cause of everything." ~ Byrne

Being a very big fan of "Law of attraction" by Byrne, I choose research and science, my career. As a woman from Pakistan where higher education is a suppressed department, undertook a PhD at my own effort and risk. I am extremely grateful to Allah Almighty for His blessings to provide me an opportunity to pursue quality education at the University of Manchester, UK. I would like to thank my highly trusted sponsors, Microsoft-Dorothy Hodgkin postgraduate award unlike the local higher education scholarship scheme in Pakistan, where merit is not a standard practise. I feel myself very lucky and fortunate to be among those who stand among the prestigious award schemes such as Microsoft-DHPA.

I would also like to pay immense thanks to my supervisor, Dr. Lee Margetts who has always shown me the right path in the time of need. His struggle to transform me into an independent research professional is remarkable. He is an immense source of scientific inspiration for me.I can never forget his efforts invested in me.

My Dad and my Mom for being an irreplaceable part of my life, without whom I would never be where I am. Their constant concerns, kind hearted words and special prayers have always healed me and never left me alone in any respect.

My 1year old boy, Mohammad Rayyan for magic hugs. My brother, Kashan Mustansar, who always lifted my morales in the low times, my younger sisters, Dr. Nayab Mustansar and Mahrukh Mustansar are the names I will never forget to mention.They were always the ones with me through thick and thin.

My co supervisors, Dr. Phil Manning (School of Earth, Atmospheric & Environmental Sciences), Dr. Bill Sellers (Faculty of life sciences) and Dr. Hillel Kugler (Microsoft research Cambridge, UK). Special thanks to Samuel McDonald for assisting me in digital image correlation, Tristan Lowe in computed tomography, Louise Leaver in visualization support, George Leaver and Michael Bane in technical problems with visualization and simulation software’s support. My uncle, Waseem Saeed for giving me quality time during my lows, aunt Saleha for cooking delicious meals. My colleagues, Ayesha Al Hijri, Nedolsa, Fabien Leonard, Zareen Syed, Mark Johnson, Peter Falkingham and Karl Bates are very important names as well.

LIST OF PUBLICATIONS RELATED TO THE THESIS

- **Mustansar Z**, McDonald S A, Sellers W.I, Mummery P, Kugler H, Manning P. L, Withers P J and Margetts L, *A study of the progression of damage in an axially loaded Branta leucopsis femur using X-ray computed tomography and digital image correlation* (submitted in the **Journal of Plos one**)

- **Mustansar Z.**, Sellers W.I, Shaukat. A., Manning P.L., Lever, M Louise and Margetts L, *A study of the effect of model resolution on elastic finite element analyses of an axially loaded Branta leucopsis femur* (submitted in the **Journal of Royal Society interface**)

- **Mustansar Z.**, Margetts L., Manning P.L and Kuglar. H, *A study of bone remodeling after injury in Tyrannosaurus rex*, (submitted in **Journal of Royal Society interface**).

- **Mustansar Z.**, and Margetts L., *The stiffness of bone*. (submitted in the **Journal of PLoS-One**)

- Manning, P., Margetts, L., Johnson, M., **Mustansar, Z**. & Mummery, P. 2009 *A finite element approach to the biomechanics of dromaeosaurid dinosaur claws.* In ***Journal of vertebrate paleontology*** (pp. 141a-141a), soc vertebrate paleontology 60 revere dr, ste 500,Northbrook, IL 60062 USA.

- Johnson, M., **Mustansar, Z.**, Manning, P., Margetts, L., Mummery, P., *Virtual repair of fossil CT Scan Data, Oral Talk:* ***Journal of vertebrate Palaeontology;*** *Society of Vertebrate* Palaeontology and the 57th Symposium of Vertebrate Palaeontology and Comparative Anatomy (SVPCA) - University of Bristol (UK), 22nd -26th September, 2009.

- Margetts, L., Manning, P. L., **Mustansar, Z**. and Johnson, M. "*Reliability of image-based finite element modeling in vertebrate palaeontology*", Symposium of Vertebrate Palaeontology, Pittsburgh (USA), October 2010.

- **Mustansar Z.**, Johnson, M., Manning P.L., *Design and evaluation of a virtual rig for mechanical testing of fossil bones*, Oral Talk: Simpleware Users Meeting-ARUP, Solihull (UK), June 2010.

- Johnson, M. R., **Mustansar, Z.**, Margetts, L., Mummery, P. M., Manning, P. L. *Image Based modeling of dinosaurs, Poster presentation: Biomedical Imaging Institute Showcase-University of Manchester (UK),* November 2009.

- **Mustansar Z.**, Margetts L., Manning P.L. and Kugler H., *Reverse engineering dinosaurs, poster presentation:* Microsoft Research Cambridge (UK), 29 June-4 July 2009.

- **Mustansar Z.**, Margetts L., Manning P.L., Kuglar. H, and Sellers W.I, *Computer aided insights into biomechanics of dinosaurs,* Poster presentation and Oral Talk: University of Arizona- Tucson (USA), 29th September-3rd October 2009.

- **Mustansar Z.**, Johnson M., Margetts L., Mummery P.M. and Manning P.L., Reverse engineering dinosaurs, poster presentation, Henry Moseley X-ray Imaging facility opening, 8 June 2009.

- Manning, P., Margetts, L., Johnson, M., **Mustansar, Z.**, Mummery, P., Finite element approach to the biomechanics of dromaeosaurid dinosaur claws, Technical session oral talk: Society of Vertebrate Palaeontology-University of Bristol (UK), 22nd-26th September, 2009.

- **Mustansar Z.**, Johnson M., Margetts L., Manning P.L. and Sellers W.I , Reverse engineering dinosaurs, Oral talk: Progressive Palaeontology Association- University of Birmingham (UK), 27-29 May 2009.

- Johnson, M. R., **Mustansar, Z**., Manning, P. L., Margetts, L., and Mummery, P. M. Breathing new life into old fossils, Progressive Palaeontology Association-University of Birmingham, (UK), May, 2009.

- Johnson M and **Mustansar Z.**, A study of the biomechanics of the terminal ungual phalanx from *Velociraptor* using computer aided engineering, 4th North West Biomechanics Research Day, Institute for Health and Social Care Research-University of Salford (UK), 15 May 2009.

LIST OF DATA SETS ON PUBLIC DOMAIN: Accession numbers of six vertebrates and scanning details available publicly on Henry Moseley X-Ray Imaging (MXIF) website.

1 INTRODUCTION

1.1 Overview

This chapter explains the motivation (section1.2) for this work and states research question (section 1.3). It then discusses the aims of this research (section 1.4). This thesis comprises of four journal papers that are outlined in section 1.5.

1.2 Motivation

The motivation of this research came from the study of locomotion in dinosaurs (locomotion is the pattern of walking in animals using limbs/legs and other locomotory organs – for details, chapter 2). Scientists have been studying dinosaurs using mathematical modelling. Mathematical modelling provides an independent means to quantitatively test specific hypotheses about the biomechanics of fossil organisms. These models are useful because they differ from conceptual models where formulation and description of natural processes are guided by observations rather than quantitative procedures.

In this technique two of the main categories that have been used by the team at the University of Manchester include, forward dynamics and inverse dynamics. Forward models make predictions based on a set of numerical inputs and boundary conditions, while inverse models attempt to solve input parameters by matching the model solution with experimental observations. In reality, there are many forces involved in locomotion. Some exerted on the ground, some exerted by the ground, others exerted from muscles, joints and tissues as well. These methods (forward and inverse dynamics) can be used to investigate these forces related to locomotor movements. The magnitude of these forces helps to understand the type of locomotion e.g. running, walking, hopping etc. While the magnitude of these forces is significant, it is not clear how large or small should the forces be, and whether the simulations result in forces that could not be supported by the owner's skeleton.

One of the recent simulations carried out by Sellers and Manning (2007) on a duck-billed dinosaur, *Hadrosaur* produced three distinct types of gaits galloping, skipping and hopping. It was inferred that it might have hopped like a kangaroo with a speed

of 61 km/h, followed by quadrupedal galloping (58 km/h), and bipedal running (50 km/h) (Sellers et al., 2009). Putting aside debates between palaeontologists as to whether hadrosaurs were bipedal or quadrupedal, it is important to know how realistic the skipping and hopping gaits might be. Was there something fundamental in the evolutionary robotics simulation (Chapter 2) that could permit unrealistic gaits to emerge as possible solutions to the analyses? Perhaps skeletal loading is an important, but overlooked, factor. If the genetic algorithm (GA) could reject gaits that damaged the owner's skeleton, would these skipping and hopping gaits still emerge? Answering this question requires modifying the genetic algorithm so that it can detect whether the skeletal loading is too high. The simplest approach is to implement a binary "yes" or "no" decision as to whether a bone would break. If the bone breaks, that particular gait could be rejected as a possible solution.

The genetic algorithm has been used by the team to produce locomotion patterns. It operates on populations of individuals which evolve as the simulation progresses forwards in time. The program, however, does not consider how high the forces are for a given organism. The reason is that the genetic algorithm used in this program does not take into account whether the forces generated might break the owner's skeleton.

The motivation for this work is to carry out a study that would serve as a benchmark for the inclusion of bone mechanics as a factor evaluated by the genetic algorithm. This will help the simulation program to make wise decisions on whether skeletal loading is reasonable (lies within the safety factors of bones) when generating locomotion/gait patterns. Therefore, the research question is addressed next.

1.3 Research question

The issue as to whether forces generated in the simulation program might be too high leads to the following research question:

"Current genetic algorithm methods used to study vertebrate locomotion do not consider whether the forces generated would damage the owner's skeleton. The purpose of this research is to explore that question using the finite element method.

Bones have a complex internal microstructure. It is not clear to what level of fidelity stress analysis is required".

Considering this, the aim of this project is to investigate the *level of detail required to reasonably predict stress-strain response in bones loaded during locomotion".*

1.4 Research Aims - The bigger picture

The ultimate aim of this research leads to the incorporation of stress as a selection criterion into GaitSym, a gait simulator developed by Dr Bill Sellers at the University of Manchester (http://www.animalsimulation.org/) However this can only be pursued by knowing what magnitude of forces are required to maintain the skeleton's integrity within the functional bone behaviour during locomotion. The research therefore undertakes this significant question of how much force can affect a bone through computer models with various levels of detail. In order to understand the connection between the skeleton and the forces during locomotion, a legitimate explanation is followed next.

It is known that pattern of locomotion is based on many factors, including the anatomy of the organism, the size of it's body and it's mass. In theory, the skeleton (which is made up of several bones) of specific weight along with muscles and joints are given to the genetic algorithm (GA) as an input. The GA interprets the input and outputs two things: a pattern of locomotion and the magnitude of force experienced by the skeleton which in turn is calculated from the weight of the animal (using F = mg). The primary question here is how the skeleton moves in this process.

Within the skeleton inputs, are given muscle and joint parameters. These muscles and joints apply some forces to the skeleton in various directions which make the skeleton move. The GA then generates a number of possible computed gaits. The resulting gaits comes out with various number of forces. However, during this process of accepting some gaits and rejecting others, the GA still might allow some forces which could damage the owner's skeleton. Therefore some of the accepted gaits might not be good solutions.

The purpose of this research is to improve this modelling. If the resulting forces are too high for the skeleton, the solution should be rejected by the GA. Conversely, if the forces are acceptable for the skeleton, it should be accepted as a solution.

To pursue this, the major aims of this research are to investigate following specific questions:

1. How can we improve the reliability of choosing material property data set for bones for accurate analysis in modelling techniques? (Chapter 6)

2. What levels of details are needed for a mechanically elastic finite element analysis in order to evaluate the constitutive response of bones to loads generated by genetic algorithm (Chapter 4) and if the mechano-elatic assumption is enough for this particular analysis? (chapter 7)

3. Is it going to be a complicated analysis if incremental loads were used such as a dynamic loading scenario? (Chapter 3)

4. Can FEM be used as a good choice for real dinosaur bones? (Chapter 5)

1.5 Thesis Layout

The thesis consists of eight chapters in total. Following this introductory chapter, the next chapter presents a logical story of how the research was undertaken. Chapter 3, 4, 5 and 6 are presented as original papers submitted for peer review in academic journals. At the end, chapter 7 discusses the overall results of the research and chapter 8 describes the future work.

As a preliminary part to conducting this research, first year of the PhD was devoted to understanding scientific articles and reading most of the relevant journal papers. This allowed the author to develop an understanding of long bone anatomy, mechanical properties and mechanical behaviour. Some of this effort, focused on the stiffness of bone, has now been written up as a discussion paper, submitted to PLoS-ONE (chapter 6).

In the second year, much of the attention was paid to the methodology and techniques to generate computer models of the bone using the finite element method.

Several computer models of vertebrates were developed by the author including a *Velociraptor Manus* (claw) and an emu, *Dromaius novaehollandiae* (femur).

In the 3rd year, the author scanned long bones from 6 vertebrates in order to select the best one to develop good quality finite element models. The predictions of simple elastic finite element modelling for four different levels of detail were investigated for the selected bone, a *Branta leucopsis* femur. This paper was submitted to the journal of Royal Society Interface (Chapter 4).

The same bone was tested under incremental axial loading to study detailed deformation mechanisms that occur beyond the elastic regime. This work was also prepared as a manuscript and submitted to the journal PLoS-ONE (Chapter 3).

A *Tyrannosaurus rex* (humerus) was also studied using imaging and finite element analysis, to investigate bone remodelling after injury. The *Tyrannosaurus rex* paper was submitted to the journal of Royal Society Interface (Chapter 5).

1.6 Authors and co-author's contribution to the paper

In accordance with the University's regulations, the author has detailed in Table 1.1 the contributions of the various authors to journal papers submitted for publication.

Chapter No.	**Conception of idea**	**Experimental design**	**Carried out experiment**	**Analysis and results**	**Structure of the paper**	**Contributed to editorial changes and provided resources**
Chap 3	ZM+LM+PLM	ZM+SM+TL	ZM+SM	ZM+LM	ZM+LM+PLM	ZM + LM + PLM+TL+ WIS+PJW
Chap 4	ZM + LM	ZM	ZM+LL	ZM+LM+AS + LL	ZM+LM	ZM + LM + WIS+ AS+PJW
Chap 5	ZM + LM	ZM+PLM	ZM+PLM	ZM+LM	ZM +LM	ZM + LM + PLM+PJW
Chap 6	ZM+LM	ZM	ZM	ZM+LM	ZM+LM	ZM+LM

Table 1-1: Contributions of various authors to the journal papers.

Abbreviations of authors, co-authors and reviewers

ZM: Zartasha Mustansar

LM: Dr. Lee Margetts

PLM: Dr Phillips Lars Manning

WIS: Dr. William Irvin Sellers

SM: Dr. Samuel McDonald

AS: Arslan Shaukat

PJW: Dr Phillip J Withers

TL: Dr Tristan Lowe

LL: Louise Lever

2 LITERATURE REVIEW

2.1 Overview

This chapter provides the necessary background and essential information related to locomotion, bones, their material properties and mechanical behavior, as well as computer modelling techniques and methods used to study them.

2.2 Vertebrate Locomotion

Locomotion is the ability of an organism to move, propel, walk, trot or jump using flagella, wings or limbs. In vertebrate locomotion, the major organs which generate forces in response to the environment are limbs.

Locomotion has always been a pivotal subject of study in the past for animal scientists (especially). There were several techniques used in the past to study locomotion. History of locomotion can be mapped down from 1878. Muyerbridge (1878) was the first to use photographic techniques. Jules (1888) found a way to record several phases of movement in one photo for flying pelicans. Similar locomotion study was observed using cinematography by Ragnard (1893) who made some experimental measurements on the fish and thrust produced by them in water. After that locomotion of paired-fin fishes was studied by Breder (1926). Being inspired from Muybridge's work, later on Magnon (1930) also started to investigate more on fish locomotion.

In 1942, a very first high speed motion picture of seahorse locomotion was produced by Breder and Edgerton (1942) to demonstrate movement of seahorse in water. Following this, Long and Siegel (1975) reports a remarkable advancement in locomotion study by using a configuration of three cameras altogether. Using this configuration, it was possible to capture more events of movements in response to the thrust force. He made his own negatives by cutting 8" x 10" plates into smaller pieces. After Muyerbridge, Gauthier (1986) used the knowledge of body morphology and function of body parts to study locomotion behaviour in *Dromaesaurids.*

In 1987, 'Grouchu running' (a form of locomotion) was given much importance where animals tend to run on bent knees more than usual was studied by (McMahon et al., 1987). Logically, a bent knee in locomotion reduces the effective vertical stiffness and diminishes the transmission of mechanical shock straight from the foot to the skull. On the contrary it is important to note that it also increases the rate of oxygen consumption as much as 50% (McMahon et al., 1987). Examples of locomotion in vertebrates also comes from the work of (Ostrum, 1969; Padian and Oslen, 1989a; Padian and Oslen, 1989b; Ostrom, 1990) and Osborn (1905) which are worth mentioning here. Now, it is understood that there are several parameters that govern locomotion patterns. These parameters sometimes depend on the size of the animal which changes with the growth process to accommodate functional integrity. However, if we compare the same parameters while using finite element analysis (FEA) it should be noted that it is the size of the animal as well that directly influences the load applied (Biewener, 1991). Likewise, the inclusion of several parameters in any locomotion study collectively forms a ‘gait guide’.

One of the evidences for gait guide came from the work of Hutchinson and Gatesy (2006) about the uncertainties in different locomotion patterns. They concluded that different orientation of animal body in different animals and a specific framework of legs may be a cause of uncertainty in locomotion. For example a short limb skeleton will move in a different way (perhaps faster) than a long limb skeleton. In biology, joints are meant to be flexible to allow movement in the bones. For example, the organs of animals like dinosaur’s hip, knee, ankle and main toe joints which can flex and extend through an arc of 90 degrees. Similarly the variation of each flexion by 1 degree increments could yield more than 67 million possible poses.

Locomotion is important to study both from extinct to extant species in order to see how the course of evolution has changed the gait style in vertebrates. However it is easier to investigate locomotion in birds compared to the extinct species like dinosaurs. One of the reasons is that the anatomy, posture and gait of most of the dinosaurs (fossil) cannot be directly observed. In living species, it is possible to observe and record motion directly and derive material properties. The soft tissues of living species can be dissected easily for finer anatomical details. Therefore, there is hardly an accurate analogue available for dinosaurs except by validating it with the

nearest relative. Further to this discussion it is important to remember, that in extinct animals, like dinosaurs the performance of locomotion seems difficult to estimate. This comes down to assumptions made through comparative anatomy and limb bone scaling about safety factors (Alexander, 2003).

Now, it is revealed that in extinct vertebrates, the bone tissue found particularly in dinosaur bones has an absolute biological significance and that, the fossil bone remains after being buried for millions years can still reveal hidden mechanical functions (Chinsamy-Turan, 2005).

In dinosaurs, the distal ends of tails of dinosaurs were transformed into dynamic stabilizers to help turning the whole body (Ostrum, 1969). It was also seen that such type of locomotion shows how animals counter balance the body weight. Certain track-ways of dinosaurs were also used to study patterns of locomotion of extinct animals during the course of evolution (Thulborn, 1990). It was also investigated by Farlow et al., (2000) that walking is a preferred means of locomotion in theropods compared to running based on the oxygen consumption and metabolic energy cost.

An important question of interest in locomotion research asks what aspects of an animal's performance in locomotion are most likely to affect fitness. The term fitness in vertebrates includes parameters like maximum achievable speed and factors like energy cost during locomotion. In all the cases the answer lies in selecting the best fitness criteria among all locomotion experiments.

Today, due to advances in science and technology, it is now possible to use engineering methods and computer techniques to study dinosaur locomotion. This is discussed in next section.

2.3 Computer modelling of vertebrate locomotion

Computer simulation is a method used to reproduce the behaviour of a system. This system can be of any type i.e. a biological, evolutionary, computer based, or natural system.

It all started with the Turing machine. In 1936, Turing developed his theoretical computational model. He based his model on how he perceived mathematicians

think. As digital computers were developed in the 1940's and 1950's, the Turing machine proved itself a very good theoretical model for computation. The first notion of efficient computation was introduced by using time polynomial in the input size. This led to complexity's most important concept, NP-completeness, and its most fundamental question, whether P = NP (Lance, July 7-10, 2003).

Later in the 1970's, more complex problems came onto the scene, as researchers started to use different models for computation. It was also discovered that the randomness from computations can be removed as well (Adleman and Huang., 1987). The 1980's saw a growth in finite element modelling. The first finite element model was the circuit that capture computation in an inherently different way (Fagin, 1973). Today, much of modern computer science deals with problems like how efficiently two or more computers communicate with each other to solve a computation. Specifically, the basic question of communication complexity is, how much information do the two parties need to exchange in order to carry out a computation? This led the researchers to adapt new ideas and new technologies to idealize the power of running a computation and/or simulation.

In this research, we use similar computer simulation for vertebrate locomotion which is a biological as well as physical phenomenon. There are several methods which can be used in computer modelling to-date. However, this research uses a method called evolutionary robotics (ER) which is discussed next.

Evolutionary robotics is a method generally used in genetic algorithms for various objectives. A genetic algorithm is a search method used in computer science to solve optimization problems. Algorithms used in ER frequently operate on a population of candidates. These candidates are used to find a solution to a given problem. The population is then repeatedly modified according to a fitness function (Nolfi and Floreano, 2000; Ofer, 2005). Therefore, in ER two things are most important while using GA:

(i). Feature selection.

(ii). Fitness function.

A feature is a binary string or an individual. Each individual has a gene ‘g’. This gene represents the value of a feature specific to the problem. The fitness function represents the most likely species to survive. If the value of a gene is (say) ‘1’ the feature is selected to be evaluated by the fitness function and if it is ‘0’ then the feature is discarded. The value of the gene is stored in a variable called an ‘allele’. An allele is the form of an individual. The combination of these values leads to a process called evolution (Ofer, 2005).

As an example to demonstrate the concept, the genetic algorithms used in this study takes ‘force’ as a feature and ‘maximum speed’ as a fitness function. At first, a random population of species with a fixed population size is generated for ‘nearly accurate’ musculoskeletal models. Each individual in the population is then evaluated by the ‘fitness function’ to determine which individual is likely to survive and progress to the next generation. The theory of evolution suggests that only those structures and patterns of movement experienced during locomotion that increase ones fitness over another individual are selected (Ijspeert and Kodjabachian, 1991). For example, in locomotion, the specie that runs the fastest is preferably the fittest individual (for running) among the whole data set. This is because the fastest running animal can easily hunt for prey and run away from possible combats. This whole process is called selection where highly fit individuals are more likely to be selected than the lower fitness ones (Kim and Uther, 2003). Since the population size is fixed, only a limited number of the best individuals are selected for reproduction. A process called ‘crossover’, where parents give rise to new individuals or offspring, generates each new individual. New individuals are also created by another mechanism called mutation where the ‘alleles’ of parent individuals are randomly changed in each evolution step (Ijspeert and Kodjabachian, 1991; Kim and Uther, 2003). This results in a near copy of the parent individual with some changes in the individual components. The same procedure is repeated in cycles many times for a fixed number of generations (Cooper, 2006). For each generation, new offspring are created by the selection, crossover and mutation processes. At last, the output is a set of the best individuals with the desired features, identified by a criterion function.

The factors that determine the efficiency of GA depend on different parameters like population size, number of generations, crossover rate and mutation rate. Crossover rate is the probability of accepting the parent individuals for crossover and the mutation rate is the probability of inverting alleles in the individuals (Siedlecki and Sklansky, 1989). Particularly in ER, the performance of GA is related to the size of the population. Initially, the population size is kept as small as possible like the ones used in (Yamazaki et al. 1996; Ogihara & Yamazaki 2001; Sellers et al. 2003, 2004, 2005). Simple models are less demanding in computational terms and the smaller the population, the easier it is to solve. Parameters for the probability of mutation and crossover are based on a careful survey of the literature. It should also be noted that altering the population size and the generation number could also affect the overall results.

A benefit of using ER in locomotion is that it can be used for both extinct and extant species. For example, if a group of vertebrates shares a number of common locomotor attributes like bipedalism, they can be placed under one phylogeny using ER.

A practical example of evolutionary robotics system is explained here using GaitSym, an ER simulation program developed by the team led by Dr Sellers in the Manchester University, UK. Designed for the study of animal locomotion, this program looks at (for e.g.) how joints exert forces in a skeletal system in vertebrates and check how the bones are articulated in an order such that locomotion is possible.

GaitSym is a forward dynamic modelling program. It generates different patterns of locomotion based on simple principles of movements in response to the input given. The inputs are usually in the form of spatial and physical properties of body segments and muscle-tendon units. It also uses the Open Dynamics Engine (ODE) physics library (www.opende.sourceforge.net). The software is open source and can be downloaded from the Animal Simulation Laboratory (ASL) website (www.animalsimulation.org).

In GaitSym, GA is the preferred optimization method. Traditional search methods rely on the particular minima or maxima to get the best values for any problem, whereas in GA we can extract any random information regardless of any specific

local function. Furthermore GA can be easily parallelized on thousands of processors to run bigger jobs compared to the traditional search methods.

Currently the locomotion of extinct vertebrates is a challenging topic because it requires a lot of work and effort to produce and construct ‘near to real’ geometrical models. However, once the models are constructed; predicted results could be used for approximately accurate analysis. Confidence in locomotion biology can be gained by using a correct method of investigation and this method involves reconstructing a logical and approximately exact biological geometry. The main problem with the state of the art methods for simulating the movement of the skeletons of dinosaurs is that the studies do not check whether the bones in the skeleton could support the applied loads. Certain patterns of locomotion or more correctly, the forces resulting from the locomotion, may result in the failure of the bones.

2.4 Bone

Bone is a heterogeneous material that has a complex structure arranged according to several levels of hierarchy (Rho et al., 1998; Weiner and Wagner, 1998). This section provides a detailed account of the structure of bone. It starts with the general structure of whole bones and zooms into the nanostructure, describing how the organization of structures at the macro, micro and nano-scale leads to different types of bone.

2.4.1 Hierarchal structure of bone

A schematic diagram of the hierarchical structure of bone is shown in figure 2.1. Each level, from the macro to nanoscale is described in detail in the following subsections.

1. Macrostructure

Two main types of bone are found at the macro-scale:

- Cortical bone – compact or cortical bone is essentially fully dense and is found in the shafts of long bones that surround marrow/medullar cavities.

The only spaces in compact bone are for osteocytes, canaliculi, blood vessels and erosion cavities (these structures are described later).

- Trabecular bone – trabecular or cancellous bone is often referred to as ‘spongy bone’. It has a porous structure which is made up of interweaving threads of bone called trabeculae that enclose relatively large cavities containing either red marrow (required for formation of red blood cells), or yellow (fatty) marrow. This type of bone is generally found in the epiphyses (ends) of long bones.

The organization of cortical and trabecular bone at the ends of long bones is illustrated in figure 2.2.

Cortical bone is found where stresses arrive from a limited range of directions. As all osteons in cortical bone have the same alignment, it is relatively stronger and stiffer in the direction parallel to the alignment (Martini, 1998). For example, the osteons in the diaphysis (shaft) of a femur are parallel to the long axis of the shaft. Hence, the shaft is stiffest along this direction.

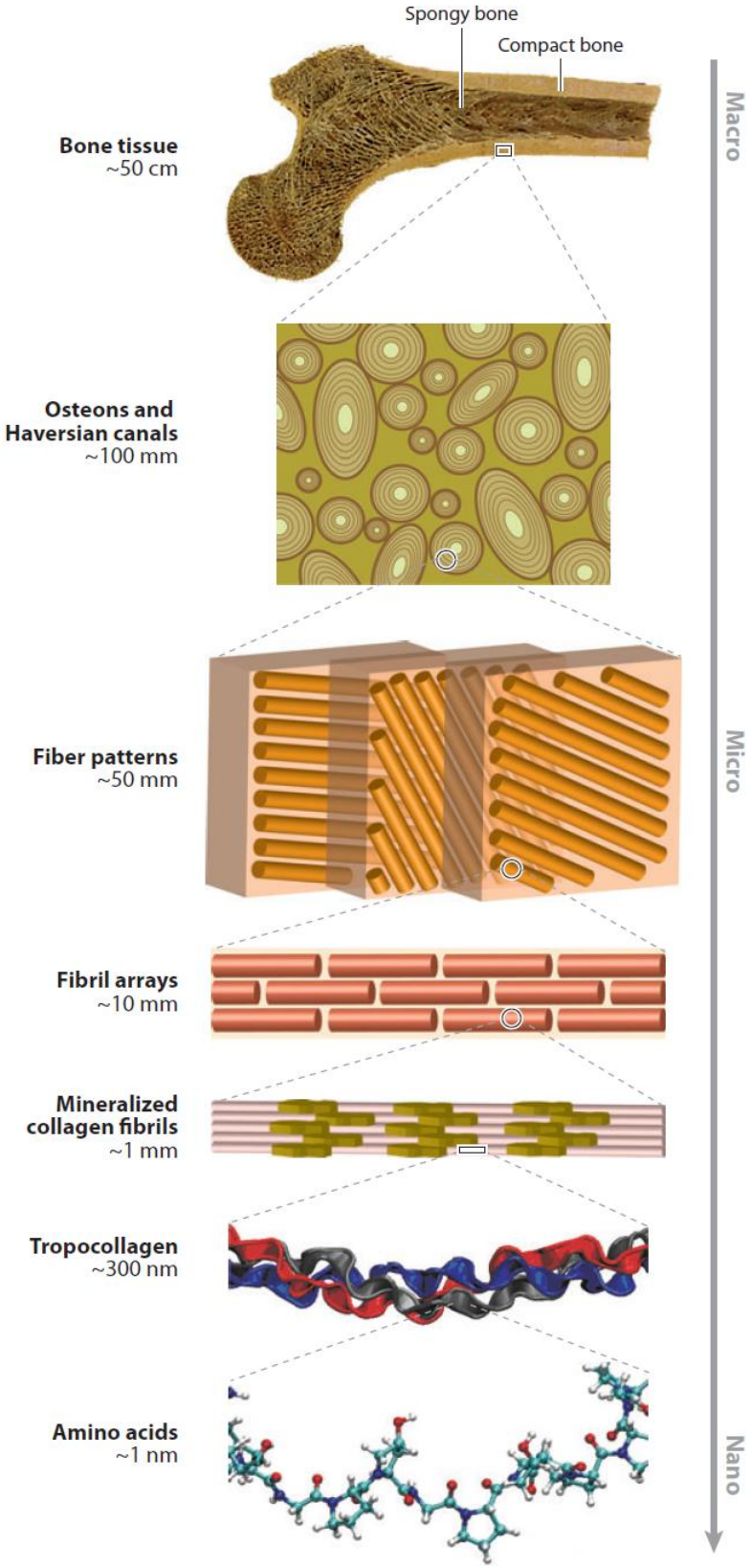

Figure 2-1: Multi-scale diagram for bone's anatomy from macro to nano-scale. Taken from Launey et al (2010).

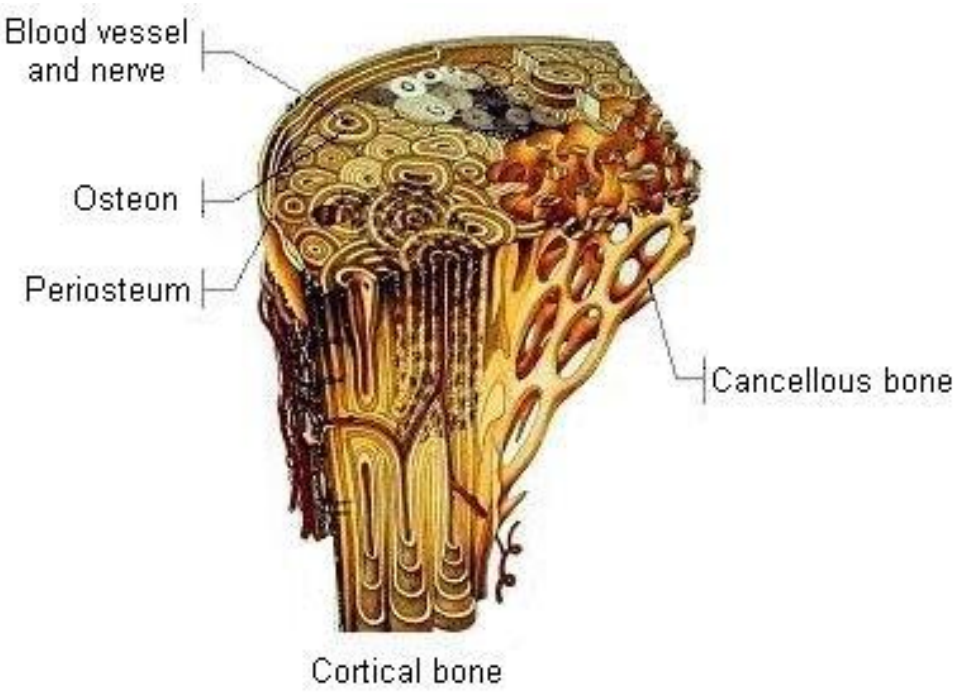

Figure 2-2: Organization of cortical and trabecular bone. The size of an osteon is typically between 200 - 500 µm. From (Warwick, 1973).

Trabecular bone is situated in regions where bone experiences the minimum stresses based on the different directions. For example, at the proximal epiphysis of the femur (the end nearest to the hip) the trabeculae are orientated along lines of stress. However, the stresses arrive from a range of directions and the trabeculae transfer the forces from the hip to the compact bone of the femoral shaft. Trabecular bone is much lighter than compact bone (per unit volume); hence it reduces the weight of the skeleton which means that the muscles can move the bones more easily. Also, the trabecular framework protects and supports the bone marrow cells. This is important because the red bone marrow, that is located within the trabecular bone of the femoral epiphyses, is an important site for blood cell formation (Martini, 1998).

Around 80% of human bone mass consists of cortical bone with the remainder being made up of trabecular bone (Genuth, 1998). Wolff (1892) hypothesised that cortical and cancellous bone were a single morphological material, with cortical bone simply being denser than the cancellous bone. Although some workers have produced data that supports this assumption (Carter and Hayes, 1976), other research has shown

that direct measurements of properties such as Young's modulus for individual trabeculae and cortical bone of similar dimensions cannot be extrapolated from a modulus-density relationship for cancellous bone (Rho et al., 1993; Rice et al., 1988). Thus, in most literature cortical and cancellous bone are treated as separate materials.

2. Microstructure

The next length scale in the structure of bone comprises fibrils that are organized into sheets, or lamellae. The width of individual lamellae is generally between 3-7μm (Rho et al., 1998). Four different fibril arrangements are found in mammalian bone, leading to woven, lamellar, plexiform (Currey, 2002) and Haversian bone (Martin and Burr, 1989; Currey, 2002)

(i) **Woven bone** is characterized by the rapid rate of formation and the random arrangement of mineralized collagen fibres (Weiner and Wagner, 1998). Both the mineral and the organic matrix are disordered. This type of bone is generally found in mammalian embryos and is the first type of bone to form after fracture and other pathological circumstances where rapid formation is a prime concern.

(ii) **Lamellar bone** is arranged more precisely than woven bone with a much slower rate of formation. The structure of lamellar bone is characterized by sets of parallel mineralized collagen fibrils present in discrete layers with the fibril orientation in each layer being different, and hence lamellar bone is often referred to as plywood-like (Weiner and Wagner, 1998). The simplest type of lamellar bone, first reported by (Gebhardt, 1906) and later described by Weiner and Wagner (1998) has parallel arrays orientated orthogonally to each other in alternate layers. Weiner and Wagner (1998) showed that the lamellae that make up this bone structure alternate in thickness and a pair of thick and thin lamellae constitute the basic repeating unit.

(iii) An intermediate structure between woven and lamellar bone is referred to as **plexiform bone**. This type of structure is highly calcified and the arrays of collagen fibrils are arranged in a much more parallel manner than in woven bone (Ascenzi et al., 1967). Plexiform bone, also referred to as laminar or fibrolamellar bone, is a type of bone characteristic of quickly growing large animals such as cows and is

composed of two distinct bone regions; woven or parallel-fibred bone and lamellar bone. A woven or parallel-fibred scaffolding is formed quickly and cavities surrounding blood vessels are then filled in by lamellar bone more slowly. A secondary scaffolding of woven bone is then formed as the amount of lamellar bone increases (Currey, 2002). In bovine plexiform bone, laminae surround a network of blood vessels (around 120 μm apart), and on either side of the laminae, layers of woven or parallel-fibred bone are found (Zioupos and Currey, 1994; Currey, 2002). A narrow hyper-mineralized sheet is present within the woven bone (Zioupos and Currey, 1994; Currey, 1962) .

(iv) The fourth type of bone structure found at this structural level is **Haversian bone**. Haversian systems, or secondary osteons, form during the bone remodelling process when small cells called osteoclasts form a cylindrical cavity with a diameter of approximately 200 μm in primary lamellar bone tissue. This cavity is then filled by osteoblasts beginning with a cement line or sheath that forms around the walls of the cavity. The structure of osteons can be described as the arrangement of cells in the form of cylinder called collagen fibres that are onion-like. Collagen fibres are a significant component of bone, giving the bone properties such as elasticity and the ability to dissipate energy during any mechanical deformation (Gao et al., 2003; Gao and Ji, 2004).

In humans, principally a few primates and carnivores, an initial plexiform bone is later replaced by Haversian bone. The Haversian system is the fundamental functional unit of much compact bone. Osteons are roughly cylindrical structures. However, in mammalian groups such as bovids and deer, the long bones generally retain their primary plexiform structure, and the structure only tends to become Haversian in small regions, generally under the insertion of strong muscles (Currey, 2002).

3. Nanostructure

One of the basic building blocks of bone is the mineralized collagen fibril. The fibril is made up of fibrous protein Type I collagen, a structural form that is also present in

the skin and tendons (Weiner and Wagner, 1998). Collagen molecules are secreted by osteoblasts. They then self-assemble into fibrils with a specific tertiary structure that has a 67 nm periodicity and 40 nm gaps between the ends of the molecules (Rho et al., 1998). The collagen fibrils are impregnated and surrounded by mineral crystals which are generally considered to be hydroxyapatite, ($Ca_{10}(PO_4)_6OH_2$), a form of calcium phosphate. However, the crystals are not in a pure form and known impurities include HPO_4 and 4-6 % carbonate which replaces the phosphate groups (Currey, 2002).

The presence of the hydroxyapatite (HA) within the collagen fibrils makes bone stiff, giving rise to a high value for Young's modulus (around 100GPa). Bone is also very brittle, increasing the chance of fracture. In addition, a deficiency of hydroxyl ions in bone apatite has been demonstrated (Rey et al., 1995; Loong et al., 2000). Hence, the mineral is better considered as a carbonate apatite ($Ca_5(PO_4,CO_3)_3(OH)$, often referred to as dahllite (Weiner and Wagner, 1998).

The apatite crystals are platelet-shaped (Landis, 1996) with an average length and width of 50 x 25 nm, and a thickness of 2-3 nm (Weiner and Price, 1986). They are thought to form within the 40 nm gaps between collagen fibrils (Rho et al., 1998), thus limiting their growth and forcing them to be discrete and discontinuous. The manner in which mineralization occurs is still poorly understood with most studies of the early mineralization of collagen fibrils having been conducted on turkey leg tendons, which are convenient to study because of the well-arranged collagen fibrils, but are not representative of typical bone structure (Currey, 2002). In turkeys, the leg bone develops in two stages, stage one is matrix addition and stage two is mineralization which takes place after two weeks of matrix formation (Parfitt, 2003). Mineralization completes the bone's development process.

2.4.2 Methods used to study the structure and mechanics of bone

Several techniques and methods have been used to study the internal structure of bone. Kabel et al.,(1999) used X-ray computed tomography (CT) to investigate the microstructure of trabecular bone. Ebinger et al. (2005) used CT to study anisotropic growth and reorientation of the microstructure. In their study, they developed a biomechanical model of bone using numerical homogenization, a process whereby

an average solution is computed for a highly heterogeneous material (Allaire and Brizzi, 2005), in order to derive microscopic material parameters for cancellous bone. A great deal of work has also been carried out for trabecular bone, particularly in the study of the effect of disease on enhanced bone fragility (Tang et al., 2007) and the risk of fracture (Ara et al., 2007).

From 2007 onwards, palaeontologists have been using CT techniques to study, for example, the internal structure of bone. Phylogenetic research (Warshaw, 2007) suggests that "History is encoded in cortical tissue" and therefore the age of bone can be determined by studying cortical bone tissue (Warshaw, 2007). The CT technique, combined with finite element analysis, has also been recently employed by Brassey et al. (2013a) in a study of the role of limb bone curvature and cross sectional geometry in supporting body weight during locomotion.

Bone naturally adapts to its mechanical environment and adjusts well to the prevailing loading conditions (Mellon and Tanner, 2012). A range of different loading regimes have been used to test bone strength and resistance to fractures. These include, two point bending (Gulati et al., 2011), three point bending (Sideridis and Papadopoulos, 2004) and four point bending tests (Szaroletta and Denton, 2002; Boyce et al., 1998). Whilst some bending tests (Belill et al., 2014) are typically used to assess material properties and strength of the bone for resistance to fracture, weight bearing capacity of bone and bone healing process, they are also employed in studies of locomotion.

Kemp (2005) conducted 3 point bending tests under static loading to test locomotion in terms of fighting and high running speeds in different breeds of dogs. The proximal limb bones of the pit bulls differed from those of the greyhounds in having relatively larger second moments of area of mid-diaphyseal cross sections and in having a more circular cross-sectional shape. The pit bull limb bones exhibited lower stresses at yield, had lower elastic moduli and failed at much higher levels of work (Kemp et al., 2005). These observations may indicate that relatively stiffer, and therefore more brittle, limb bones belong to owner's with a propensity for running quickly. In contrast, bones with a higher resistance to fracture are more suitable for fighting.

In another example of the use of three point bending tests, strains were determined for alligator femora in order to test locomotor traits (Blob and Biewener, 1999). Whole bone specimens were tested for a tibia bone in tension such that the loading orientation was representative of a locomotion scenario. The tests were performed on four long bones by positioning the bones in test rig and applying strain gauges. In most of the long bone specimens (tibia & fibula), the anterior surface experiences the highest tensile magnitudes, the medial surface experiences relatively lower tensile magnitudes, and the posterior surface remains in compression (Blob and Biewener, 1999).

Although a variety of bending tests are used to assess the strength of bones, axial compression appears to be one of the most commonly applied methods (Ara et al., 2007; Benoit et al., 2009; Das and Cleary, 2006; Müller et al., 1998; Müller et al., 2005).

2.4.3 Biomechanics of Bone

Biomechanics is the science which deals with the forces involved in a biological system (Ratner, 2004). Any internal/external forces acting on/within a biological system and the effects produced in response to these forces are studied in biomechanics. In biomechanics, biomaterials hold an important role. A biomaterial is any material, which can be natural or man-made, that comprises whole or part of a living structure intended to interact with a biological system (Ratner, 2004). Bone is an important constituent in the evolution of organisms. Organisms have evolved according to their mechanical environment (Wolff, 1892) and their design is a response to environmental factors. The internal organs/structures (e.g. bones) in organisms are well suited to the environment they live in. The resistance of bone to the application of loads is determined by two factors:

- Its strength.
- The loads that bones are likely to encounter.

The factors (a) and (b) in bones have been investigated by one of the three methods which are explained in detail next.

1. Theory (e.g. beam theory)

2. Experiment (e.g. Mechanical testing)
3. Simulation (e.g. Modelling forces)

Beam theory plays an important role in structural analysis because it provides the designer with a simple tool to analyze numerous structures. A beam is defined as a structure having one of its dimensions much larger than the other two. There are various structures in real life that can be treated as a beam for analysis. For example, a number of machine parts have beam-like structures such as lever arms and drive shafts. Several aeronautical structures such as wings and fuselages can also be treated as thin-walled beams. Bones can also be treated as long cylindrical beam like structures. Beam models are often used in manufacturing at a pre-design stage because they provide valuable insight into the behaviour of structures. Such calculations are also quite useful when trying to validate more complicated computational solutions. Today beam theory is mostly overlooked by the adoption of more sophisticated tools, such as the finite element method (Bauchau and Craig, 2009).

Mechanical testing is a common experiment-based approach where a compressive or a tensile test is used to test the failure strength of bone. It is possible to apply strain gauges on bones in regions of interest to measure strain and assess strength. Several mechanical testing methods exist in the literature. Mechanical testing procedures have been used for various reasons. They can be used to determine the material properties in bones (Warshaw, 2007; Boyda et al., 2008; Gupta and Zioupos, 2008) and to study complex biological behaviour in order to trace localized deformation (Rodríguez-Martín et al., 2010; Verhulp et al., 2008). In-vitro femoral fractures can also be studied by using mechanical testing procedures . One such example came from the mechanical tests conducted in human trabecuale for the quantification of the effects of osteoporosis treatment (Lenaerts and Lenthe, 2008).

In simulation, various numerical methods are used, such as the finite element method (discussed in 2.5).

The science of mechanical properties (e.g. elasticity or inelasticity) seeks to understand the mechanical behaviour of structures when they are loaded. It aims to predict a material's behaviour under given loads and can be used to estimate when a

structure might fail. This depends on the properties of the material that the structure is made of and the size and shape of the structure. For example, it is easier to stretch rubber than plastic; similarly, a long thin structure is easier to break than a short and wide structure.

The response of a material or structure to loading is a function of:

- Tensile strength.
- Compression.
- Shearing.
- Torsion.
- Bending and fatigue strength.
- Anisotropy/heterogeneity.

Anisotropy is particularly significant in bones, where it arises due to the complex internal geometry and arrangement of (especially) the trabecular bone in different directions. Variation in the material properties of bone is a function of direction as shown by the simple sketch in figure 2.3, where planes orientated in different directions across a sample can yield different values for stress. This is important because the mechanical response of bone to load is not only nonlinear in terms of stress and strain (as indicated by the shape of the curve), but also variable spatially, that is location in the bone and orientation (as indicated by the different curves).

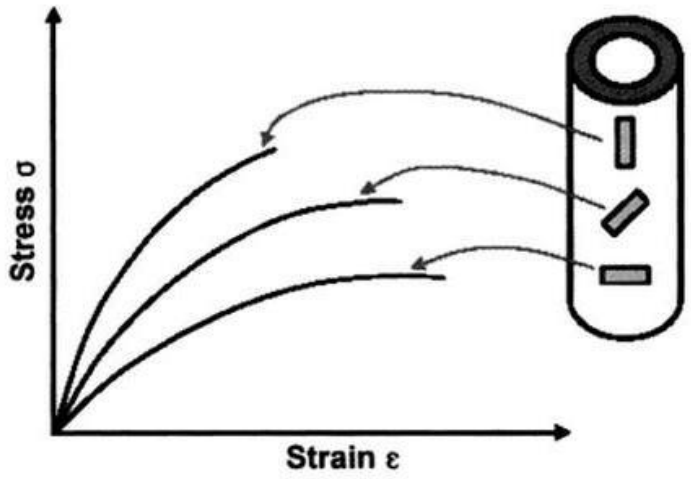

Figure 2-3: Anisotropic behaviour of cortical bone prepared in various directions to the long axis of the bone. Taken from Deng et al (2005).

Two important material properties are the Young's modulus and Poisson's ratio. These define elastic behaviour. Young's modulus is the stiffness of the material. It is the relationship of the stress/force applied to a sample to the resulting strain. It is named after Thomas Young, the 19th century British scientist. Young's modulus can be determined by a simple experiment where a sample of the material is subjected to a load, the strain is measured and the stress is determined. Young's modulus is the slope of the linear portion of the stress–strain curve in figure 2.3.

Poisson's ratio helps determine the amount of expansion in a material under compression. Formally, Poisson's ratio (ν) is the negative ratio of transverse strain to the longitudinal strain (Sharir et al., 2008). It is named after Siméon Poisson, a French mathematician. When a specimen with a positive Poisson's ratio is loaded in compression, it will shorten in the direction of the load and elongate across its width. If the specimen is loaded in tension it enlarges in the direction of the load but becomes narrower in width. Materials with a negative Poisson's ratio behave in the opposite way. In bone, Poisson's ratio ranges from 0.1 – 0.33 (Gercek, 2007; Lakes, 2008; Reilly and Burstein, 1974; Reilly and Burstein, 1975; Reilly et al., 1974).

The selection of values for material properties is a key decision in any mechanical analysis. Any change in the property may lead to a significant change in the results. A full discussion of how and why elastic properties vary in bone is contained in the paper 'The stiffness of bone' (See chapter 6). Here, a few examples are presented.

Table 2.1 shows the variation of mechanical properties of bone due to age. The table shows that with the increase of age the resistance to load decreases. McCalden R. W. et al., (1997) considered ageing as a major loss of bone's strength. As bone porosity increases with age, or due to disease, the compressive strength of the bone becomes more anisotropic, figure 2.4.

Property		Age						
Ultimate Strength (MPa)		10-20	20-30	30-40	40-50	50-60	60-70	70-80
	Tension	114	123	120	112	93	86	86
	Compression	-	167	167	161	155	145	-
	Bending	151	173	173	162	154	139	139
	Torsion	-	57	57	52	52	49	49
Ultimate Strain (%)	Tension	1.5	1.4	1.4	1.3	1.3	1.3	1.3
	Compression	-	1.9	1.8	1.8	1.8	1.8	-
	Torsion	-	2.8	2.8	2.5	2.5	2.7	2.7

Table 2-1: Ultimate strength and strain (%) of cortical bone from the human femur, subject to the function of age (Leuven, 2005).

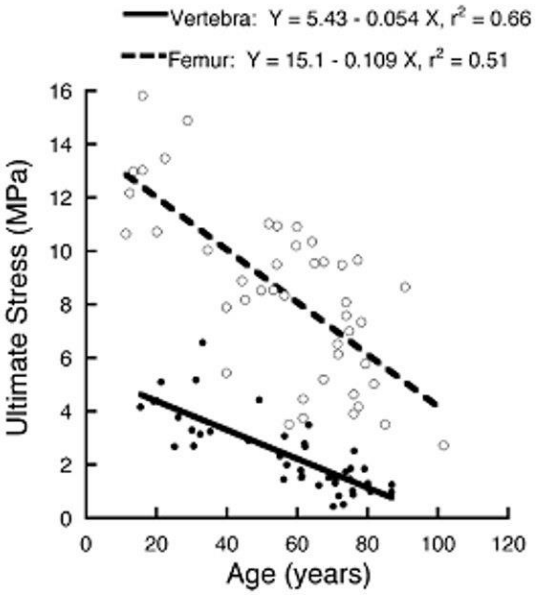

Figure 2-4: Graph showing dependencies of compressive modulus on age for human vertebra and proximal femoral trabecular bone cores (McCalden et al., 1997).

The material properties of bone are also related to function, which varies in different animals and different bones. Currey (1999) studied deer and the use of antlers in fighting. When the antler is dry, just after it sheds its velvet, it is at its strongest compared to wet bone.

Bone mineralization is also important in mechanical properties, the higher the percentage of mineralization, the higher the modulus of elasticity (Currey, 1999). The effect of anisotropy (discussed in section 2.4.2) on material properties has been studied by Keaveny et al (2001), Natali (2008) and Seto et al (2008); the latter paying attention to the effects of variation in fibril structure and orientation on elastic modulus and ultimate tensile strength. The arrangement of cells is also an indicative of the strength of bone in terms of toughness and elasticity (Wille et al., 2012). The complex hierarchical bone-matrix structure at both small and large length-scales is proficient in resisting the initiation and propagation of major cracks that can cause bone fractures (Elizabeth et al., 2014).

In the research carried out in this thesis, bone is assumed to be an elastic material. This is because the aim is to quickly estimate whether a vertebrate long bone might break under a particular set of loads generated by the evolutionary robotics program, GaitSym. Assuming bone to be linearly elastic means that the properties of the bone are same in all the directions. However, in reality a bone is a highly anisotropic and heterogonous material. Taking into account nonlinearity and anisotropy would lead to simulations with excessively long run times. The pros and cons of these elastic assumptions are discussed in the discussion section (Chapter 7).

The literature shows that many researchers have gained insights into the behaviour of biological materials and structures assuming simple linear material behaviour. For example, in two of the many studies of human face tissue modelling (Chabanas et al., 2004; Lotz et al., 1991), linear elastic analyses have proven sufficient to carry out quick and simple evaluations of surgical procedures. These studies do not consider the anisotropic nature of the tissues or their nonlinear stress-strain response to loading, yet they provide useful indications of tissue response from the point of view of the investigators and their target audience. In another example, bone is modelled as an elastic solid, but with non-homogenous properties (Vicecont, 2012).

Incorporating a degree of spatial variability in the elastic properties of the bone provides results that are more consistent with biological reality.

Certain long bones experience elastic instability when subjected to high compression loading. According to Currey and Alexander (1985), the local instability in elasticity of the bone (in other terms buckling) is due to the relation R/t, where R is the mid radius and t is the wall thickness. The maximum threshold for this proportionality is 2.00. If the bone under loading exceeds this threshold value it will experience buckling and if it is below this value, it will deform locally (Guilherme and da Silva, 2004).

In the study of bone deformation, fracture mechanics is a particularly important area of research. Bones (particularly the cortical material) provide a skeletal framework for the protection of an organism's internal organs. A number of factors influence bone's susceptibility to fracture. Ageing is important. Over time, bone deteriorates and cracks (Jennings and de Boer, 1999). This type of fracture is called a stress fracture. Some fractures occur due to dynamic overloading (Ritchie et al., 2005). Cortical bone shows least resistance to fracture under tensile loading (Ritchie et al., 2005). The stress distribution and the resulting damage in bone due to compressive forces is often very complicated, mainly due to the anisotropic structure of the material that makes up bone (Seto et al., 2008). Unlike failure in tension, compressive failure in bones does not always proceed along the actual perpendicular plane of maximum stress (Cristofolini et al., 2010). This is demonstrated by the research presented in this thesis (see Chapter 3 for more details).

Three of the fractures that most commonly occur in daily life are described next (Taylor, October 2012). The first type is *comminuted fracture*, which involves the bone breaking into several smaller pieces. The second type is *greenstick fracture*, where a bone breaks on one side only, typically due to the application of a force perpendicular to the bone's long axis. In this type of fracture, the bone usually bends and breaks only partially. This is the type of fracture that is closest to the one observed as a result of the *Branta leucopsis* mechanical test, although the load was applied in line with the bone's long axis rather than perpendicular to it. A partial fracture was observed and the bone did not break into several small pieces. The final type of fracture is an *avulsion fracture*. This involves a small piece of bone being

torn off from the main bone due to an extreme force applied to a ligament or tendon. Avulsion fractures may be caused by muscle overexertion or sudden traumatic pulling of part of the body during an accident or a combat. This type of stress fracture is addressed in the journal paper given in chapter 5, in which a purported avulsion injury in *Tyrannosaurus rex* is studied.

The fracture toughness of bone (or resistance to fracture) has been shown to be a function of age. In human (cadaveric cortical bone), experiments have shown that fracture toughness of bones including the humerus, the tibia and femur decrease by 5–11% per decade in the longitudinal direction under the crack opening mode (Wang et al., 2002; Sroga and Vashishth, 2012). A detailed review of bone toughness, considering the hierarchical nature of bone, ranging from the nano to macroscale has been carried out by Ural and Vashishth (2014).

The mechanical properties of bone, characterized by quantities such as modulus of elasticity, tension and compression yield stress are independent of body mass of the animal. Furthermore, any structures that support stresses experienced during a particular function (e.g. locomotion) have not evolved due to the mass of the body but the direction of the forces applied to it (McMahon, 1973; McMahon, 1975a; McElhaney, 1965; McMahon et al., 1987; McElhaney and Byarse., 1965). Bone responds to forces in a certain way. This application of forces or loads determines the stress-strain response in bone, which is discussed next.

2.4.4 Stress-Strain relationship in bone

Stress is generated in a structure as a result of an applied force across a certain cross sectional area. For example, if it takes a unit force to stretch one elastic band, it will take twice the amount of force to stretch the two elastic bands placed side by side. Therefore, this proves that resistance to stretch is directly proportional to the thickness of the structure. Hence, stress is the resistance to the applied force in a unit area. It is usually represented by the symbol, σ so that;

$$\sigma = P/A$$

Where P is the applied load and A the cross sectional area of the sample.

Stress is usually represented in Newtons per square metre (Nm-2) or Pascals (Pa) in SI units. Other units used for stress are MPa (Nm-2 x 106) and GPa (Nm-2 x 109).

If a rubber of length L is stretched by a distance of dL, this change of length from L to dL is known as strain. It is usually represented by the symbol ε, so that:

$$\varepsilon = dL/L$$

Where dL is the change in length and L the original length of the sample.

Strain is a unit less ratio expressed in microstrain such that 0.01 (1%) strain will be expressed as 10,000 microstrain (Sharir et al., 2008).

During the incremental loading of bone, at first there is a linear relationship between stress and strain (or load-displacement) in a stress-strain curve, which is called the elastic region (Figure 2.5). At some point, known as the yield stress, any further increase in load causes a nonlinear response, where even small increases in load can cause big strains. Bone deforms plastically beyond this point and eventually the bone breaks at a point called the ultimate stress. The ultimate stress determines the strength of the material.

Mathematical models which show particular stress and strain response under specific loading conditions are called constitutive models. In constitutive modelling, bone can be modelled either as a mechanically elastic or mechanically plastic material. The research presented in this thesis considers elastic modelling only.

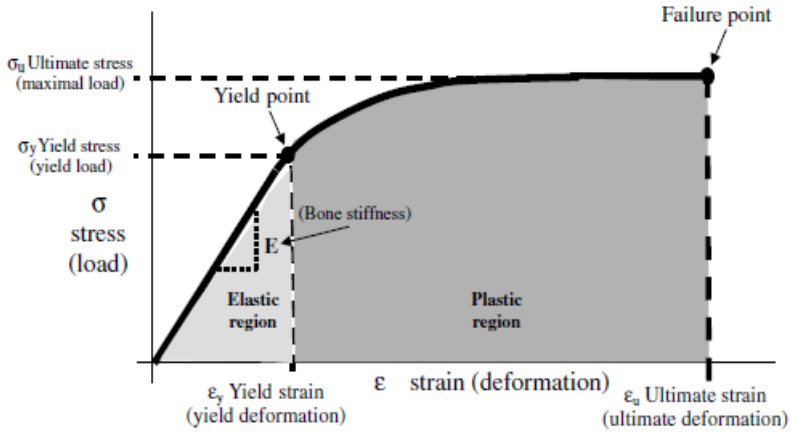

Figure 2-5: The stress–strain curve of a compact bone sample, from (Sharir et al., 2008).

A number of different constitutive models have been developed for biomaterials and this is still a very active research area, particularly for bone, whose behaviour is so complex, it is difficult to represent using a simple mathematical description. Georgeanu et al (2014) have developed constitutive models to help investigate periprosthetic bone remodelling, for the complete full-term functioning of tibial long bones. These models can be used to study the malpositioning of bone, improving prosthesis survival and adaptation to new stress during normal walking cycles in humans. Yang et al (2014) use nonlinear constitutive equations with the finite element method to study the impact of head injury. The nonlinear finite element method has recently been used, together with novel constitutive models for damage and fracture, to study failure response in trabecular bone under continuous loading (Harrison et al., 2013).

2.4.5 Safety factors in bones

A bone will grow and adapt to support a specific loading regime that it experiences during the lifetime of the owner. Evolution has given bones the capacity to support a load that is higher than normal. This extra capacity, beyond what might be called a normal service load, is called a "safety factor". The safety factor is formally defined as the ratio of bone failure strain to maximum functional strain (Biewener, 1993), described by the following expression:

$$\textit{Safety factor} = \textit{Strength of structure} / \textit{Maximum load}$$

Safety factors tend to be small. A larger value for a safety factor would imply that a bone is over-designed for a particular function. The natural evolutionary process usually strikes a balance between safety factor and normal functioning of bones. Over-design implies a cost in terms of the commitment of an animal's resources, such as nutrition or energy consumption and this may be to the animal's detriment.

As far as the safety factor of bones is concerned, it is clear that there is always a limit to the functionality of any organ or system. Bones therefore can and do fail. That failure might occur due to a higher than expected load that is more than the bone can bear. Different authors have investigated typical values for the safety factor of bone. Alexander (1984) suggests that the safety factor of bone should not exceed

a value of 3.4. Biewener (1993) states that this margin is calculated by "the relationship between the load that bone can potentially bear and the loads encountered in life". Biewener (1993) reports that bone has a considerable ability to absorb strain energy. This capability is what determines its safety factor. Several studies have therefore been conducted on the strain energy density within bone when a certain amount of load is applied to it (Rubin, 1984; Skedros et al., 2003; Chiang and Wang, 2006). These studies revealed a non uniform distribution of stress and strains in bone.

Safety factors in the long bones of running animals is generally reported, ranging from 2-6 (Alexander, 1981). Main and Biewener (2007) further elaborated the findings from Alexander's (1984) work; showing that a trade-off between the risk of fracture of bone and the locomotive speed of an organism contributes to the safety factor of bone. Moreover, because of this, the energetic cost of maintaining bones is not uniform in all bones, especially in long bones. For example, in limb bones, the epiphyseal regions incur a higher energetic cost than the middle of the shaft.

In recent research, it has been suggested that the curvature of the shaft in limb bones may help bones support a higher load than they may experience under normal conditions (Brassey et al., 2013 (in press)). Thus, it is not only the base material of the bone or the microstructure that improves the load bearing capacity of bone, but also the macrostructure or external geometry of the bone.

Every improvement in some aspect of a particular bone will have a cost associated with it. For example, small changes in mineralization of bone, can produce definite changes in its elasticity and mechanical properties (Currey, 2002). There is an evidence that bones have safety factors lower than those suggested by Alexander (1984). Alexander's findings did not specifically take into account bone's ability to remodel. Neither he takes into account the fact that the distal parts of locomoting limbs are lightened and hence weakened to reduce the cost of locomotion (Main and Biewener, 2007). This is an important area because bone can remodel itself according to the mechanical environment that it experiences during life.

2.5 Finite Element Method

The finite element method (FEM) is a mathematical approach used to obtain an approximate numerical solution to a complex problem from any discipline. It works by dividing a system into large number of smaller elements connected by nodes, which mimics the physical reality of a system (Kolston, 2000).

Clough first coined the term in 1960s. From the early 1960s onwards, engineers have used the method to obtain approximate solutions to problems in stress analysis, fluid flow, heat transfer, and other areas. This generality is explained in depth in one of the key books on the FEM, by Zienkiewicz and Cheung (1967). Most commercial FEM software packages originated in the 1970s, such as Abaqus, Adina and Ansys. They came about through adaptation and commercialization of source code developed and released by NASA in the USA. In the past few decades, the FEM has seen growing use in biomechanics. An early example of the adoption of FEM in biomechanics is in the analysis of the human skeletal system, through the design and analysis of orthopedic devices (Kazuo Tanne et al., 1987).

2.5.1 Workflow in FEM

A typical finite element workflow is shown in figure 2.6.

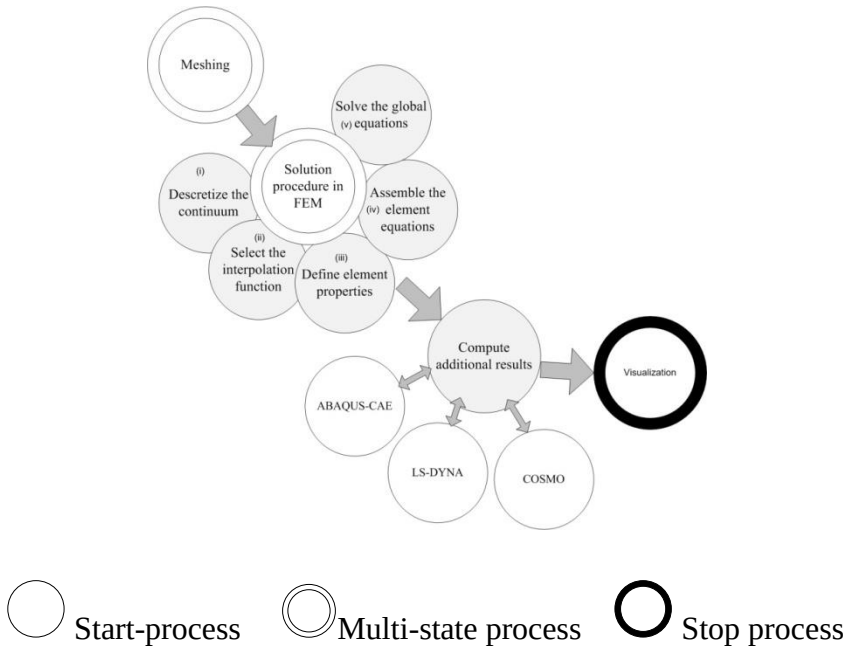

Figure 2-6: Steps in finite element model development.

It is important to carefully plan finite element analyses. This is because a small mistake in geometry, boundary conditions, choice of material model or simulation parameters can cause the final result to be erroneous. Furthermore, the FEM uses different types of elements in a mesh. Each type of element in a mesh is associated with different assumptions and hence element choice can also influence the results. Commonly used elements include beams, shells, 2D and 3D elements.

The general numerical solution steps in FEM are listed as follows (Nikishkov, 2004):

- Discretize the continuum.
- Select interpolation functions.
- Define element properties.
- Assemble the element equations.
- Solve the global equations.
- Compute the additional results.

Discretizing the continuum involves dividing the input geometry into a number of small elements. It is normally carried out using a pre-processor or meshing program. Discretization produces files containing a list of nodal coordinates and element connectivity. The mechanical behaviour of the individual elements is defined by a set differential equations that are converted to finite element form using interpolation or shape functions.

Each finite element is then assigned material properties, for example, the Young's modulus and Poisson's ratio in an elastic analysis. These properties are carefully selected either from the literature or determined experimentally. The elemental matrices are then, typically, assembled into a global matrix. Boundary restraints and loads are applied to an equilibrium equation. For a static elastic equilibrium problem, this system is normally sparse, symmetric and positive definite. The deflections of all the nodes are calculated as the result of the solution to this equation. The equation to be solved is given by:

$$\mathbf{F = ku}$$

where,

F = column matrix of the externally applied load.

K = stiffness matrix of the structure.

U = column matrix representing deflection of all the node points, that results when loads are applied.

Once the displacements have been obtained, additional quantities such as stress and strain can be computed in the post-processing stage of the analysis. This typical finite element procedure is summarized in figure 2.7

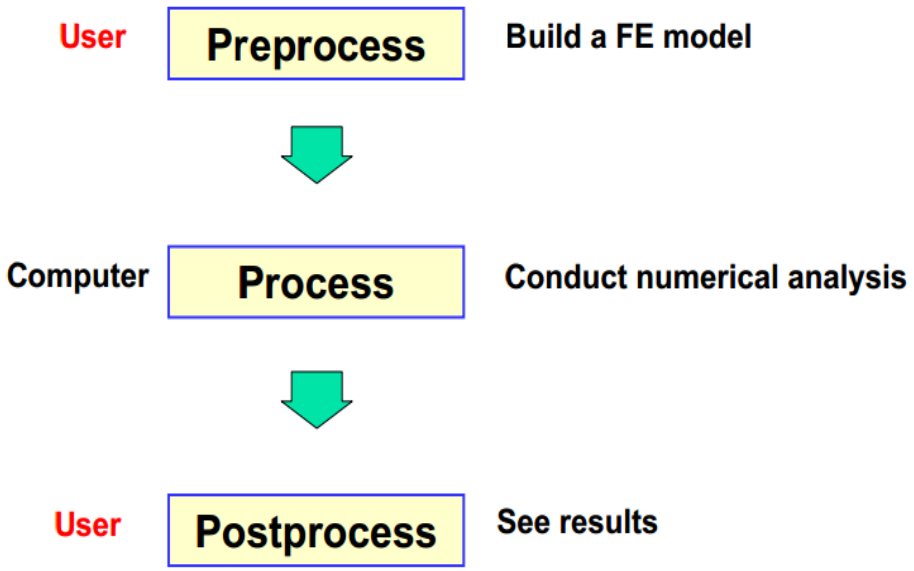

Figure 2-7: Workflow of fem using commercial software.

2.5.2 Constitutive models in FEM

A constitutive model is the mathematical description of how materials respond to different loads. An example in computational mechanics is the stress-strain response to load. The development of constitutive models involves converting experimental data, derived from physical testing (which may involve many different types of test in different orientations or at different strain rates) into its mathematical description. To derive a constitutive model, first the material behavior is characterized, then the appropriate measurements are made and the formulation of the specific constitutive model is derived. There are many constitutive models to cover a whole range of

material responses that are found in the natural world and man-made structures. For example, in static loading scenarios, typical constitutive models may describe the following types of behaviour: mechanically elastic isotropic, mechanically inelastic isotropic, mechanically elastic anisotropic or mechanically inelastic anisotropic.

2.5.3 Precision and accuracy in FEM

Currently two major issues of finite element method are accuracy and precision in relation to validation. This is sometimes due to a lack of computing power and/or computational cost. As the number of finite elements in a model increases, and the complexity of the physics included in the simulation increases, the computational load increases. Computational requirements increase very quickly with increasing element counts.

Model validation involves assessing the degree to which the finite element model (and the results that it outputs) represents the real system being modelled. In simple words, the analyst must assess whether the model correctly represents the geometry, loading conditions, material properties (and correct constitutive model), boundary restraints and interface conditions of the real structure. The accuracy of a finite element model is determined by performing convergence tests. A convergence test is carried out by analyzing essentially the same problem a number of times, but with increasing numbers of finite elements. When further increase in mesh refinement result in no significant changes to the result, the solution is said to be independent of the mesh. Automated convergence tests has been a built-in feature of commercial finite element packages such as Abaqus-CAE since the 1990s (Biewener, 1991).

2.5.4 Typical Mistakes to Avoid in Finite Element Modelling

There is always a chance of encountering analytical, numerical or experimental errors while carrying out finite element analyses. Many of these errors are due to assumptions or scientific judgment, whilst others are due to human error. Mistakes can be avoided by considering the following check list before carrying out any analysis.

- All input data needs to be carefully handled. The analyst needs to ensure that all units (length, stress, material properties) follow a consistent scheme.

- It is not easy to find mistakes when the model is large and the outputs are large. Therefore, the analyst is recommended to start with small, simple models that can be executed and checked very quickly, before proceeding with larger, more accurate analyses.
- Often errors arise as human error. For example, poor choices in the mesh generation stages may lead to distorted elements and therefore incorrect answers. Another example might be the input of the wrong values for material properties or loads.
- Numerical approximation in computing may lead to round off errors. These may accumulate in a long running simulation and affect the final results. The analyst should test sensitivity of the results to the simulation parameters in the software used.
- Access to high performance computing facilities can enable the researcher to carry out complicated analyses. However, it is expensive and therefore its use needs careful planning. The analyst needs to be confident that simpler preliminary models are giving reasonable results before using high performance computers.

While these points are extremely important to consider, another way to validate finite element method results is to compare them with hand calculations. In the case of the finite element modelling of bones, beam mechanics can be used. Examples of this type of calculation can be seen in Brassey et al (2013b) and Alotta et al (2014). There are other examples where the finite element method has been used to study the mechanics of bone. These are discussed in the next section.

2.6 Application of FEM in the study of bone of extant species

As the finite element method is widely used in nearly all the disciplines of science, especially biomechanics, it is difficult to provide a comprehensive review. Here, the thesis therefore focuses its attention on bone. A number of studies use the FEM to address problems in biomechanics, more specifically in musculoskeletal structural analysis.

In the past, there were many computational limitations to analysis (such as slower processor speeds and small computer memories). This is why FEM models were

greatly simplified to study structures using two-dimensional or axi-symmetric models (Rybicki et al., 1972; Svesnsson et al., 1977; Pedersen et al., 1982; Crowninshield et al., 1980; Berkelmans et al., 1992). As a consequence, finite element modelling in the past had poor geometric conformity. However, the scope of FEM has greatly improved due to advances in computer hardware as well as computational methods and techniques. Thorough reviews of the use of the finite element method in the 1980s and 1990s were carried out by Huiskes and Chao (1983) and Huiskes and Hollister (1993)

The first applications of FEM in biomechanics found by the author appeared in 1972. This research involved carrying out isotropic linear structural analyses of bone in the elastic regime by Rybicki et al (1972) in America and Brekelmans et al (1972) in the Netherlands. This was the first time it was possible to calculate mechanical stresses in bodies having complicated shapes, complicated material distributions and loading conditions.

In 1982, a 2D FE model of acetabular region I and II from a human (a ball and socket joint in the form of cup to provide an attachment site for the femur head) was developed by Carter et al (1982) in order to calculate values of stress/strain that may arise during hip replacement procedures. This represented a significant breakthrough in the field of bone implants. Based on this work, it was noted that an increased thickness of the implant resulted in relatively smaller stress values in the implant and the cancellous bone. Later, with further advancements in engineering techniques and methods, the use of the FEM in medical applications included image-based modelling with the interactive positioning of computer aided design hip joints within the scan of an actual patient and modelling the insertion of a cannula into a patient's artery (Said et al., 2008) and (Young et al., 2008).

The FEM is also used extensively in vertebrate morphology. An early example uses a 3D finite element mesh to model the bill of a Shoebill (African wading bird). The bird's bill was loaded on two different regions wherein the amount of displacement and stress maps were calculated and studied Guillet et al (1985). It is noteworthy that due to the constraints of computing hardware in the 1980s, the model only comprised two hundred 3D elements.

As stated elsewhere in the thesis, it is generally accepted that bone remodelling occurs as a consequence of normal physiological loading patterns (Wolff, 1892). This hypothesis was tested in 1990, using a 2D finite element model of a proximal femur (Beaupr´e et al., 1990). The bone was loaded over time, in-vivo, to distribute the stress over all the bone such that it strongly correlated with Wolff's hypothesis regarding the modelling of bone.

By 1999, efforts had been made to deploy the FEM technique at the micro-scale, for 3D reconstructions and 3D architectural analyses that were used to help understand the influence of connectivity over strength in cancellous bone. It was also found out through image-based FEM, that the strength of the cancellous bone is dependent on its elastic properties (Pedersen and Bendsøe, 1999). From then onwards, an effort to elucidate the importance of model resolution has been taking place, studying the relationship between voxel/pixel resolution and the quality of the solvable domains.

In 1998 and 1999, Ulrich performed a high resolution image-based study on human trabecular bone using the FEM. Cubes of human trabecular bone from the femur, illiac crest (ilium bone) and spine were imaged at 28 microns using an X-ray computed tomography scanner. The images were later coarsened to 168 microns for mesh generation. This led to the formation of disconnected regions in the image of the trabecular bone, resulting in an effective loss of stiffness when used to generate a finite element model. The loss in information (due to image downsampling) was compensated by two different meshing methods: (i) Tetrahedral element meshing based on marching cube algorithms (ii) modified hexahedral meshing (figure 2.8). The elastic modulus and computed von Mises stress in the tissue using the hexahedral mesh gave relatively poorer results than those obtained using the tetrahedral mesh.

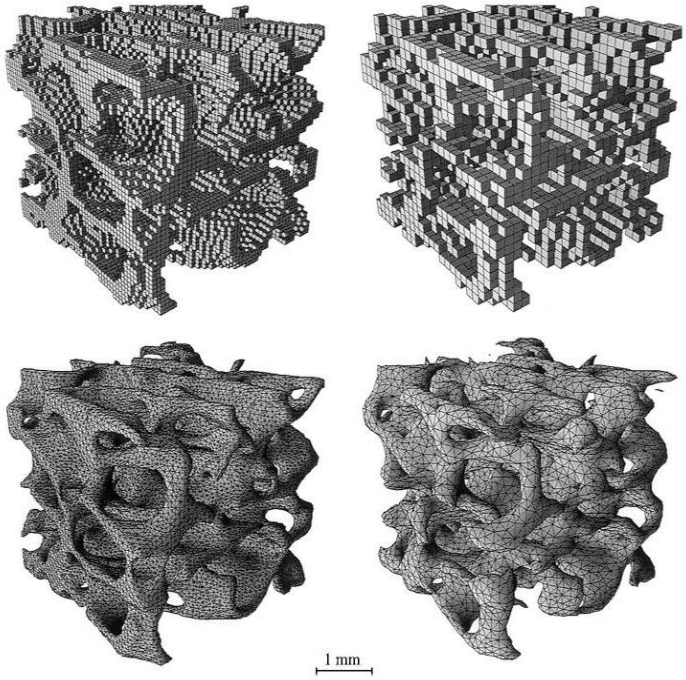

Figure 2-8: FE models of femoral head specimens from human, created at the voxel resolution of 84 microns (left) and 168microns (right) with hexahedron meshing (top) and tetrahedron meshing (bottom); source:(Ulrich, 1998).

Another study revealed the importance of resolution on the results of analyses obtained for cubic domains of trabecular bone. Again, this work involved converting digital images into numerically supported FE models (Keaveny et al., 2001).

Brown (2004) suggested that if FEM is going to be a major tool in biomechanics, then the geometrical facts of the material itself should not be denied. This geometry can sometimes be man-made (e.g. surgical implants), sometimes natural (anatomical structures), and sometimes both (Brown, 2004). In case of man-made geometries, meshes are based on the geometrical abstractions of the structure. Nowadays, they are typically user-built to investigate an approximate solution for the physical objects at an appropriate level of detail. In other cases, they are generated automatically and/or semi-automatically by utility routines which translate data held in computer aided engineering files for further processing. Regarding natural geometries, a key consideration is whether the anatomic representation is generic or not. Source geometric data nowadays come from three-dimensional imaging modalities such as computed tomography (CT), magnetic resonance imaging (MRI), or con-focal microscopy. Therefore, geometric fidelity typically

depends on the resolution of the pixel or voxels in the source image. Another consideration is that such image sources often have limited capability for defining sub-regions of different material behaviour. To overcome these shortcomings, the finite element programs now incorporate a wide range of options for material property representation, including linear and nonlinear elasticity, plasticity and bimodal behaviour for tension versus compression (Brown, 2004). Since the type of meshing technique also affects the overall results, researchers have developed efficient, fast and robust mesh generation methods for complicated specimens (Young et al., 2008). Recently, increased computational power in desktop systems (particularly large random access memory) has meant that solving large models with many millions of 3D finite elements has become feasible.

The FEM has been used to study the underlying structure-function relations in trabecular bone for complex mechanical behaviour, such as multiaxial loading, time-dependent failure, and damage accumulation (Berkelmans et al., 1992). This can be done by assigning highly anisotropic and heterogeneous properties to different finite elements in a mesh. Micros-structurally faithful models of bone have also been used to derive good predictions of the apparent elastic properties of bone for macros-scale analyses (figure 2.9).

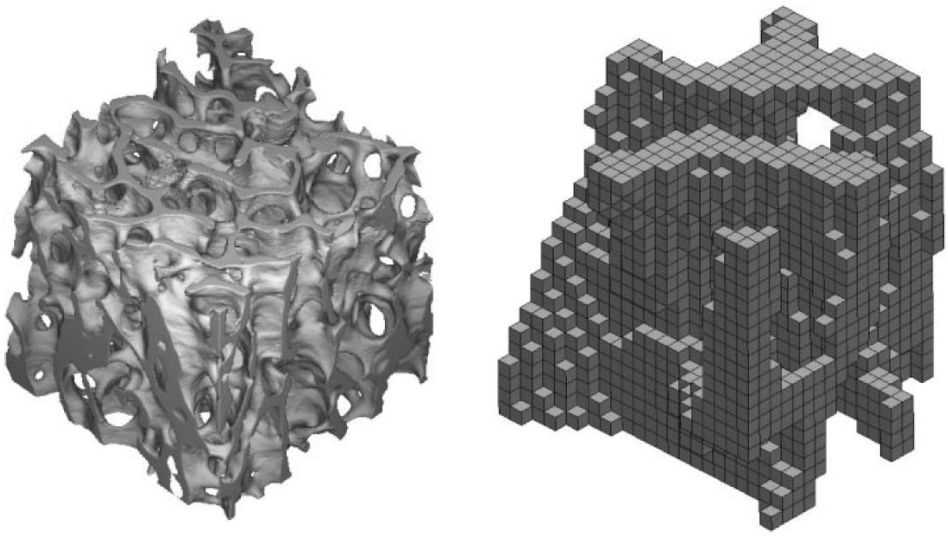

Figure 2-9: A bovine tibia model (left) at resolution of 20 microns and finite element model (right) source:(Kabel et al., 1999).

In order to follow a practical approach in biomechanics FEA, the realism of material representation in biomechanical problems is very important. This can be achieved by applying real loads/forces to the specific structure. There are two primary sources of complexity in the loadings typically encountered in biomechanical finite element studies:

- The first complexity is temporal: this means some systems are analyzed with a single static loading, other systems with a series of different directional loadings, yet other systems use a fully dynamic treatment (i.e. inertial effects included).

- The second source of complexity is the spatial distribution of loading. This includes point loadings (the simplest situation) and they are relatively rare.

Another consideration is the use of an appropriate constitutive model that can cope with different types of loading. Dynamic loading scenarios with inelastic behaviour of highly anisotropic material have been studied by (Lanir, 1983). Constitutive equations have also been developed to study the fibrous connective tissues in bones to seek an insight into the function, structure and mechanics of tissue components. In another instance, cancellous bone architecture was used to define constitutive relationship between density and elastic properties of bone (Kabel et al., 1999). Moreover, to study failure in terms of cohesion loss between fibres, constitutive models of the fibrous structures of compact bone have been developed to study the response to dynamic loading (Pithioux et al., 2002).

It has also been reported in the literature that ontogenic transformations (changes in morphology) have an impact on functional behaviour. This has been demonstrated in studies of skulls using the FEM (Callum (2005); whose work led to a simple formulation of complex structure-function relationships.

The effect of voxel resolution on the elastic as well as plastic characteristics of three-dimensional (3D) osteoporotic lumbar trabecular bone models has been studied by Woo et al (2006). They studied six levels of image resolution: 21μm, 42μm, 63μm, 84μm, 105μm and 126μm. After careful FE analysis, it was found out, the size of specimen (representative elementary volume) has a great impact on the results of

trabecular modelling. In Woo et al. (2006), 6.5mm was suggested as the standard specimen dimension to be used. If small changes in shape and diameter of a specimen can affect the effective strength of the bone, then it will completely change the results if a full femur model at varying resolution is used (Woo et al., 2006).

Boyda et al (2008) have carried out similar research, using the FEM on small cubes of trabecular bone to determine effective material properties. A similar effort, studying the effect of voxel resolution on FEM results, has been reported by Bevill and Keaveny (2009) who used forty six trabecular bone samples, of varying size and resolution, to study the elastic and inelastic response to loading. Their study revealed that non-linear FE analysis is a better predictor of yield stress than linear FEM because material response appears to dominate structure.

Over the past 5-10 years, FEM of the complex microstructure of trabecular bone has been used to demonstrate the computational power of the world's largest supercomputing facilities. Arbenz and Müller (July, 2008) used a mesh of cube of human vertebrate bone to carry out a mechanically elastic FE analysis. The maximum stress bearing locations are highlighted in figure 2.10. These regions depict the zone of possible failures. Effective use of supercomputing with high resolution details was made possible because the smaller the specimen the better resolution and hence magnification. This problem had a size of 1.6 billion degrees of freedom. The analysis was run on an IBM BG/L supercomputer. Visualization of the results of the simulation was carried out using a high performance workstation.

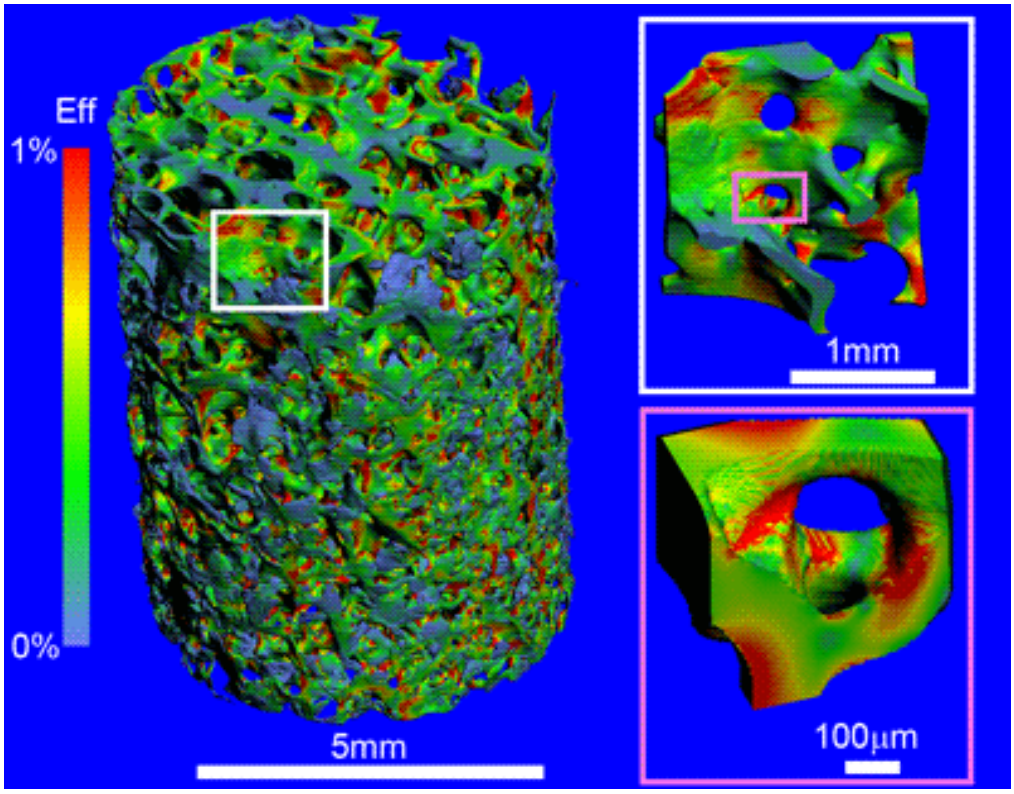

Figure 2-10: Effective strains in vertebral bone specimens, source: (Arbenz and Müller, July, 2008).

Doube et al (2011) used the FEM to compare the bulk stiffness of trabecular bone across a group of mammals and birds (Figure 2.11). A wide variety of terrestrial mammals were chosen (around 90); whose weight ranged from 3g to 3400kg. It was revealed that trabecular scaling does not alter the bulk stiffness of trabecular bone. However it does significantly alter the strain within trabeculae under equal applied loads. In this study, the FEM provided new insight into the science of bones.

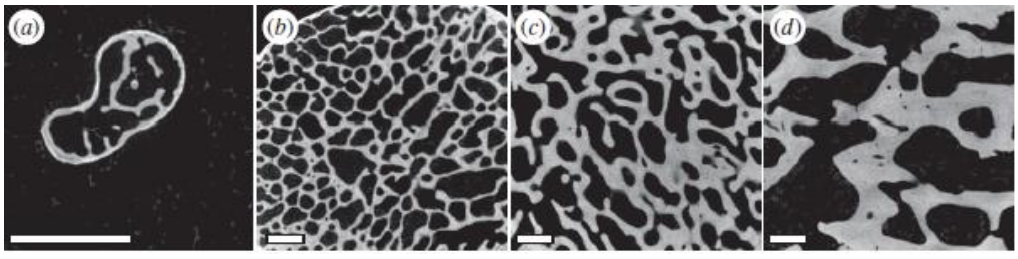

Figure 2-11: Trabecular scale with increasing animal size from a to d of four mammalian species (Doube et al., 2011).

A paper by Panagiotopoulou et al (2011) presents an empirical model of an elephant (Elephas maximus) femur with heterogeneous material properties. This is the first

work to run a full FEM model of a femur using heterogeneous material properties. Before this study, mostly isotropic homogenous FE models of long bones were carried out. Two femoras of an adult female elephant were used. Three different sets of FE models were produced to study the effect of element size, element type and material property values. This work particularly informed the preparatory work and modelling carried out in this thesis. In the work carried out in this thesis it is noted that:

- The acquired resolution for the elephant femora was 742 microns. In theory, most of the information is lost at this resolution. Hence, work carried out in this thesis, uses a small preferably.
- Isopropanol and pumice powder were used for the chemical treatment of the femur prior to mechanically testing in the elephant study. This means, direct human error is introduced via the contamination of the bone by using chemical agents. In the preparation of the goose bone used in the thesis, simple boiling and drying was therefore preferred.
- The trabecular structure was treated as solid in the elephant femora. In this thesis, the rule of mixtures was applied to introduce an effective bulk modulus.

2.7 Application of FEM in extinct bones

2.7.1 The Dinosaurs

Dinosauria comprise one of the most morphologically diverse groups of terrestrial vertebrates that has existed in the history of life (Alexander, 1989). This group includes extinct vertebrates ranging in size from a few grams to many tons. The bones of these vertebrates (as well as their relatives, modern birds) are an important subject of research not only in palaeontology, but also in advanced sciences such as computer science and engineering. Using advanced methods and techniques in combination with incredible computational power, it is possible to generate models of extinct (fossil) bones in an accurate fashion to study their functional properties and hypothesize their operational mechanical forces over the course of evolution.

Dinosaur's bone biology is important because it opens channels to uncover the secrets tied up in the evolutionary history of life. Extinct organisms equally have complex internal geometry and strain functions in bones comparable with living animals. In dinosaur biology, the biggest problem is determining the absolute values of material properties of tissues and bones. This is because soft tissue is not preserved in the fossilization process. Another challenge in dealing with dinosaur bones is unveiling the complex structural geometry despite a long fossilization process with an expected loss of information. Fortunately, X-ray tomography systems have been developed for industrial applications and with sufficient power, can penetrate rock.

Physical testing is not possible with dinosaur bones as the bones are mineralized during the fossilization process, and of course there are no living examples to collect and study. Therefore, computational approaches such as FEM, used in conjunction with X-ray computed tomography (to define the geometry), are perfect for studies in palaeontology, enabling quantifiable and repeatable "virtual" experiments. The greatest advantage comes from being able to try out different values of input parameters, which is one area of considerable uncertainty.

After a long discussion on mechanical testing procedures in the initial section of this chapter, it is now clear that in order to measure a bone's ultimate strength, or determine the properties of its constituent materials, physical testing methods are essential and have been employed in related work (Das and Cleary, 2006; Verhulp et al., 2008; Lieversa et al., 2010; Rodríguez-Martín et al., 2010; Singh et al., 2010). However, these methods cannot be applied to determine the properties of dinosaur bones. Instead, the properties of the material of bone from the dinosaur's nearest living relatives may be used. The strength of dinosaur bones is then determined using the FEM.

There are many examples where dinosaur bones have been studied using the FEM (especially) for the determination of forces they experience during their life, giving insight to how they lived many millions of years ago. The form and function of dinosaur limbs is also considered in the literature, particularly in relation to movement and locomotion. In the context of strength, an interesting study concerns the role of the short arms of Tyrannosaurus rex. It has been assumed by scientists

that its arms were used for pushing itself up; to hold its body weight or to lift up its chest while in a sitting position (Newman, 1970). However some scientists argue that the arms have evolved as a strong weapon for clutching its prey (Carpenter and Smith, 2001). Support for this argument is the presence of a large caracoid, shortened forelimb and powerful adductor muscle. Furthermore, the small size of the forelimb makes it more robust and mechanically stronger than the large slenderical forelimbs of other dinosaur species such as Deinonychus. The limited functionality of the Tyrannosaurs rex arms is said to be significant and perfectly designed for the biomechanical movement (Carpenter et.al 2001). In one of the Carpenter's papers, the Tyrannosaurs rex arms are described as an 'efficiently designed force based system'. A FEM study of this arm has been carried out as part of this thesis, in order to demonstrate its strength after the healing of a purported tendon avulsion injury (See chapter 5).

The function of the forelimb may vary in extinct animal's life for example to get up from a prune position (Newman, 1970) or to aid in copulation (Osborn and Brown, 1906) and for locomotion (Farlow et al., 2000; Hutchinson and Gatesy, 2006).

One of the most prolific scientists to use the FEM in the study of dinosaurs is Rayfield. She has pioneered the use of the FEM in the study of dinosaur skulls and the forces acting upon them (Rayfield, 2005; Rayfield, 2004; Rayfield, 2001). This work has been further continued and developed by her students, including studies of the cranial biomechanics of basal *Ornithischians* and the feeding and jaw mechanism of *Heterrodontosaurus tucki* (Porro, 2006; Porro, 2007). She has developed FEM models of the dinosaur *Allosaurus fragilis* to investigate the mechanical significance of intracranial flexibility in the skulls of these dinosaurs (Rayfield, 2005). She has also constructed a 2D model of a Tyrannosaurus rex skull using the FEM to investigate functional morphology. In this work, Rayfield suggests that a large number of loosely held bones within the skull functioned as a shock absorber, an evolutionary adaptation for fights with other dinosaurs (prey or aggressors) that involve biting. Rayfield's work gives rise to questions applicable to all the finite element studies i.e. how accurate the FEM reflects the reality which forms a central question in the vertebrate morphology (Rayfield, 2007). At the same time, the shortcomings of her work include factors such as the level of detail in

terms of geometrical fidelity. For example, in cranial mechanics factors like soft tissues at tooth sockets and further sutural contacts are missing. That said, the work provides a starting point towards experimenting and testing models from fossil specimens (Rayfield, 2004).

In another example from the literature, a virtual synthesis of a sauropod skull was used with the FEM to study stress and strain during skull evolution in *Diplodocus* (Witzel and Preuschoft (2005). Margetts et al (2006) have used the FEM with soil mechanics to study dinosaur trackway formation. The tracks of dinosaurs not only reveal how big those animals were, but also provide useful insight into other factors such as the walking style and locomotion pattern of these extinct organisms, during the course of evolution. Manning et al (2009) have used finite element analysis, with models derived from 3D X-ray computed tomography images to study the form and function of a *Velociraptor* claw.

Based on the brief review of the dinosaur literature presented in this section, it is evident that modern engineering techniques such as tomography and the FEM can contribute significantly to our understanding of dinosaurs and the evolution of vertebrates.

2.8 Summary of key insights

- So far, a large number of techniques and methods have been used to study gait patterns in vertebrates e.g. mathematical modelling using genetic algorithms and evolutionary robotics on high performance computing platforms. However, these methods do not take into account whether the bones in the skeleton can support the loads that may arise due to the computed gaits.
- Use of finite element modelling is now a widespread tool for biologists to study the behaviour of bone. Some researchers have studied the mechanical aspects of trabecular bone at the micro-scale whilst others have focused on modelling bones as a solid material. However, no one has modelled a whole bone including internal geometry. All studies considering trabecular micro-structure have studied small cubes of bone only, as a means to generate effective material properties.

- Current genetic algorithms that are used to study locomotion, especially in dinosaurs, use enhanced optimization methods. However these methods lack the ability to determine whether the forces generated may damage the owner's skeleton. As a result, the algorithms may produce solutions for patterns of gait that are not realistic.

On a concluding note, based on the literature described in this thesis, it is seen that so far studies on investigating the level of detail required in bones with complex internal microstructure has only been used on small cubes of trabeculae or a cortical bone alone. Only one study conducted by (Torcasio et al., 2011) uses a full femur, but here the trabecular bone is still treated as a solid. Nowhere in literature shows any results, where full bone microstructure is taken into account at reasonable detail to study the overall behaviour of bone.

This thesis contributes to research by taking into account the following factors:

- Reasonable resolution.
- Specimen length.
- Imaging modalities.
- Computational resources.
- Numerical validation.

3 A study of the progression of damage at multiple length-scales in an axially loaded *Branta leucopsis* femur

Zartasha Mustansar[1], Samuel A. McDonald [2], William Irvin Sellers[3], Philip Lars Manning[1], Philip J. Withers[5] and Lee Margetts[6]

---

1 Interdisciplinary Centre for Ancient Life, School of Earth, Atmospheric and Environmental Science, University of Manchester

2 School of Materials, University of Manchester, Oxford Road, Manchester, M13 9PL, UK.

3 Faculty of Life Sciences, University of Manchester, Manchester, M13 9PT, UK. Email:

4 School of Earth Atmospheric and Environmental Sciences, University of Manchester,

5 School of Materials, University of Manchester, Manchester, M13 9PL, UK.

6 Oxford e-Science Research Centre, University of Oxford

A paper submitted to the Journal of PLoS-ONE.

A study of the progression of damage in an axially loaded *Branta leucopsis* femur using X-ray computed tomography and digital image correlation

Zartasha Mustansar[1], Samuel A. McDonald[2], William Irvin Sellers[3], Philip Lars Manning[4], Tristan Lowe[5], Philip J. Withers[6] and Lee Margetts[7,8]*

[1] Interdisciplinary Centre for Ancient Life, School of Earth, Atmospheric and Environmental Science, University of Manchester, Manchester, M13 9PL, UK. Email: zartasha.bi@gmail.com

[2] School of Materials, University of Manchester, Oxford Road, Manchester, M13 9PL, UK. Email: sam.mcdonald@manchester.ac.uk

[3] Faculty of Life Sciences, University of Manchester, Manchester, M13 9PT, UK. Email: william.sellers@manchester.ac.uk

[4] Interdisciplinary Centre for Ancient Life, School of Earth, Atmospheric and Environmental Science, University of Manchester, Manchester, M13 9PL, UK. Email: phil.manning@manchester.ac.uk

[5] School of Materials, University of Manchester, Oxford Road, Manchester, M13 9PL, UK. Email: tristan.lowe@manchester.ac.uk

[6] School of Materials, University of Manchester, Manchester, M13 9PL, UK. Email: philip.withers@manchester.ac.uk

[7]* Interdisciplinary Centre for Ancient Life, School of Earth, Atmospheric and Environmental Science, University of Manchester, Manchester, M13 9PL, UK. Corresponding author. Email: lee.margetts@manchester.ac.uk

[8] Oxford e-Science Research Centre, University of Oxford, OX1 3QG, UK.

Abstract

This paper investigates the mechanical response of a vertebrate long bone subjected to a compressive load, applied in the direction of the bone's long axis, which is increased gradually until failure. The study was carried out using a test rig mounted in an X-ray computed tomography facility so that three-dimensional images of the bone's internal structure could be recorded at certain intervals in the loading path. Five distinct types of deformation mechanism were observed in the cancellous part of the bone. These were (i) cracking (ii) thinning (iii) tearing of cell walls and struts, (iv) notch formation (v) necking and (vi) buckling. Progressive deformation leading to cracking was studied in detail using digital image correlation. The resulting strain maps were consistent with mechanisms occurring at a lower length scale. This study serves as a unique reference for researchers interested in how bone responds to loading, particularly those using computer modelling who may require qualitative information for verification and validation of their simulations.

Introduction

Bone has a complex geometry, both through its external appearance and its internal structure. Bone grows and remodels itself according to the mechanical environment it is subjected to [1] and reflects a combination of influences, from the functional constraints of a particular bone to the animal's habitat. Femora support the transmission of load due to the weight of the owner's body. Structurally, it is a long beam like cylinder with a distinct head, neck and shaft. It develops in a way that uses the minimum material to provide the maximum mechanical strength [2,3]. The material that bone is made of comprises cascaded building blocks at specific nano, micro and macro scales. This hierarchical arrangement of bone is responsible for controlling properties like deformation and toughness [4,5]. Femoral bone consists of two distinct regions, cortical bone which constitutes the denser part and trabecular or spongy bone consisting of struts as small as 100-200 microns in diameter [6]. Distribution of trabeculae in the femur is such that the most of bony trabeculae lie in the neck and tension-compression trabeculae lie in the medial cortex region. This forms an efficient system to withstand stresses during locomotion and/or other load bearing scenarios [7]. In the femur, the most fracture prone part is called the

Trigomeum intenum femoris or 'Ward's triangle' which is made of diminished density of trabeculae lying in the upper epiphyseal femoral neck [2,4]. Within the trabeculae in the head and tail of the femur are 'interstitial lamella' which hold the struts together. During loading scenarios where the load exceeds the strength of bone, these interstitial lamella break apart causing the bone to fail [4,7,8].

The three-dimensional (3-D) nature of vertebrate long bones makes it difficult to accurately observe the microstructure from 2-D microscopy investigations [9]. Consequently, to fully observe and understand in 3-D the deformation mechanisms and overall mechanical response occurring during an axial loading test, a means of imaging the evolution of structure in 3-D is required. As a non-destructive imaging technique, X-ray computed micro-tomography enables the virtual reconstruction of a 3-D 'image' and can reveal detailed information about the evolution of internal structure of an object when subjected to mechanical loading. It involves reconstructing the 3-D spatial distribution of the local X-ray attenuation of the materials/phases contained within the object. Combined with digital image correlation (DIC) [10] or digital volume correlation (DVC) [10,11] as applied to fully 3-D tomographic volumes, the technique is rapidly gaining interest for mapping the heterogeneous deformation within the bulk of microstructured materials [12]. It works by correlating successive images so as to infer the displacement vectors relating one to the other. In order to measure and extract the displacements the presence of a readily observable microstructure with an internal contrast to X-ray absorption is required. While contrast can be introduced artificially by adding high attenuation contrast markers, in many cases the material microstructure itself has sufficient contrast, such as for the study of the uniaxial mechanical response of cellular polymeric foam structures [13,14,15] and trabecular bone [16].

There are many examples where X-ray computed micro-tomography and digital image correlation are used to examine 3D local trabecular strains for small cubes of bone in mammals [17], rodents [18,19] and humans [20], [21]. This paper presents, for the first time, a study of a whole *Branta leucopsis* (*Barnacle goose*) femur, which has been subjected to incrementally applied loading to failure whilst being monitored through the entire loading regime by 4-D imaging.

Methods

This section describes the rationale behind the selection of the specimen. It then details the procedures followed in the preparation of the specimen and the scanning of the specimen. The tools and methodology used to interpret the results are also explained.

Selection of Vertebrate Long Bone

The characteristics of the test rig and scanning system place constraints on the size of bone and size of internal features that can be studied. Simply stated, the bone cannot be longer than the test rig and only micro-structural features roughly larger than one voxel can be captured. With respect to the latter, the high aspect ratio of long bones (long bones are significantly narrower than they are long) limits the resolution of scan that can be acquired.

Therefore, at the beginning of the study, a selection of bones from different species were identified as potential test specimens on the basis of their length. The bones were individual femora from each of the following vertebrates: pigeon (*Columba livia*); partridge (*Perdix perdix*); Barnacle goose (*Branta leucopsis*); Guinea fowl (*Numida meleagris*); pheasant (*Phasianus colchicum*) and rabbit (*Oryctolagus cuniculus*). These were sourced and prepared according to the procedure outlined in the next section. A static X-ray tomography scan was carried out for each femur. Details of the scanning arrangements are given later. The scans were reconstructed and the quality of each was assessed. In many of the specimens, micro-structural features in the cancellous bone were not captured. The features were smaller than the resolution of the scan. The goose bone produced a high quality scan and the micro-structure of the cancellous bone was very clearly defined. The goose was therefore selected for this study. The other scan data is not published here, but is available on request.

Sample Preparation

The right and left femora were obtained from an adult Barnacle goose (*Branta leucopsis*) with accession number SF320. Both femora were 59 mm long. The intact

adult weighed 2.034kg. All soft tissues were carefully removed using standard laboratory procedures such that the distal and proximal epiphyses remained intact.

The bones were then cleaned following the methodology of [22] and [23]. Care needs to be taken that the preparation does not weaken the bones before carrying out the mechanical test [24,25,26]. All bones (including those in the previous section) were first treated with 75% saline solution to avoid use of organic/chemical detergent. The bones were then subjected to 'supervised boiling' in tap water with a small amount of detergent for 6 hours. The boiling time was divided into two sessions. The water was changed after 3 hours. This released most of the soft tissue on the surface and the fats held within the marrow. The bones were then kept for air drying for three to four weeks. Drying was considered complete when the weight of the bone stayed constant over a few days.

The right femur was used as a 'test specimen' to devise, evaluate and improve the experimental protocols before carrying out the final destructive axial loading test on the left femur.

Safety assessment procedures and protocols were followed in compliance with the BIOCOSSH procedures set out by the Medical School at the University of Manchester, UK [27].

X-ray Tomography

The system used for this work was a Nikon Custom Bay 320kV micro CT scanner at the School of Materials, University of Manchester, UK (Fig 1)

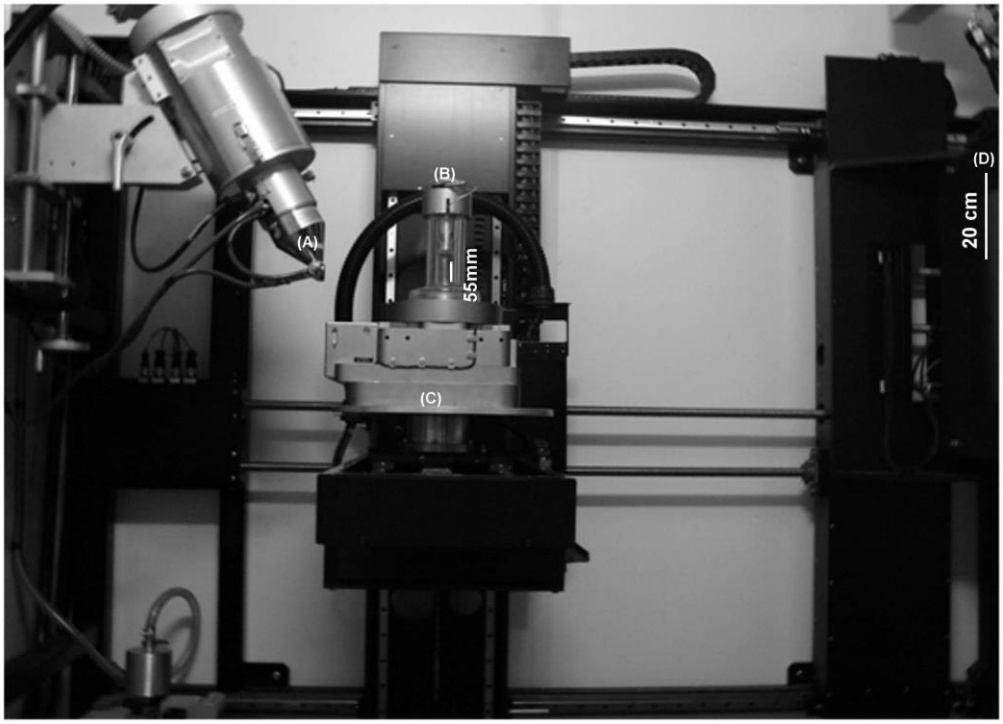

Fig. 1. Nikon Custom Bay 320Kv X-ray micro-tomography system. The figure shows the (A) source, (B) the mechanical rig with the bone mounted for testing in the glass tube, (C) the detector, and (D) the load assembly.

A mechanical tension-compression loading rig specially designed for use with this scanner was used to carry out the axial loading. The rig has two adjustable steel platens, one on the top and the other on the base. The left goose femur was mounted in the loading rig vertically along its axis. Epoxy resin disc spacers were specially manufactured and introduced between the bone and the steel platens at both the top and bottom of the loading rig. The purpose of the spacers is to avoid the steel platens casting a shadow on the tomography scans at the distal ends of the bone. Discs of abrasive paper of equal dimension to the epoxy resin were used between the bone and the resin. The purpose of the abrasive paper was to stop the bone moving in the plane perpendicular to the axis of loading. Open cell phenolic foam (Smithers Oasis) was glued over the bottom epoxy resin disc, holding the bone upright. The foam is radio-transparent which avoids introducing any unwanted artefacts into the scan. The loading rig and mounting of the specimen are shown in Fig. 2.

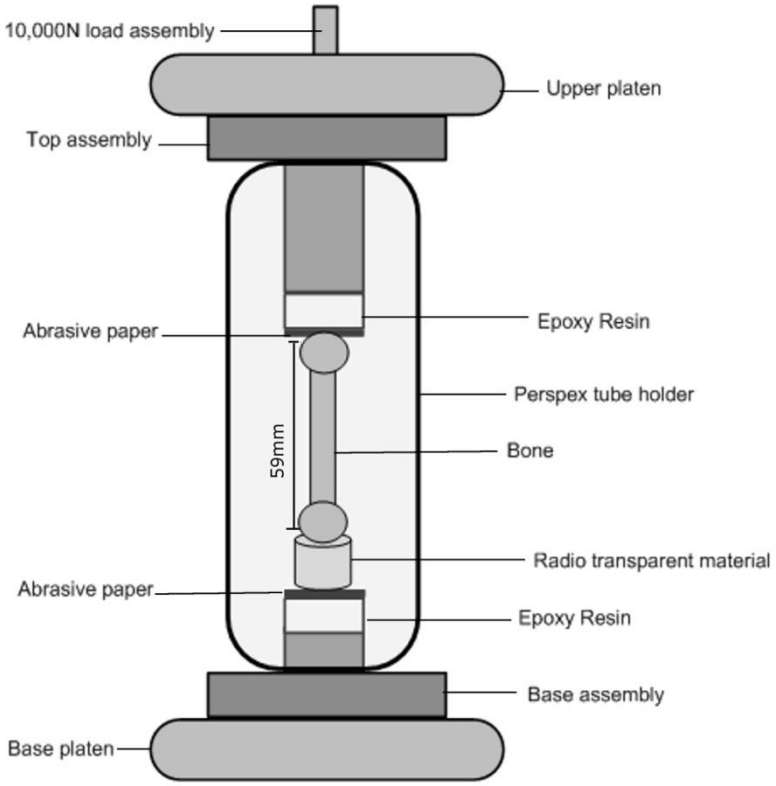

Fig. 2. Loading cell. A schematic of the rig used for the mechanical compression test.

A 10,000N load cell was used to load the bone through the upper platen. The lower platen was fixed. A compressive pre-load of 10.2 N was applied at the beginning of the experiment to take up any slack between the bone, the spacers and the rig. Once a stable force reading was reached (after approximately 100-150 seconds), the load step was increased. In total 11 incremental loads, numbered from 0 to 10, were applied at a rate of 0.5mm/min. Loading was stopped when the bone had completely failed. The magnitudes of the displacement increments applied along with the corresponding loads are given in the results section.

At the end of each displacement increment and when a stable force reading was acquired, a full three-dimensional scan was carried out. The resolution acquired was 32 microns using 59kV and 195microAmperes. The distance between the source and the sample was 234.3 mm.

Image Processing

The images were reconstructed using the commercial CTMetris Pro software (Nikon Metrology, Tring, UK). The center of rotation was determined and the noise levels were reduced. After that, the level of beam hardening was chosen. Data was then exported in unsigned 16-bit DICOM format (VG Studio Max v. 2.0, Volume Graphics, Heidelberg, Germany). They were then processed using Avizo 7 [28]. First a median filter, with a kernel size of 3x3x3 pixels, was applied in order to reduce the effects of noise. Virtual isosurface renderings were then created for selected features of interest that were found in the scans. Isosurfaces for each scan captured through the loading sequence were generated using the same parameters. This allowed the evolution of the features of interest to be followed from one scan to the next. The number of times each type of feature was present in each scan was counted manually to see whether there was a pattern of feature growth or feature emergence as the bone progressed to failure.

Digital Image Correlation

Digital Image Correlation was used to evaluate the evolution of a small crack feature. Digital Image Correlation can infer particle movements by matching the locations of patches from two different images. Methods that have been developed include least-squares approaches [13] and Bayesian probability methods [29]. In this study, correlation was performed using an algorithm developed by LaVision, Göttingen (originally conceived for particle image velocimetry (PIV)), which is part of the StrainmasterTM software package. It uses fast Fourier transform (FFT) cross-correlation to compare small sub-regions of the images [10]. The method is based on generalized texture mapping functions and on the fact that, under suitable conditions, groups of particles or regions of image texture will retain similar appearances under small translations and deformations. The particles or texture regions can then be tracked as a group using a correlation function to perform pattern matching as a function of the displacement. The algorithms thus use the characteristic local intensity variation to identify a region before and after deformation and thereby estimating the associated displacements. The actual displacement is determined from the location of the maximum value of the

correlation function, and is always done to sub-pixel accuracy, with a local curve fit of the correlation data. If the correlations are performed correctly, the maximum value represents the most likely displacement of the image in each interrogation window. Multiple iterations are used during which the search sub-region is iteratively translated and deformed, using interpolation, until the highest correlation possible is achieved with accuracies of 0.01 pixels.

All the volumes were imported into ImageJ [30]. Scan 0, which is an unloaded and therefore undeformed volume, was selected as a reference image. The background was cropped for each image. Boundary pixels near the shaft in each image were aligned with reference to the first scan. All the images were then exported as a set of 'raww' files. These were imported into Avizo7 and accurately aligned with one another using the affine registration module. Digital Image Correlation was then performed on the sequence of three dimensional sub-images containing the crack feature. Correlation was performed on a sub-region of decreasing size, from 32x32 pixels to 16x16 pixels and with a sub-region overlap of 25%. This was found to provide a good compromise between spatial resolution and displacement accuracy, giving an uncertainty in strain resolution of around 0.05%. Strains were calculated by measuring the change in length/displacement between the original and the deformed volumes. The output was a sequence of three-dimensional strain maps corresponding to the associated loading increments.

Results

The results are presented at three different levels of detail, defined here as macro-scale (the length scale of the whole bone), meso-scale (the length scale of individual trabeculae) and micro-scale (the length-scale of crystalline lamellae that form the trabeculae). These correlate with the increasing fidelity provided by the different investigative tools employed. Firstly, the overall macro-scale load-displacement response is presented. Next, the authors present their study of the meso-scale deformation features captured by the X-ray tomography data. Finally, the results of the digital image correlation are presented, giving insight into processes at the micro-scale.

Macro-scale load-displacement response

The load displacement response is shown in Fig. 3. the consecutive numbers “0” to “10” mark the points at which loading was interrupted to carry out the tomography scans. Whilst the scans were taken, the loads decreased, probably due to creep in the bone material. The load-displacement data are also presented in Table 1. The first data point “0” corresponds with the first tomography scan. A displacement of around 2mm was recorded for an insignificant load reading. This represents the loading required for all the slack to be taken up in the testing rig and for the bone to be held firmly in position. The reconstructed volume for the unloaded scan 0 is shown in Fig. 4.

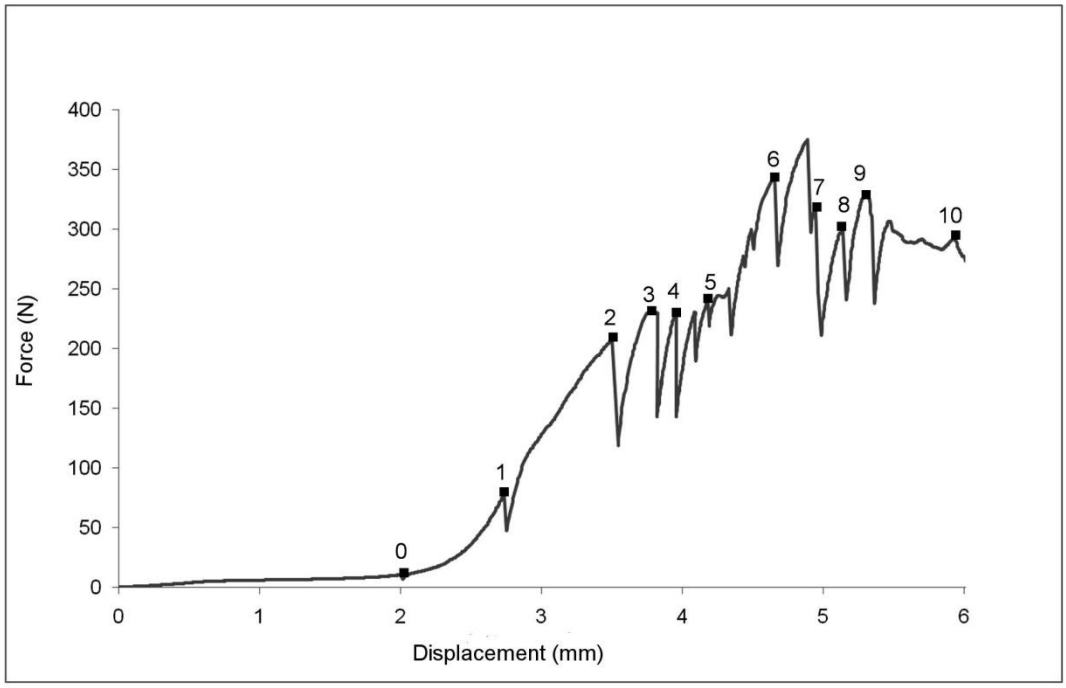

Fig. 3. Load-displacement curve. Each scan is indicated on the graph using a unique scan number.

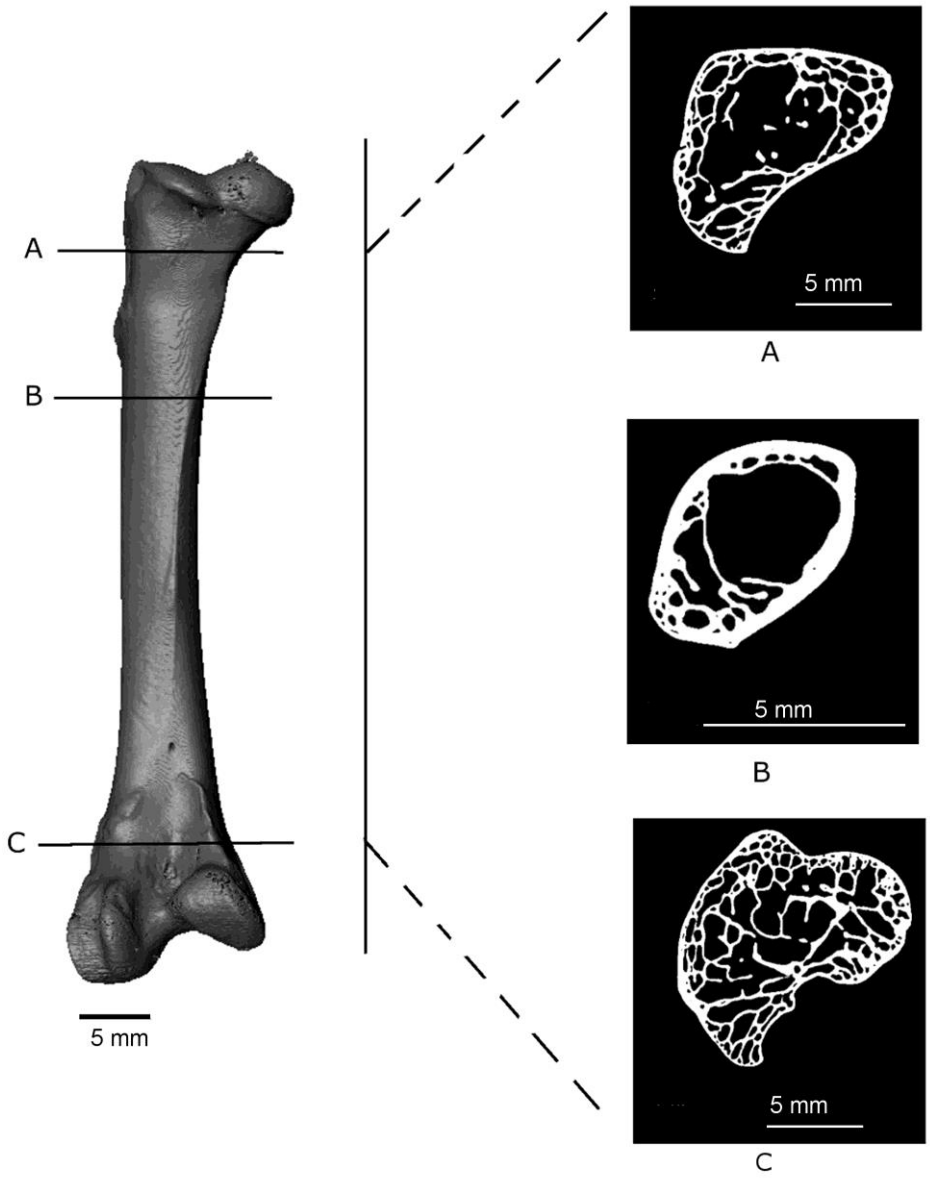

Fig. 4. Volume reconstruction of the *Branta leucopsis* femur before loading. The figure shows 2D sections from the upper condyle (A), the shaft near the epiphyseal neck (B) and the lower condyle (C) to highlight the internal structure.

Scan number	Force (Newton)	Displacement (mm)
0	10	2.04
1	77	2.73
2	208	3.50
3	230	3.75
4	229	3.96
5	250	4.24
6	343	4.65
7	247	5.02
8	296	5.11
9	310	5.25
10	273	6.02

Table 1. Force-displacement data for the *Branta leucopsis* femur

Based on the load-displacement curve, there appear to be 4 phases in the macro-scopic response to loading. These are identified as follows: (i) The part of the curve from scan 0 to 2 appears to show an approximately linear load-displacement response; (ii) Scans 2 to 4 correspond with a region of displacement (3.5 to 4.5mm) that is not matched by an increase in load bearing capacity (load stays at around 200-250N); (iii) Scans 5 to 7 show an increase in load (to ~375N) for a small displacement (~0.5mm). This is matched by the macro-scopic observation of a visible crack in the greater trochanter region of the head of the femur. (iv) Finally, scans 7 to 10 show a reduction in load bearing capacity of the bone which corresponds with shear failure in the epiphyseal region of the femur. Fig. 5 shows the external surface view of the progression of the crack and Fig. 6 shows 2D slices of the tomography scan for the same set of features. These results are similar to those described in [31].

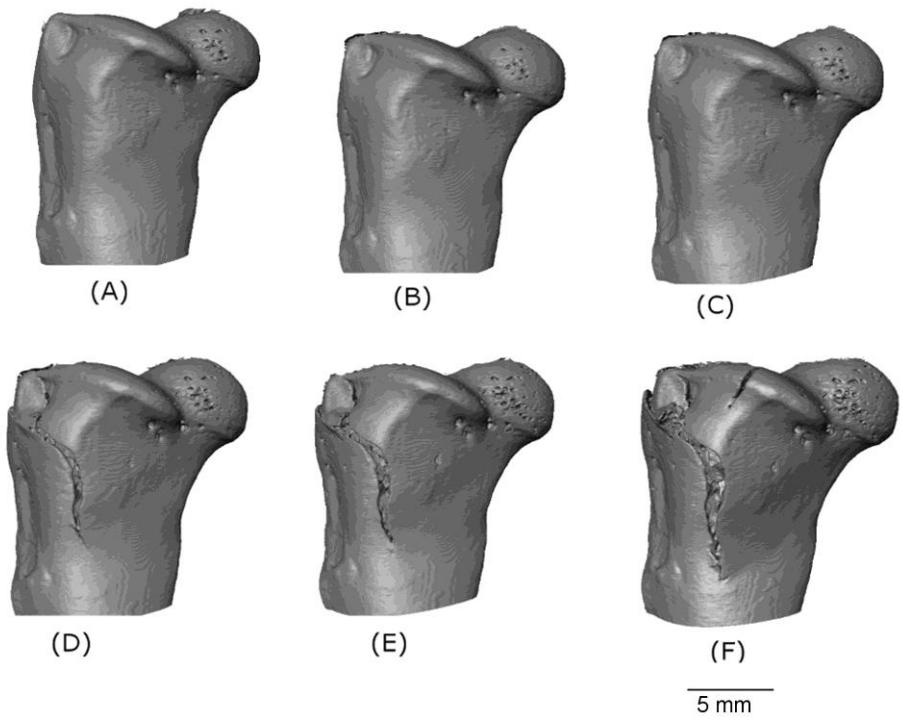

Fig. 5. 3D volume reconstruction of the macro-scale cracking. The evolution of the macro-scale crack on the upper part of the femur is illustrated for scans 0 (A), 4 (B), 6 (C), 7 (D), 8 (E) and 9 (F).

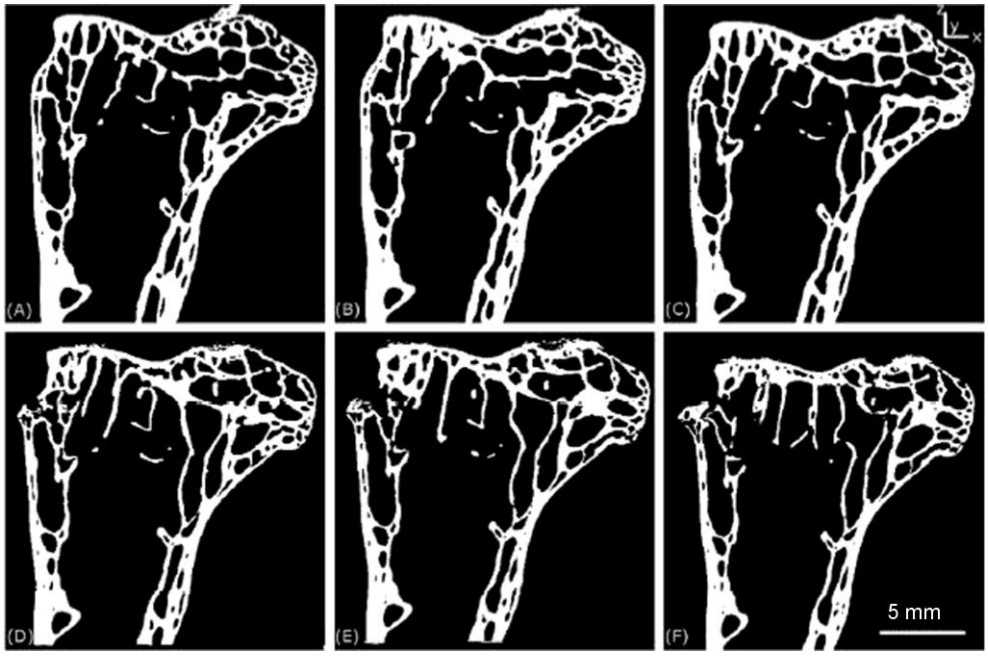

Fig. 6. 2D tomography slices of the macroscopic crack. The evolution of the macroscopic crack on the upper part of the femur is shown for scans 0 (A), 4 (B), 6 (C), 7 (D), 8 (E) and 9 (F).

Meso-scale deformation features

Five distinct types of deformation mechanism in the cancellous bone were identified in the reconstructed tomography data. Each of these appeared at specific points in the loading path. The evolution of these features could be followed to a certain degree at subsequent loading intervals. Both brittle and ductile mechanisms were observed, reflecting the varied influence of bone's complex architecture. The mechanisms observed included (i) cracking (Fig. 7); (ii) thinning (iii) tearing of cell walls and struts (Fig. 8); (iv) notch formation (Fig. 9) and (v) buckling of struts (Fig. 10). The features in Figs 7 to 10 are located in the upper condoyle near the greater trochanter of the femoral head.

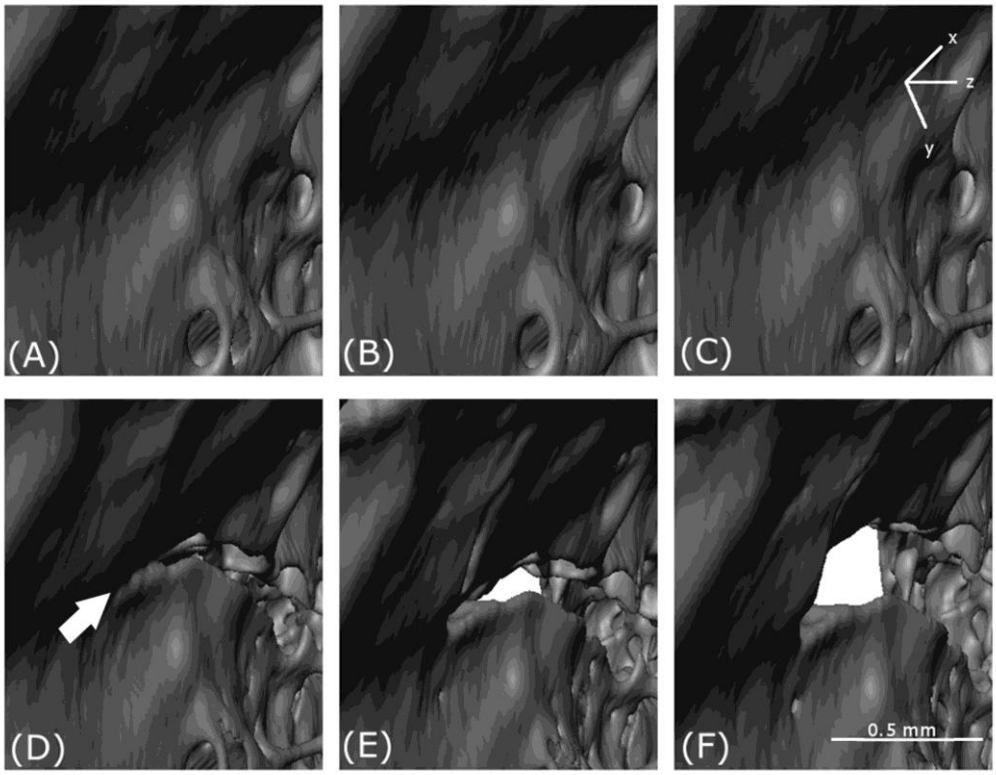

Fig. 7. Localized crack opening and crack extension. (A), (B), (C), (D), (E) and (F) show reconstructed volumes from scan 0, scan 4, scan 6, scan 7, scan 8 and scan 9 respectively.

In Fig. 7, a crack appears at scan 7 (D) and then opens with increasing load through scan 8 (E) and scan 9 (F). However, no obvious crack initiation mechanism is visible

in the preceding scans. Cracking is examined more closely using digital volume correlation later in the paper.

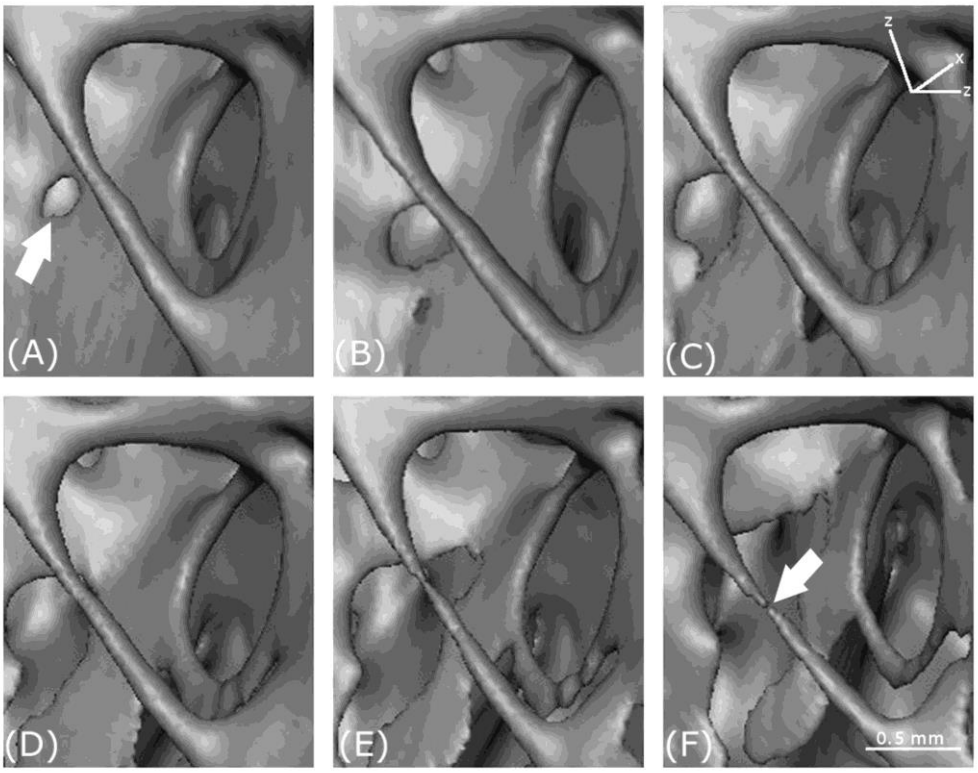

Fig. 8. Thinning and tearing. Thinning and tearing of a cell wall and necking in a strut. (A), (B), (C), (D), (E) and (F) show reconstructed volumes from scan 0, scan 4, scan 6, scan 7, scan 8 and scan 9 respectively.

In the background of Fig. 8, a roughly circular hole in a cell wall in the first scan increases in size with increasing loading. The increase in size is accompanied by cell wall thinning, leading to the creation of a new hole (B) and tearing as the holes coalesce; (C) and (D). In the foreground, a strut thins (D) then necks (E) and eventually breaks (F).

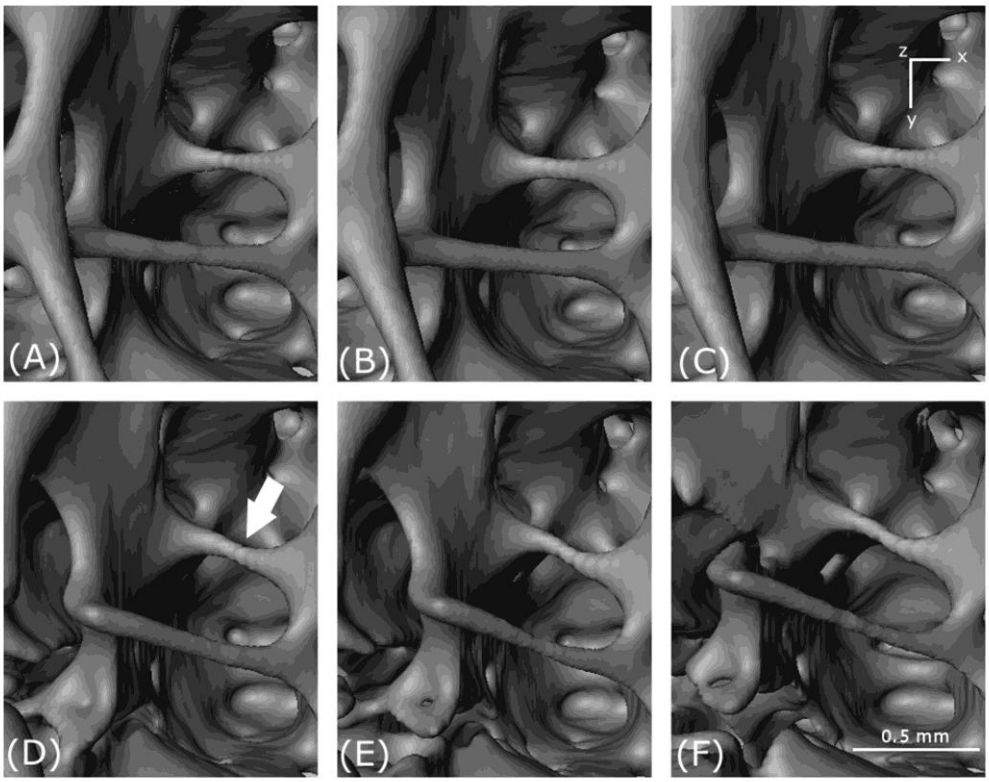

Fig. 9. Notch formation. (A), (B), (C), (D), (E) and (F) show reconstructed volumes from scan 0, scan 4, scan 6, scan 7, scan 8 and scan 9 respectively. The location of the notch is indicated by the arrow in (C).

Fig. 9. shows the appearance and development of a notch in a hole in a cell wall. The hole in the cell wall was approximately circular in shape before loading. The notch is a stress concentrator that could lead to cracking. Here cracking does not occur as other mechanisms such as cell wall thinning and tearing are more dominant. The formation of the notch is probably governed by mechanisms occurring in the crystalline microstructure that exists at a lower length scale.

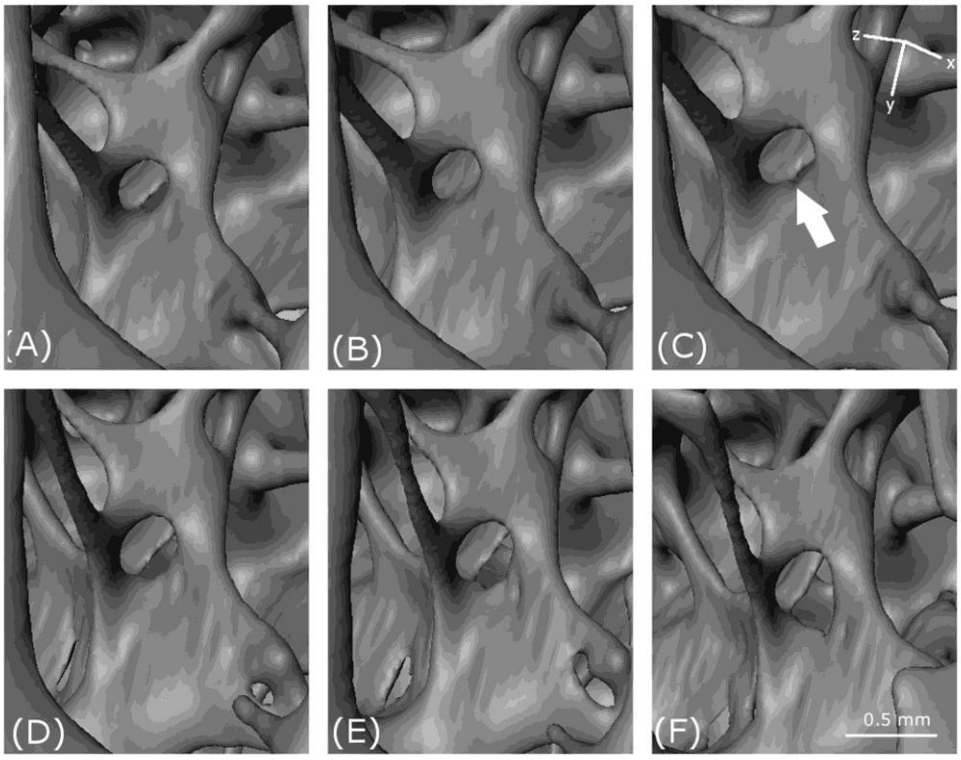

Fig. 10. Buckling of struts. (A), (B), (C), (D), (E) and (F) show reconstructed volumes from scan 0, scan 4, scan 6, scan 7, scan 8 and scan 9 respectively. The strut undergoing buckling is indicated by the arrow in (D).

The last mechanism noted in the meso-scale was the buckling of struts. An example is shown in Fig 10. Buckling is a classic mode of elastic deformation, in which a beam adopts a s-shaped geometry.

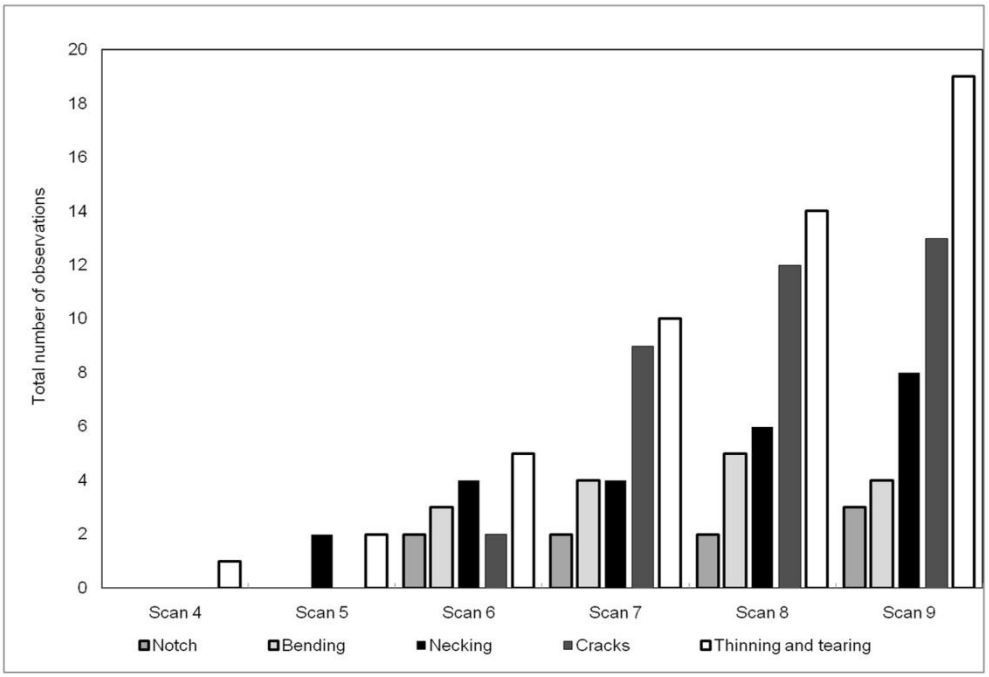

Fig. 11. Histogram showing counts of meso-scale deformation features.

The number of times each of the meso-scale deformation features occurs in each scan is plotted in Fig 11. This gives an indication of the relative dominance of the mechanisms observed in this particular bone for this particular test. The features rank from most to least dominant as follows: (1) thinning and tearing (2) cracking (3) necking (4) notch formation and (5) bending.

Micro-scale deformation

The reconstructed tomography data in the first three scans of Fig. 7 does not indicate that a crack is about to form. However, digital volume correlation applied between subsequent scans can give an indication that something is happening at a lower length-scale. Fig. 12 shows a crack feature that was selected for investigation using digital image correlation.

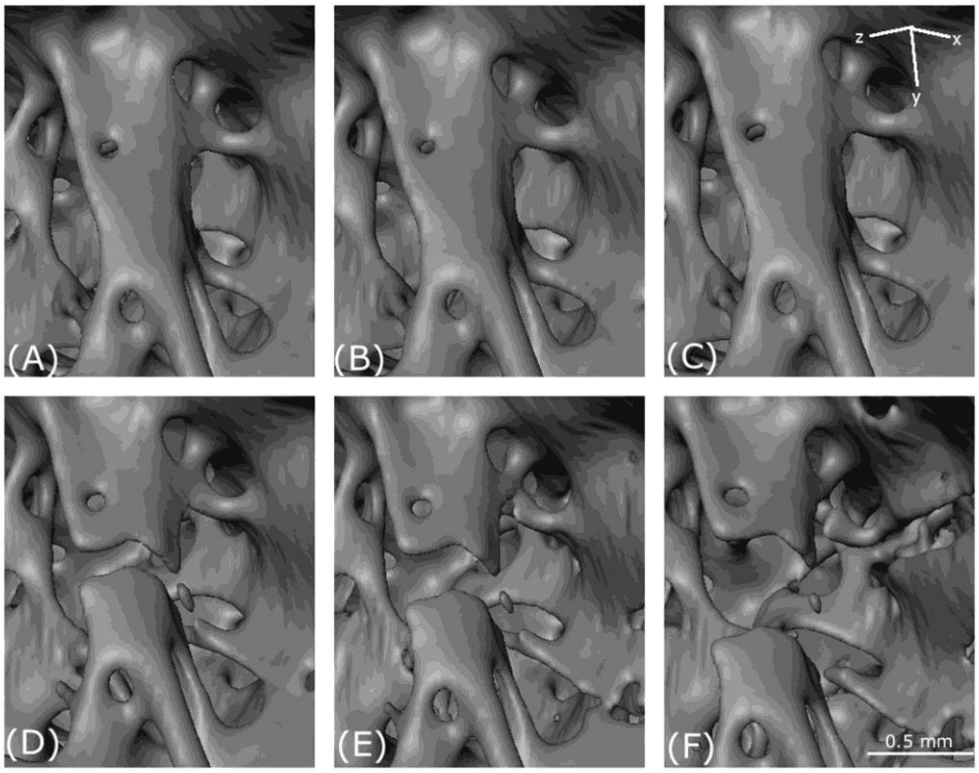

Fig. 12. Crack Propagation. Crack propagation across external surface visible from internal bone structure. (A), (B), (C), (D), (E) and (F) shows incremental load steps from scan 0, scan 4, scan 6, scan 7, scan 8 and scan 9 (detailed data from table 1). This crack was visible from the external morphology of bone with an eye. View in this fig. is taken from the inside of the bone. Progression is more evident from (D) to (F). Scale bar is 1 mm long.

Digital image correlation

The results of the digital image correlation exercise are presented in Fig. 13. Figs 13A, 13B and 13C show contour plots of the strain component in the x-direction for scans 2, 4 and 6 respectively. The reference, undeformed state, is scan 0. Figures 13D, 13E and 13F show strains in the y-direction for the same scans and the corresponding displacement maps are given in Figures 13F, 13G and 13H. The crack feature appears in scan 7 (Fig. 12D) and digital image correlation cannot therefore be used for scans 7 to 10.

The displacement vectors in Fig. 13 show that the bottom half of this section of bone is being displaced to the right as the top half moves upwards. In the strain maps, the

y-component increases up to a value of 6% strain (Fig. 13F) in the region where the crack occurs (Fig 12D).

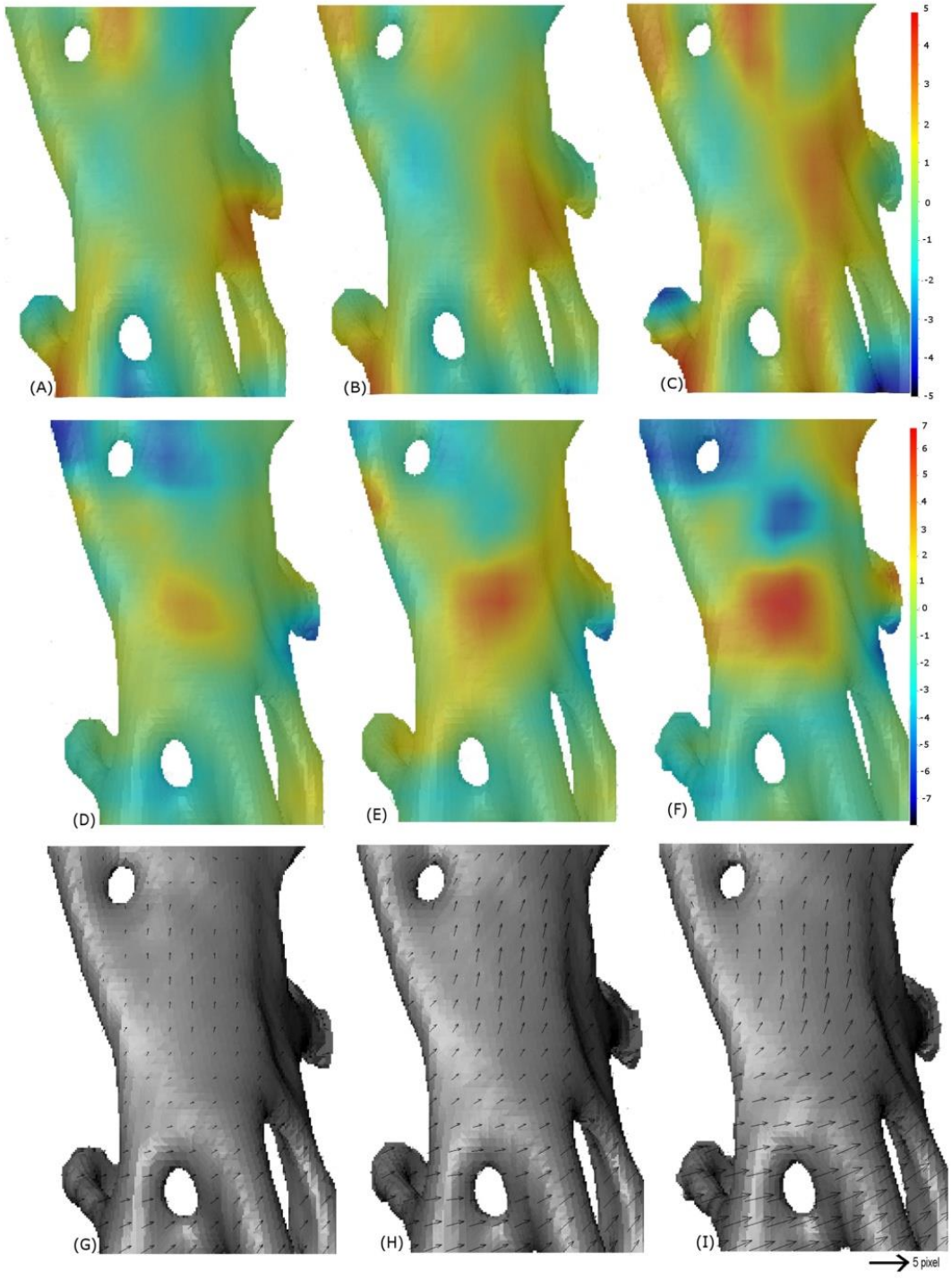

Fig. 13. Digital image correlation. Progression of strain in x direction (A to C), progression of strain in y direction (D to E) and displacement maps (F to I) for scans 2, 4 and 6.

Discussion

In this study, a *Branta leucopsis* femur has been loaded to failure within a specially designed rig mounted in an X-ray computed tomography system. The scans highlighted six distinct types of deformation mechanism in the cancellous part of the bone. These were (i) cracking, (ii) thinning and (iii) tearing of cell walls and struts, (iv) notch formation, (v) necking and (vi) buckling. The results highlight that bone experiences brittle (notch formation and cracking), ductile (thinning, tearing and necking) and elastic (buckling) modes of deformation.

The digital image correlation study shows that the development of these features is quite complex characterized by the irregular development and evolution of localized strain fields. These fields appear not to be linked to features at the resolution of the X-ray computed tomography scan, but instead to mechanisms that develop at a lower length scale.

The relative frequency of the features, as indicated in the histogram of Fig. 11, shows that, for this particular bone, the ductile modes are more dominant than the brittle modes. Strut buckling is not common and probably relies on there being a near perfect axisymmetrical strut that is subject to loading in line with the strut's long axis. Care must be taken in the interpreting the data, however, as large intervals of time 30-45 minutes passed between each individual load increment so that a scan could be carried out. In future tomography simulation, it will be possible to carry out this type of 4D scan in real time. This will help determine whether any of the ductile deformation arose due to relaxation creep in between successive scans.

In conclusion, the results of this study will be of interest to a broad community of researchers who are using computer modelling to predict the load bearing capabilities of bone in various scenarios. Bone's response to loading is complex and occurs due to mechanisms that occur at a lower length scale than the resolution of the X-ray computed tomography data.

Acknowledgements

This work was funded by the Microsoft-BBSRC Dorothy Hodgkin Award FA01546 and the BBSRC grant BB/K006029/1. The X-ray tomography facilities and computer systems used were provided by the Henry Moseley X-ray Imaging Facility at the University of Manchester, UK. The authors would like to thank Louise Lever in IT Services at the University of Manchester who assisted in the visualization aspects of the paper.

Author Contributions

Conception and design of experiments: ZM, LM, TL

Experimentation: ZM, SM, TL

Analysis of results: ZM, LM, SM

Paper written and checked/reviewed by: ZM, LM, PLM, WPJ, WIS, TL and SM

Contributed regents/materials/tools: ZM, LM, PLM, WPJ, WIS and SM

References

1. Wolff JD (1892) Gesetz der Transformation der Knochen. Berlin: Hirschwald.

2. Tomáš M (2006) Geometry and internal structure of thigh bone. Bulletin of Applied Mechanics 7: 141-150.

3. Currey JD, Alexander RM (1985) The thickness of the walls of tubular bones. Journal of Zoology 206: 453-468.

4. Nagarajaa S, Couseb LT, Guldberg ER (2005) Trabecular bone microdamage and microstructural stresses under uniaxial compression. Journal of biomechanics 38: 707–716.

5. Rudman EK, Aspden MR, Meakin RJ (2006) Compression or tension? The stress distribution in the proximal femur. Biomedical engineering online 5: 12.

6. Currey JD (2000) Bones: Structure and Mechanics.: Oxford, Princeton University Press.

7. Weiner S, Wagner HD (1998) The material bone: Structure-mechanical function relations. Annual Reviews Materials Science 28: 271-298.

8. Launey EM, Ritchie OR (May 25, 2009) On the Fracture Toughness of Advanced Materials. Advanced materials 21: 2103–2110.

9. J. Quinta Da Fonseca, P.M. Mummery, Withers. PJ (2005) Full-field strain mapping by optical correlation of micrographs acquired during deformation. J Microsc 218: 9.

10. Bay KB (2008) Methods and applications of digital volume correlation. The Journal of Strain Analysis for Engineering Design 43: 745-760.

11. Bay KB, Smith ST, Fyhrie PD, Saad M (1999) Digital Volume Correlation: Three-dimensional Strain Mapping Using X-ray Tomography. Journal of Experimental mechanics 39: 217-225.

12. Brémand F (June 2-5, 2008) Study of mechanical behavior of cancellous bone by Digital Volume Correlation and X-ray Micro-Computed Tomography. Proceedings of the XIth International Congress and Exposition. Orlando, Florida USA.

13. Roux S (2008) Three-dimensional image correlation from X-Ray computed tomography of solid foam. Composites Part A, 39: 1253.

14. McDonald SA, Dedreuil-Monet G, Yao AA YT, J WP (2011) In Situ 3D X-Ray Microtomography Study Comparing Auxetic and Non-Auxetic Polymeric Foams Under Tension. Phys Stat Sol B 248: 45.

15. McDonald SA, Ravirala N, Withers PJ, Alderson A (2009) In-Situ Three-dimensional X-Ray Microtomography of an Auxetic Foam Under Tension. Scr Mater 60: 232.

16. Verhulp E, Rietbergen BV, Huiskes R (2004) A three-dimensional digital image correlation technique for strain measurements in microstructures. journal of biomechanics 37: 1313–1320.

17. Doube M, Kłosowski M, Michał., Wiktorowicz-Conroy M, Alexis., Hutchinson R, John., Shefelbine J, Sandra. (2011) Trabecular bone scales allometrically in mammals and birds. Proceedings of Royal society.

18. Sawall S, Bergner F, Hess A, Lapp R, Mronz M, et al. Functional phase-correlated micro-CT imaging of small rodents with low dose; 2011. pp. 796124-796124-796127.

19. Liu L, Morgan EF (2007) Accuracy and precision of digital volume correlation in uantifying displacements and strains in traecular bone. Journal of biomechanics 40: 3516–3520.

20. Libertiaux V, Pascon F, Cescotto S (2011) Experimental verification of brain tissue incompressibility using digital image correlation. Journal of mechanical behaviour of biomedical materials 4: 1177 – 1185.

21. Pan B, Wu D, Wang Z (2012) Internal displacement and strain measurement using digital volume correlation: a least-squares framework Measurement science and technology 23: 13pp.

22. Cauble R (2010) The Bone Room; Available at: http://www.boneroom.com/faqs/bones.html. Berkeley, CA.

23. Nawrocki S (1997) Cleaning Bones. . University of Indianapolis Archeology & Forensics Laboratory.

24. Onwuama K, Tobechukwu, Sulaiman SO, Ali M, Nzalak (2012) Effect of Different Methods of Bone Preparation on the Skeleton of the African Giant Pouched Rat (Cricetomys gambianus). International journal of morphology 30425-427.

25. Grygon (2010) Tutorial cleaning of Bones PART 1. [Online]. pp. Available:http://fav.me/d2lxlel [Accessed.

26. Boyle C (2010) Maceration and preparation of mamma skeletons for long term curation.

27. https://www.safety.ncl.ac.uk/.

28. www.fei.com/software/avizo3d/.

29. Quinta Da Fonseca J, Mummery MP, Withers JP (2005) Full-field strain mapping by optical correlation of micrographs acquired during deformation. Journal of Microscopy 218: 9-21.

30. imagej.nih.gov/ij/.

31. Ritchie OR (1988) Mechanisms of fatigue crack-propagation in metals, ceramics and composites: role of crack tip shielding. . Mater Sci Eng A 103: 15–28.

4 A study of the effect of model resolution on elastic finite element analyses of an axially loaded *Branta leucopsis* femur

Mustansar Z[1], Sellers W.I.[2], Withers P.W.[3], Shaukat., A[4] Lowe T[3], Manning P. L[1], and Margetts L.[1,5,6,7]

---

[1] Interdisciplinary Centre for Ancient Life, University of Manchester, UK

[2] Faculty of Life Sciences, University of Manchester, UK.

[3] School of Materials, University of Manchester, UK.

[4]College of Electrical and Mechanical Engineering, NUST Pakistan.

[5]Research Computing, University of Manchester, UK.

[6] Oxford eResearch Centre, University of Oxford, UK.

[7]School of Mechanical, Aerospace and Civil Engineering, University of Manchester, UK.

A paper submitted in Journal of Royal society Interface.

A study of the effect of model resolution on elastic finite element analyses of an axially loaded *Branta leucopsis* femur

Mustansar Z.[1], Sellers W.I.1,[2] Shaukat. A[3],

Manning P. L.[1], Lever L.M.[4] and Margetts L.[1,5,6]

1 Interdisciplinary Centre for Ancient Life, University of Manchester, Williamson Building, Oxford Road, Manchester, M13 9PL, UK.

2 Faculty of Life Sciences, University of Manchester, Michael Smith Building, Dover Street, Manchester, M13 9PL, UK.

3 College of Electrical and Mechanical Engineering, National University of Sciences and Technology (NUST), H-12, Islamabad, Pakistan.

4 Research Computing, University of Manchester, Devonshire House, Oxford Road, Manchester, M13 9PL, UK.

5 Oxford eResearch Centre, University of Oxford, 7 Keble Road, Oxford, UK.

6 School of Mechanical, Aerospace and Civil Engineering, University of Manchester, Manchester, M13 9PL, UK.

Corresponding author: lee.margetts@manchester.ac.uk

ABSTRACT

The purpose of this paper is to evaluate whether elastic finite element analyses can be used as a quick indicator as to whether a vertebrate long bone would break under an axial load. The study uses X-ray computed tomography to capture the external geometry and internal microstructure of a *Branta leucopsis* femur. Finite element analyses were carried out for three levels of detail assuming: (i) the femur is a solid bone; (ii) the femur is made of cortical bone only that is hollow in the shaft, but solid at both ends and (iii) the same as (ii) but with separate material properties for regions with cortical and cancellous bone. Sensitivity to mesh resolution was also studied. The results showed that all the analyses significantly overestimate the load bearing capacity of the femur. The authors conclude that simple elastic finite element analyses may not be suitable for obtaining reasonable estimates of stress-strain response in vertebrate long bones.

Key words: Finite element analysis; *Branta leucopsis*; bone microstructure; simulation; computed tomography; validation

1. INTRODUCTION

The principal motivation for this work is the study of locomotion in extant and extinct vertebrates. We have been using computer simulation to investigate and characterize gaits in hominids [1], chimpanzees [2] and dinosaurs [3] using genetic algorithms that use various input parameters such as body mass and joint kinematics. The modelling techniques use solid body mechanics together with genetic algorithms on distributed computer systems to predict possible gaits in a field called evolutionary robotics. When applied to extant vertebrates, the output of the simulations can be verified by comparison with the results of observational methods. In contrast, studies of extinct vertebrates rely on comparing the results with what we might expect from theory or the closest living relatives.

A recent simulation of a duck billed dinosaur (hadrosaur) produced three distinct types of gait: Galloping, skipping and hopping [4]. Putting aside debates between palaeontologists as to whether hadrosaurs were bipedal or quadrupedal, we

wondered how realistic the skipping and hopping gaits might be. Was there something fundamental in the evolutionary robotics simulation that could permit unrealistic gaits to emerge as possible solutions to the analyses? Perhaps skeletal loading is an important, but overlooked, factor. If the genetic algorithm could reject gaits that damaged the owner's skeleton, would these skipping and hopping gaits still emerge? Answering this question requires modifying the genetic algorithm so that it can detect whether the skeletal loading is too high. The simplest approach is to implement a binary "yes" or "no" decision as to whether a bone would break. If the bone breaks, that particular gait could be rejected as a possible solution.

The genetic algorithm operates on populations of individuals which evolve as the simulation progresses forwards in time. In computing terms, each individual is evaluated using a single CPU (core in a multi-core processor) in less than 1 second. We use highly parallel multi-processor systems for our work as the total run time for a simulation becomes very large considering a population of individuals evolving over generations. Therefore, if we wish to evaluate whether bones will break, then we need to do this in as short a time as possible. For example, adding another 1 second of computation for each individual may double the run time of the analysis.

Simple beam theory has been considered for carrying out a quick structural analysis and failure assessment [5], but bones are more complex than beams in terms of external morphology, internal structure and material stress-strain response. We are therefore looking at carrying out structural computations using open source libraries for finite element analysis [6], embedded in the evolutionary robotics software. Considering the target run times, the finite element analysis needs to be quick. It also needs to share the memory of one cpu with the gait simulation. We know that bone is a complex biocomposite [7-11] with a nonlinear material response to load [12]. However nonlinear finite element analysis is very time consuming. Solution times increase (roughly) proportionally to the cube of problem size. So for our quick evaluation of whether skeletal loading is too high, ideally we need to use a small model that has some approximate (for example, linear) material behaviour.

In the literature, bone has been modelled, using the finite element method, in many different ways. Whole bones have been modelled as linear elastic solids, with neither an internal cavity nor the fine structure of trabeculae, even if present in the real

specimen [13-15]. Small samples of bone have been imaged using X-ray tomography, to generate high resolution meshes of the microstructure [16-17] and investigate how microstructure governs mechanical properties at the macroscale [18-20]. Here, we report the evaluation of a methodology that lies between these two extremes.

2. OBJECTIVES

The main objective of this paper is to investigate whether a linear elastic analysis is good enough to predict failure, as required in our gait simulations. We also investigate whether different levels of geometric complexity and mesh resolution improve the predictions made when assuming bone behaves as a linear elastic material. We report on our success in building a finite element model of a complete vertebrate long bone that includes all the internal microstructure. We believe that this is the first time that this has been achieved, but we have not been able to run a full analysis.

3. MATERIALS AND METHODS

This section describes the rationale behind the selection of the specimen. It then details the procedures followed in preparing the specimen, scanning the specimen, processing the images and the generation of the finite element models.

3.1. Selection of the specimen

The study required selecting a long bone that could be scanned at a high enough resolution to capture the internal micro-structural features present in the trabecular bone. As it was not possible to know a-priori what bone would be suitable, a selection of femora from different species was chosen for scanning. These bones were selected on the basis of length, so that they could be mounted in the scanning

facility. A *Barnacle goose* femur (accession number SF230) gave the best quality scan with individual trabeculae clearly defined and was selected for the study.

3.2. **Specimen preparation**

The *Branta leucopsis* specimen was a wild bird that died naturally and had no apparent injuries. All soft tissues were carefully removed using standard laboratory procedures such that the distal and proximal epiphyses remained intact. The femur was 59mm long and the intact adult weighed 2.034kg. All bones (including those in the previous section) were cleaned according to the methodology used in [21] and [22]. They were first treated with 75% saline solution and then subjected to 'supervised boiling' in tap water with a small amount of detergent for 6 hours. Boiling was divided into two sessions, with the water being changed after 3 hours. The bones were air dried until the weight of the bone stayed constant for a few days. Preparation of the specimen was carried out in compliance with the BIOCOSSH procedures set out by the Medical School at the University of Manchester, UK [23].

3.3**. Image Acquisition**

The X-ray micro-computed tomography scan of the *Branta leucopsis* femur was acquired using a Nikon Custom Bay 320kV micro CT scanner at the School of Materials, University of Manchester, UK. A resolution of 31 microns was achieved using scanner settings of 59kV and 195microAmperes. The distance between source and sample was 234 mm. The scan was carried out with the bone mounted diagonally within the detector window in order to increase the acquired resolution. The tomography dataset was reconstructed using VG Studio MAX 3.0 [24]. Example 2D slices and reconstructed 3D volumes are shown in Figure 1.

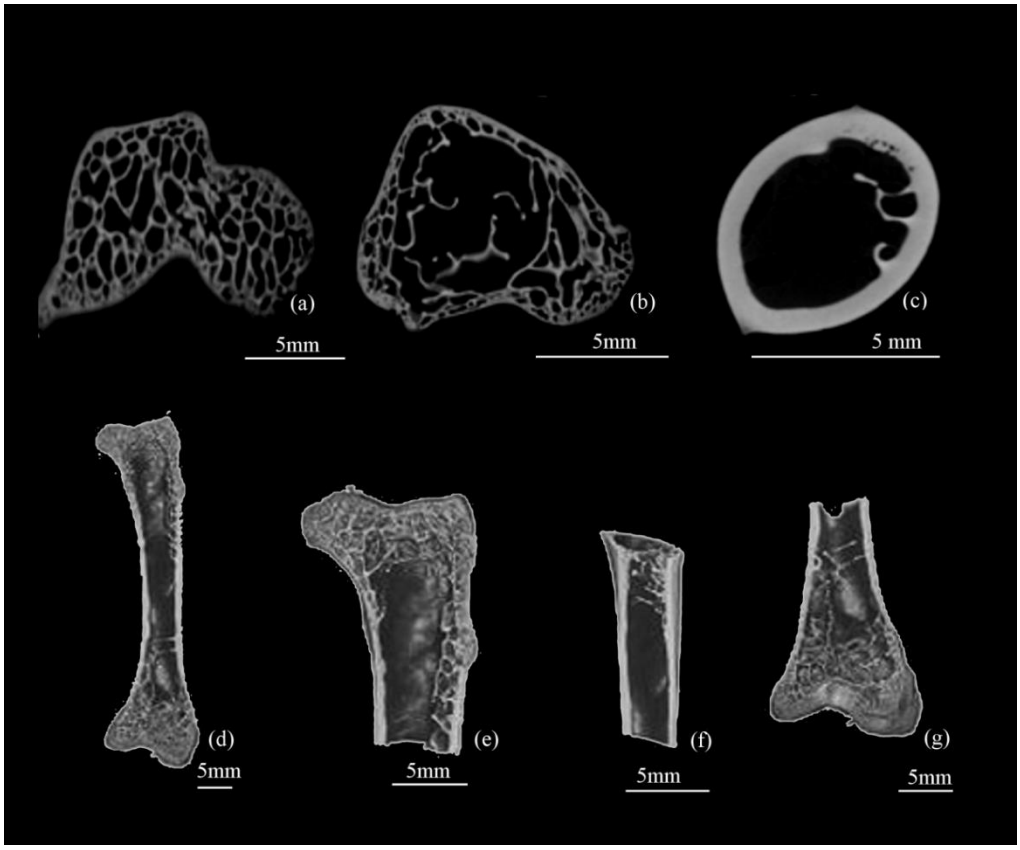

Figure 1. 2D slices and 3D volumes from the *Branta leucopsis* femur. 2D sections through (a) the lower condyle; (b) the upper condyle and (c) the shaft. 3D volumes showing (d) vertical cross-section through whole bone; (e) the upper epiphyseal region to the start of the diaphysis: (f) the shaft and (g) the lower epiphyseal region.

3.4. Finite element meshes

The femur was segmented using the software ScanIP from Simpleware Ltd [25] into the three separate phases representing the (i) cortical bone, (ii) trabecular bone and (iii) medullary cavity. Using the same software, a "morphological" filter was used to smooth out some of the geometric features in the dataset. Next a combination of "cavity fill", "flood fill", "close" and "dilate and erode" filters were used to ensure that there were no islands of unconnected material. A finite element model should be a single domain and the presence of islands may be problematic in some finite element software.

Finite element models were created from the image data for four different levels of detail (Figure 2). Level 1 (Figure 2a) treated the bone as a single phase solid that was given the elastic properties of cortical bone. Likewise, level 2 (Figure 2b) assumed that the bone was a single phase, but with a hollow cavity. In level 3 (Figure 2d), the trabecular bone was modelled as a solid phase (not spongy) which had a reduced stiffness compared with the cortical bone. Levels 1 to 3 considered the trabecular bone as a continuous solid and therefore the image data could be downsampled to reduce the size of the finite element model. In contrast, the trabecular bone in level 4 (Figure 2e) was meshed as an interconnecting network of pores at the full resolution of the scan. Five finite element meshes, ranging from coarse to fine, were created for each of the levels 1 to 3 (Figure 3) in order to test mesh sensitivity. The number of elements in each mesh is given in Table. 1 for levels 1 to 3. Only one mesh was created for level 4 (Figure 4). This mesh comprises 120 million finite elements and captures all the full detail of the trabeculae. The cortical and cancellous bone were meshed as separate parts, so each could be given different material properties.

3.5. **Boundary conditions**

Each finite element model was subject to the same boundary conditions. A region on the base of the femur (the lower condoyle) was fixed in the x, y and z directions. An axial, compressive load was applied to the bone in a direction aligned with the long axis of the bone. The load was distributed across a region of nodes on the top of the bone through a virtual stiff platen. This platen was constrained to move only in the z-direction, thus eliminating any off axis motion in the same way as the test might have been carried out experimentally, using an Instron rig.

Figure 2 Two dimensional slices through the segmented image showing masks for (a) level 1 - a solid bone with one type of material; (b) level 2 - a solid bone with one type of material and a hollow cavity; (c) level 3 – a two phase bone with solid cancellous bone, solid cortical bone and a hollow cavity (shown in yellow); (d) level 3 – with the mask for the hollow cavity removed using a Boolean operation and (e) level 4 – with a full resolution mask for the cancellous bone including all the internal micro-structure.

Level 1	Number of elements	Level 2	Number of elements	Level 3	Number of elements
Model 1	2,989	**Model 1**	4563	**Model 1**	8,180
Model 2	4,687	**Model 2**	10,382	**Model 2**	23,508
Model 3	21,495	**Model 3**	23,998	**Model 3**	394,546
Model 4	145,242	**Model 4**	187,676	**Model 4**	1,431,561
Model 5	492,029	**Model 5**	488,214	**Model 5**	2,161,525

Table 1. Number of elements in each model for levels 1 to 3

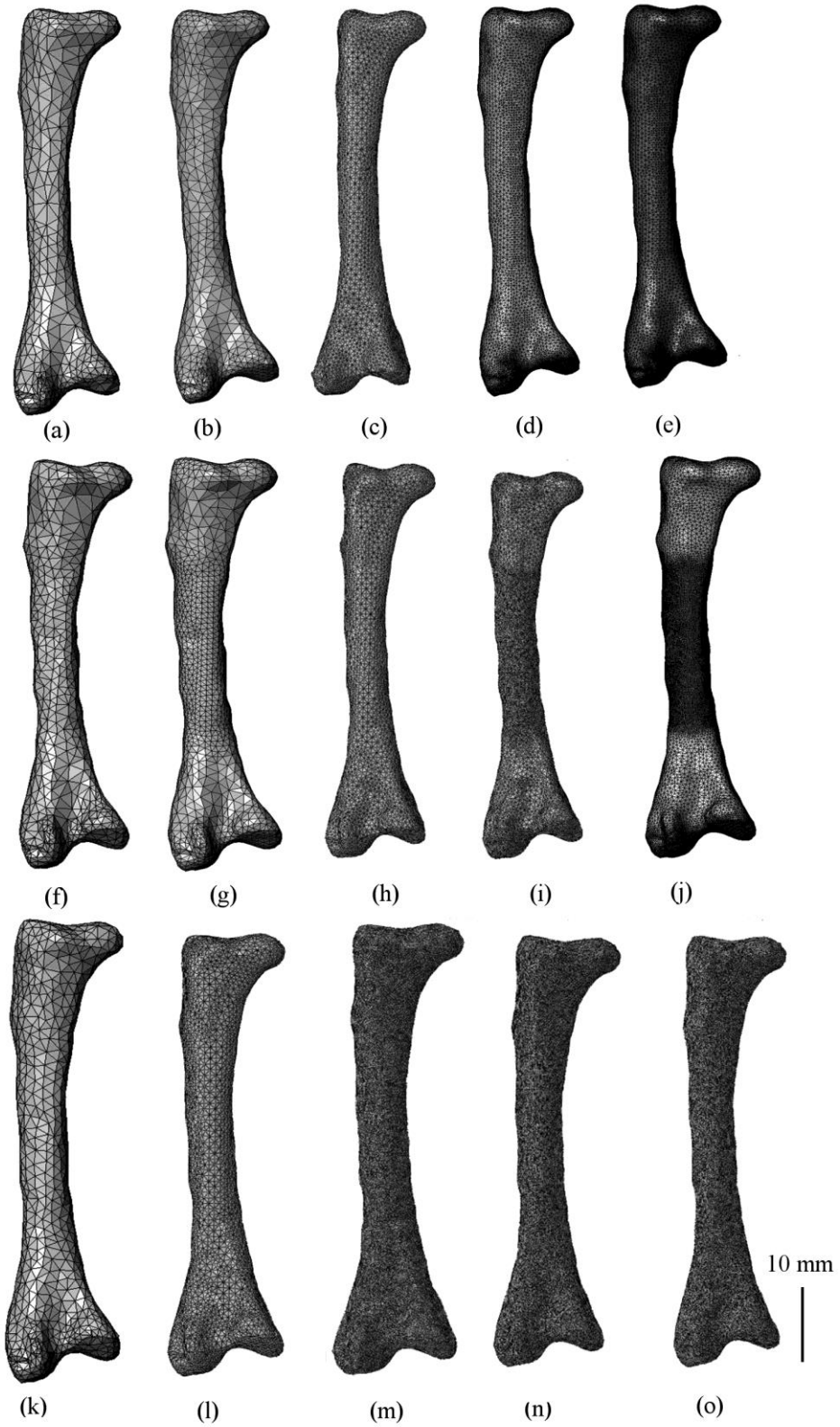

Figure 3. Finite element meshes for levels 1 to 3: (a-e) Level 1, models 1 to 5; (f-j) level 2, models 1 to 5 and (k-o) level 3, models 1 to 5.

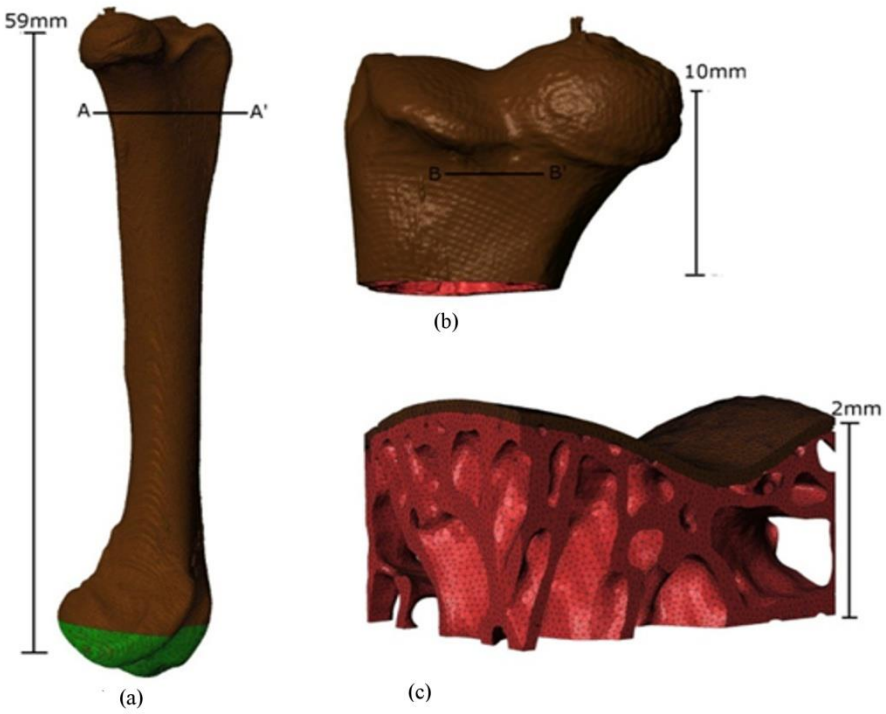

Figure 4. Mesh showing a model of an optimized mesh from level4 in a 2mm section from 59mm long *Branta leucopsis* femur. AA' indicates the boundary line where 10mm section was chopped for further analysis of refinement, BB' indicates the region where 2mm section was chopped out to work of if further refinement was required or not. This figure aims to show a full resolution mesh across the single strut of trabeculae in 2mm section.

The regions for application of the boundary conditions were selected at the image-processing stage, resulting in the definition of additional masks (to those used for meshing) in the Simpleware software. After mesh generation, these masks were then used to identify all the nodes in the region to be fixed and the region to be loaded. The Simpleware software outputs lists of nodes which can then be read into a finite element package as node sets, allowing the user to configure the boundary conditions as required. This procedure was important to ensure, as far as practically possible, that each finite element mesh was subject to essentially the same boundary conditions, thus enabling us to have confidence that any differences in results were due to the level of detail and mesh refinement.

The load applied to the femur was 540N. This figure is our estimated maximum failure load for an adult goose, as our aim is to investigate if any of the simple models predict failure. The safety factor for long bones is reported to be between 2 and 6 by Alexander [26] and 2 by Biewener [27]. The mass of an adult goose can reach 9 kilograms [28]. Multiplying the highest safety factor (6) by the highest mass (9) by gravity gives us the load of 540N.

3.6. **Material properties**

The analyses assume elastic behaviour, which requires input values for the Young's modulus and Poisson's ratio in the finite element method. Values for Young's modulus for both the cortical bone (24 GPa) and individual trabeculae in the cancellous bone (15 GPa) were determined by the authors for this particular specimen using the nano-indentation technique [29]. Level 1 is assumed to be a solid bone with the properties of cortical bone. Level 2 is hollow, again with the properties of cortical bone. The Young's modulus used in levels 1 and 2 was 24 GPa. The rule of mixtures was used to estimate the bulk Young's modulus of cancellous bone for the level 3 models. The equation used was:

$$Escb = EsVs + E\upsilon V\upsilon$$

Where Escb = the effective stiffness of homogenized cancellous bone; Es = measured stiffness of the trabeculae; Vs = the volume fraction of the cancellous bone; Eυ= elastic modulus of the voids (assumed zero) and Vυ= the volume fraction of the voids. The volume fraction of cancellous bone without air was calculated to be 0.53 using the Simpleware software. Using the rule of mixtures formula, the effective elastic modulus of the cancellous bone was estimated to be 7.89 GPa.

3.7**. Analytical solution**

In order to gain some measure of confidence regarding the finite element analyses, the results were compared with an analytical solution for an idealised problem: an axial load applied to a right cylinder. The equation for change in length in a right cylinder due to the application of an axially applied load is given by:

$$dl = \sigma l_0 / E$$

Where dl is the change in the length of the bone, σ is the stress, l_0 is the original length of the bone and is the Young's modulus [30]. A hollow cylinder has a smaller cross-sectional area than a solid cylinder and therefore the change in length of the former will be greater than that of the latter. If the finite element analyses are reliable, the finite element predictions for the change in length of the bone should be of a similar order of magnitude, and may lie between these two extremes. Here, the following values were used: The wall thickness is 3mm; the mean diameter of the shaft is 11.7mm; the original length of the bone is 59mm and the Young's modulus is 24.4GPa.

4. RESULTS

4.1. Software

The analyses for levels 1 to 3 were run successfully using Abaqus [31] on a high memory workstation, with 64GB RAM. The model for level 4, which included all the internal microstructure could not be run on the same system.

4.2. Displacements

Figure 5 shows plots of displacement in the z-direction, in line with the applied load, for each of the fifteen finite element meshes used for the study. The range of values used for the contour intervals is exactly the same in each of the images (a) to (o) to facilitate easy visual comparison. The contour interval at the top of the bone for level 1 ranges from 0.039mm to 0.043mm (Figures 5a, b and c). The range is 0.043mm to 0.088 in the same location for levels 2 and 3. These values are essentially the change in length of the bone. The analytical problem estimated the change in length to be 0.03 for a solid cylinder and 0.045 for a hollow one, confirming that the results of the analyses are reasonable.

4.3. Mises stress

Plots of mises stress are shown in Figures 6 and 7. As with the displacements, the range of values used for the contour intervals is exactly the same in each of the images (a) to (o). Scanning each plot from (a) to (o) in Figure 6, there is a clear

pattern of increasing stress value as the mesh size increases (a) to (e) and as the model includes more complexity from level 1 to level 3. The maximum value of mises stress in Figure 6 (a) to (n) is in the range 50 to 60 MPa (colour red). Only the highest resolution model in level 3 exceeds this value, with stress in the range 60 to 236 MPa (colour grey). Figure 7 gives some examples of how the stress varies in a cross-section through the bone. Figure 8 shows histograms of mises stress to highlight how the distribution of stress (calculated at the centre of each element) varies with level of detail and model resolution.

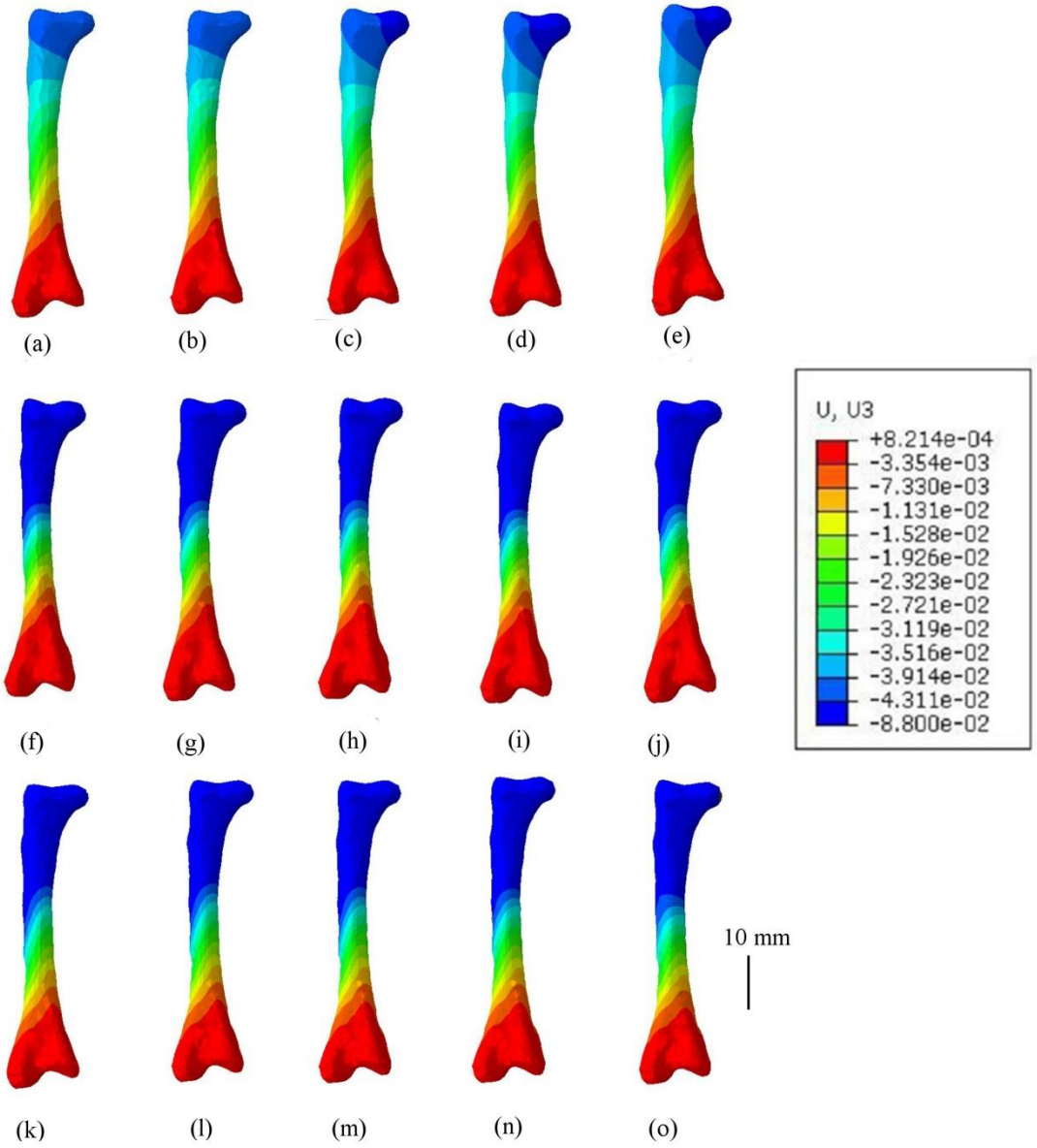

Figure 5: Plots of z-displacement. Level 1 - models 1-5 are shown as (a) to (e) respectively; Level 2 - models 1 to 5 are shown as (f) to (j) respectively; Level 3 – models 1 to 5 are shown as (k) to (o) respectively.

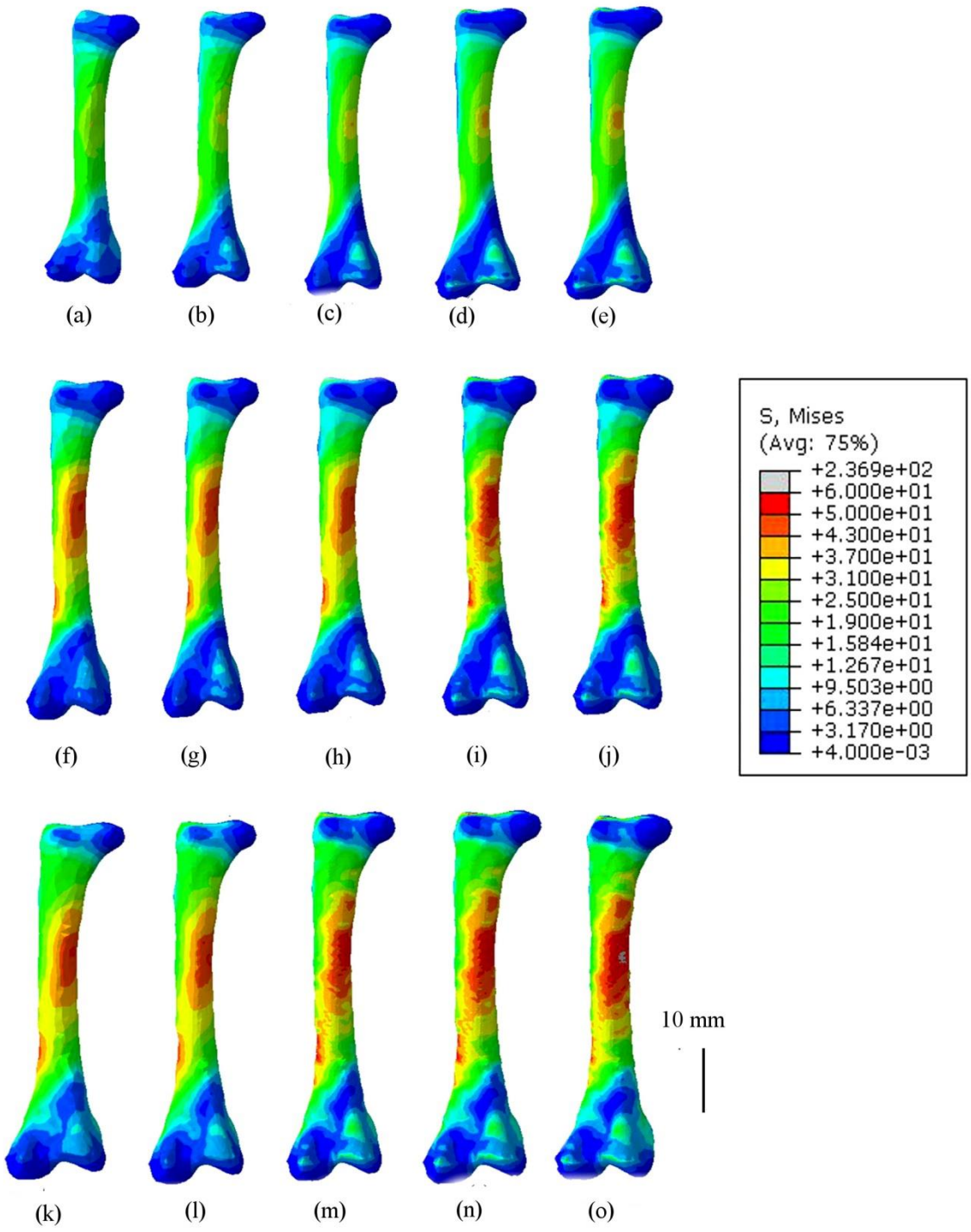

Figure 6. Plots of z-displacement. Level 1 - models 1-5 are shown as (a) to (e) respectively; Level 2 - models 1 to 5 are shown as (f) to (j) respectively; Level 3 – models 1 to 5 are shown as (k) to (o) respectively.

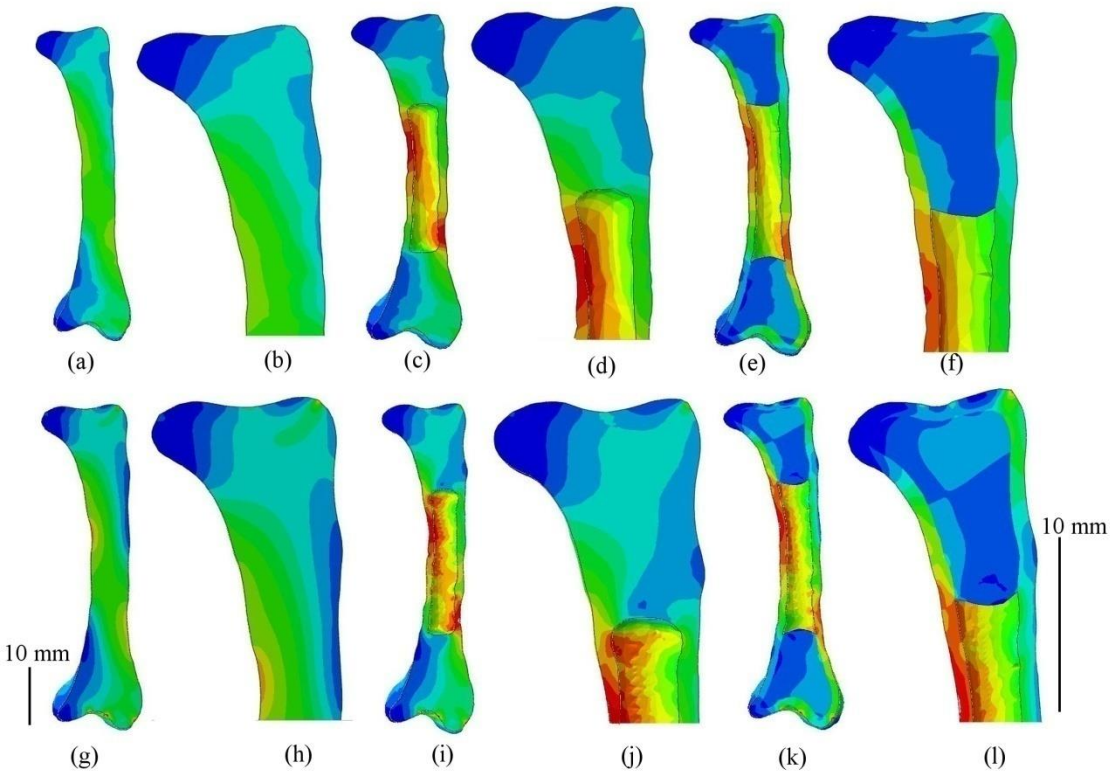

Figure 7. Mises stress in cross-section. The key for the contour intervals is shown in Figure 6. (a) level 1 model 1; (b) level 2 model 1; (c) level3 model 1; (d) level 1 model 5; (e) level 2 model 5; (f) level 3 model 5.

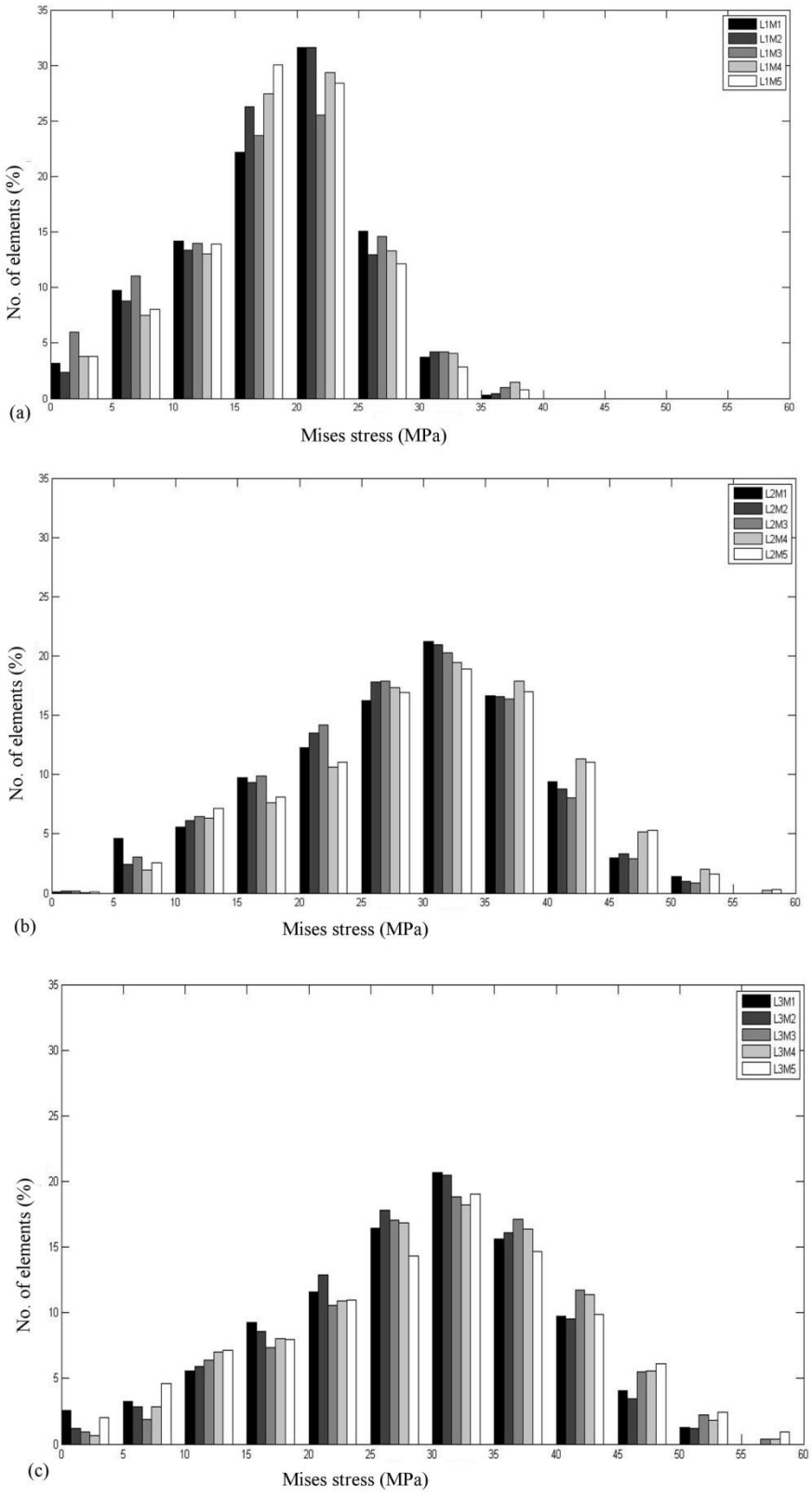

Figure 8. (a) Distribution of Mises stress (MPa) in models 1-5 in level 1 (b) model 1-5 level 2 (c) model 1-5 level 3.

4. **DISCUSSION**

The assumption of a completely solid bone (Figure 6a to 6e), which has been used in studies where a particular bone has been compared across a number of species [15], is clearly demonstrated to give both different values and different stress distributions to slightly more complicated analyses with hollow bone (Figure 6f to 6o). The maximum value for von Mises stress is only around 25% of the value obtained for the hollow bones. Increases in mesh density do not bring the values obtained with solid bone models closer to those obtained with hollow bone models, as is to be expected.

The highest stress values, which are in the range 60MPa to 236MPa according to the contour interval, occur in models 4 and 5 for level 2 (high resolution, single material, hollow bone) and models 3, 4 and 5 for level 3 (high resolution, separate values for cancellous and cortical material, hollow bone). The location of the highest stress values is in the shaft, just below the upper condyle, indicating a reasonable location where the bone may fail. The histogram in figure 8 shows that the range of von Mises stress values is similar for both sets of hollow bone models, but is very different for the solid bone. It also highlights a degree of mesh sensitivity as the histogram shifts to the right for the meshes with higher element counts.

Figure 6 shows very clearly that von Mises stress increases with increasing model complexity and increasing mesh resolution. The most complex model (level 3) with the highest resolution mesh predicts the highest values of stress. That said, there is an issue with the results of the analyses. Even assuming the highest value for a reasonable safety factor and the highest value for a reasonable load, the model with the highest stresses does not predict a stress high enough to reach the published failure stress of 180-200MPa [32-34]. We would need to increase the factor of safety to 18. This does not seem realistic.

It is possible that the published failure stress is too high. It is also possible that the meshed thickness of the shaft wall is too thick, although quick hand calculations with the analytical expression show that the shaft would need to be very thin indeed to achieve stresses of 180-200MPa. This could be confirmed by carrying out a sensitivity analysis, changing parameters in the image segmentation and meshing.

The most likely reason that the predicted stresses are too low is that the isotropic elastic material model is too simple to predict realistic stress values in bone. It ignores the complex structure of bone and how bone really behaves under loading.

We believe our work is along the right lines and that the level 3 model, with elasto-plastic material behaviour, may give reasonable predictions of the response to loading. The distribution of stress in the bone is very different for each of the levels of detail studied. This is highlighted in the cross-section of Figure 7. Contrast the von Mises stress plot for a coarse model of solid femur (Figure 7a and 7d) with a fine model for a hollow femur that has different elastic properties for the cortical and homogenized cancellous bone (Figure 7c and 7f).

5. **CONCLUSIONS**

Our study shows that elastic finite element analyses may greatly underestimate expected maximum stress values in an axially loaded goose femur, even when incorporating (i) a certain degree of complexity in the geometry and assuming (ii) generous values for animal weight, (iii) safety factors and (iv) material properties.

The findings highlight that a working estimate of stress-strain response, needed for a quick yes or no decision in a computer program, probably requires undertaking finite element analyses that incorporate more realistic stress-strain responses described by anisotropic material models.

Our need is to evaluate, in less than 1 second, whether a bone would break in a certain loading regime. To do this, the authors would probably need to parameterize a more complicated analysis using emerging numerical techniques such as model order reduction.

Acknowledgements

Zartasha Mustansar was funded by a Microsoft-BBSRC Dorothy Hodgkins Postgraduate Award FA01546. Lee Margetts and William Sellers were funded by

BBSRC grant BB/K006029/1. The X-ray tomography facilities and computer systems used were provided by the Henry Moseley X-ray Imaging Facility at the University of Manchester, UK. The Henry Moseley X-ray Imaging Facilities have been made available through the following EPSRC grants: EP/F007906, EP/F028431, EP/I02249X/1, EP/K004530/1 and EP/M010619/1.

References

[1] Sellers, W.I., Cain, G.M., Wang, W. & Crompton, R.H. 2005 Stride lengths, speed and energy costs in walking of Australopithecus afarensis: using evolutionary robotics to predict locomotion of early human ancestors. . Journal of the Royal Society, Interface 2, 431-441.

[2] Sellers, W., Margetts, L., Bates, K. & Chamberlain, A. 2013 Exploring Diagonal Gait Using a Forward Dynamic Three-Dimensional Chimpanzee Simulation. Folia Primatol 84, 180-200.

[3] Sellers, W.I., Margetts, L., Coria, R.A. & Manning, P.L. 2013 March of the Titans: The Locomotor Capabilities of Sauropod Dinosaurs. Plos One 8, e78733. (doi:10.1371/journal.pone.0078733).

[4] Sellers, W.I., Manning, P.L., Lyson, T., Stevens, K. & Margetts, L. 2009 Vrtual palaeontology: Gait constructuction of extinct vertebrate using high performance computing. Palaeontologea electronica 12.

[5] Brassey, C.A., Margetts, L., Kitchener, A.C., Withers, P.J., Manning, P.L. & Sellers, W.I. 2013 Finite element modelling versus classic beam theory: comparing methods for stress estimation in a morphologically diverse sample of vertebrate long bones. Journal of The Royal Society Interface 10.

[6] Smith, I.M., Griffiths, D.V. & Margetts, L. 2013 Programming the Finite Element Method, 5th Edition .

[7] Natali, A.N., Carniel, E.L., Pavan, P.G. 2008 Constitutive modelling of inelastic behaviour of cortical bone. Medical Engineering & Phy.

[8] Christen, P., Ito, K., Ellouz, R., Boutroy, S., Sornay-Rendu, E., Chapurlat, R.D. & van Rietbergen, B. 2014 Bone remodelling in humans is load-driven but not lazy. Nat Commun 5. (doi:10.1038/ncomms5855).

[9] Currey, D.J. 1962 Stress concentrations in bone. Journal of microscopical Science 103, 111-133.

[10] Currey, J.D. 2002 Bones: Structure and Mechanics. Oxford, Princeton University Press.

[11] Currey, J.D. 2003 How Well Are Bones Designed to Resist Fracture? J Bone Miner Res 18, 591–598.

[12] Mellon, S.J. & Tanner, K.E. 2012 Bone and its adaptation to mechanical loading: a review. International Materials Reviews 57, 235-255.

[13] Rayfield, E.J. 2005 Using finite-element analysis to investigate suture morphology: A case study using large carnivorous dinosaurs. Anatomical Record Part a-Discoveries in Molecular Cellular and Evolutionary Biology 283A, 349-365.

[14] Rayfield, E.J. 2007 Finite Element Analysis and Understanding the Biomechanics and Evolution of Living and Fossil Organisms. Annual Review of Earth and Planetary Sciences 35, 541–576.

[15] Panagiotopoulou, O., Wilshin, S.D., Rayfield, E.J., Shefelbine, S.J. & Hutchinson, J.R. 2011 What makes an accurate and reliable subject-specific finite element model? A case study of an elephant femur. Journal of Royal Society interface. 9, 351–361.

[16] Ebinger, T., Steeb, H., Diebels, S., Ripplinger, W. & Tjardesy, T. 2005 A biomechanical model based on a FE2 approach using data from computer tomography. In VIII International Conference on Computational Plasticity (ed. C. VIII).

[17] Woo, D.G., Lee, T.W., Ko, C.Y., Kim, H.S. & Won, Y.-Y. 2006 Biomechanical Tests of Osteoporotic Vertebral Trabecular Bone using Finite Element Analysis

Based on Micro-CT. In Intl. Conf. on Biomedical and Pharmaceutical Engineering (ICBPE)

[18] Sansalone, V., Lemaire, T. & Naili, S. 2007 Multiscale modelling of mechanical properties of bone: study at the fibrillar scale. Comptes Rendus Mecanique 335, 436–442.

[19] Zaideman, O. & Fischer, A. 2010 Geometric Bone Modelling: From Macro to Micro Structures. J. Comput. Sci. Technol. 25, 614-622. (doi:10.1007/s11390-010-9350-0).

[20] Idhammad, A., Abdali, A. & Alaa, N. 2013 Computational simulation of the bone remodelling using the finite element method: an elastic-damage theory for small displacements. Theor Biol Med Model 10, 1-11. (doi:10.1186/1742-4682-10-32).

[21] Nawrocki, S. 1997 Cleaning Bones. . (University of Indianapolis Archeology & Forensics Laboratory).

[22] Cauble, R. 2010 The Bone Room; Available at: http://www.boneroom.com/faqs/bones.html. (Berkeley, CA).

[23] Guidance notes; The University of Manchester health and safety rules (BIOCOSH) to handle biological materials and assessment of risk.

[24] http://www.volumegraphics.com/en/products/vgstudio-max.html.

[25] www.simpleware.com.

[26] Alexander, R.M. 1981 Factors of safety in the structure of animals. Science Progress (Oxf.) 67, 109–130.

[27] Biewener, A.A. 1993 Safety Factors in Bone Strength. Calcified tissue international 53, S68-S74.

[28] Scientist, G. 2010 Mystery Bird: Barnacle Goose, Branta leucopsis. In Mystery Bird: Barnacle Goose, Branta leucopsis (Finland, University of Helsinki Museum of Natural History).

[29] Rho, J.Y., Roy, M., Tsui, T.Y. & Pharr, G.M. 1997 Young's modulus and hardness of trabecular and cortical bone in various directions determined by nanoindentation. In In: Transactions of the 43rd Annual Meetings of the Orthopaedic Research Society. (p. 891).

[30] Young, W.C. & Budynas, R.G. 2002 Roark's Formulas for Stress and Strain. In 7th edition (7ed, McGraw-Hill: Chicago, USA).

[31] http://www.3ds.com/products-services/simulia/products/abaqus/.

[32] Reilly, T.D. & Burstein, H.A. 1974 The Mechanical Properties of Cortical Bone. The Journal of Bone and Joint Surgery. 56, 1001-1022.

[33] Reilly, T.D. & Burstein, H.A. 1975 The elastic and ultimate properties of compact bone tissue. Journal of biomechanics 8.

[34] Razak, A.S.I., Fadzliana, N.S.a. & Aizan Wan, A.R. 2012 Biodegradable Polymers and their Bone Applications: A Review. International Journal of Basic & Applied Sciences

5 Finite element analysis of a tendon avulsion injury and its impact upon forelimb function in a specimen of *Tyrannosaurus rex*

Margetts L.[1,2] Mustansar Z[1] Mackovicky, P[3]. and Manning PL[1*].

---

[1]Interdisciplinary Centre for Ancient Life, School of Earth, Atmospheric and Environmental Science, University of Manchester, UK

[2]Oxford eScience Research Centre, University of Oxford, Oxford, UK

[3]The Field Museum, Lake Shore Drive, Chicago, USA

A paper submitted to the Royal Society Interface.

Finite element analysis of a purported tendon avulsion injury and its impact upon forelimb function in a *Tyrannosaurus rex*

Margetts L.[1,2] Mustansar Z[1] Mackovicky, P[3]. and Manning PL[1*],

[1]Interdisciplinary Centre for Ancient Life, School of Earth, Atmospheric and Environmental Science, University of Manchester, Williamson Building, Oxford Road, Manchester, M13 9PL, UK

[2]Oxford eScience Research Centre, University of Oxford, Oxford, UK

[3]The Field Museum, Lake Shore Drive, Chicago, USA

*Corresponding author (e-mail: phil.manning@manchester.ac.uk)

ABSTRACT

The most complete specimen of *Tyrannosaurus rex* (FMNH PR2081) is housed at the Field Museum in Chicago (USA). This remarkable specimen displays several pathologies in its skeleton (both in the skull and post-cranial elements), including a 3 cm long, 0.5 cm deep pit on the posterior surface of the right humerus (with a 1 cm long posterodistal bony spur at the proximal edge of the pit). The abnormal morphology has previously been suggested to be either an abscess resulting from necrosis of bone tissue with probable infection-induced osteomyelitis or alternatively a tendon avulsion injury with subsequent infection and healing. This study used X-Ray Computed Tomography (XRCT) and Finite Element Analysis (FEA) to investigate the structure, morphology and subsequent repair of the humeral pathology. The 3D data generated by the XRCT shows evidence that the injury suffered a probable bacterial infection and healing was accompanied by both external and extensive internal bone re-modelling, in what seems a non-fatal injury. While the XRCT shows that the avulsion site on the humerus of FMNH PR2081 healed, the FEA indicates that it could subsequently support a higher compressive load than adjacent healthy bone. The position and geometry of the pathology

suggests that a tendonous attachment might well have existed in *T. rex* for the medial head of the triceps that tore free from its origin resulting in the trauma and observed healing. The FEA result supports the XRCT data that the injury was non-fatal. Our results backs-up previous studies that suggest a single trauma event gave rise to the distinct pathology in the humerus and maybe associated with additional skeletal trauma observed on FMNH PR2081. This work also provides quantitative approach to the imaging of palaeopathologies along with interpretation and functional analysis of the humerus of the *Tyrannosaurus rex* 'Sue' (FMNH PR2081).

Keywords

Tyrannosaurus rex, Palaeopathology, Finite Element Analysis, X-ray computed tomography

Introduction

Tyrannosaurus rex [1] is possibly the most instantly recognizable of all dinosauria [2]. The most complete specimen (FMNH PR2081) currently known to science is housed at the Field Museum of Natural History in Chicago (USA) and has been extensively studied [3-6]. Previous studies have identified evidence of healed trauma on the skeletons of extinct vertebrates, but this is especially apparent in theropod dinosaurs [7]. Brochu [3] identified many pathologies on FMNH PR2081, but here we focus on the distinct pathologic feature present on the proximal anterior surface of the right humerus.

The only humerus recovered for FMNH PR2081 was from the right-hand side of the skeleton. This beautifully preserved element displays an abnormal 3 cm long, 0.5 cm deep pit and proximal to the pit is a 1 cm long posterodistal process (osteophyte) on the posterior surface of the humeral shaft. Brochu [3] noted that this feature did not correspond with any structure normally seen in the theropod forelimb skeleton. Rothschild and Martin [8] suggest that pits similar to the one observed on the humerus of FMNH PR2081 might be a function of an abscess resulting from necrosis of bone tissue. Brochu [3] further compared the structures with abnormalities in living tetrapods suggesting a similarity with infection-induced osteomyelitis. However, others have suggested the pathology is a function of a

tendon avulsion as a result of unusual stress loading of the forearm [6, 9]. Hudson [10] noted that the medial triceps in extant birds consists a fleshy and not tendonous origin suggesting the pathology in the humerus of FMNH PR2081 is not a tendon avulsion related to the medial triceps. In this study we apply both imaging and numerical modelling approaches to aid in the interpretation of the humeral pathology observed in FMNH PR2081.

In this paper we use engineering techniques, including X-Ray Computed Tomography (XRCT) and Finite Element Analysis (FEA) to investigate the structure, morphology and subsequent repair of the humeral pathology. X-ray tomography is a non-destructive means by which palaeontologists can investigate internal biological structures that have been preserved in fossils [11]. This method is preferred to the traditional physical sectioning techniques that destroy what are often unique and/or rare specimens. The use of X-ray light sources in palaeontology is growing in importance and has even been used to identify and characterise chemical traces in fossils [7, 12-15]. FEA is a numerical method used to estimate the response of a structure to an externally applied load [16]. It is traditionally used in engineering disciplines such as civil engineering [17-18] and has recently seen a growing uptake in palaeontology [19-21] especially vertebrate palaeontology [5, 11].

Rayfield [5, 22-24] has used FEA to study the biomechanics of skulls, particularly bite force and the distribution of cranial load, in *Tyrannosaurus rex*, *Allosaurus fragilis* and other carnivorous dinosaurs. Preuschoft [25] has used finite element analysis to study growth stages in the skull of Diplodocus. Both Rayfield [22] and Manning et al. [11] have combined imaging with computer modelling [11, 24]. The latter has used X-ray tomography scans to generate finite element models that were used to investigate form and function in a *Velociraptor* claw [11].

This paper analyses for first time a pathologic bone in a *Tyrannosaurus rex* (FMNH PR2081) humerus using a combination of both XRCT and the finite element method.

Figure 1. Skeleton of *Tyrannosaurus rex* (FMNH PR2081) with volume rendering of the right humerus generated from XRCT data.

Materials and methods

The original fossil of the *Tyrannosaurus rex* humerus, with acquisition number FMNH PR 2081, was briefly borrowed from the Field Museum of Natural History in Chicago (USA) and scanned at the Loyola University Hospital (Illinois).

Image Acquisition and Processing

The humerus was mounted and scanned in a General Electric Lightspeed VCT X-ray tomography system at the Loyola University Hospital CT scanning facility. The following settings were used in order to penetrate the fossil and produce a good quality image: Slice spacing of 0.75 mm, slice thickness 1.25 mm, scanned in helical mode at 140 Kv and 500 mA. The data was reconstructed using Osirix to produce a stack of 312 gray-scale slices through the humerus with a 512 x 512 field of view. The Osirix 3D volume render tool was used to render the images and produce three-dimensional volumes. These are presented in the results section along with descriptions of the purported injury.

The XRCT data was used to generate volumetric renderings of the humerus of FMNH PR 2081 as the source of the geometry for an FEA model. Several steps in processing the data were followed in order to create the model. Firstly, the cracks in the fossil, which are not of biological origin or related to the injury, were removed from the image. This was achieved through a combination of manual painting and the use of dilation, erosion and flood fill filters available in the ScanIP software from Simpleware Ltd [26]. The procedure followed for "virtual fossil repair" is described in more detail by [27]. The next step was to segment the image into different phases, again using ScanIP. Three phases were identified, each relating to a different biological material, namely cortical and cancellous bone, and also the volume that would once have contained bone marrow (the core of the bone). For modelling simplicity the cancellous bone was segmented as a solid phase. Figure 2 illustrates the image processing steps using a two dimensional slice of the scan. All slices were processed in the same way.

A Boolean operation was used to remove the mask of the marrow cavity. It was assumed that this material would not provide resistance to loading. The removal of this phase reduced the size of finite element model to be solved.

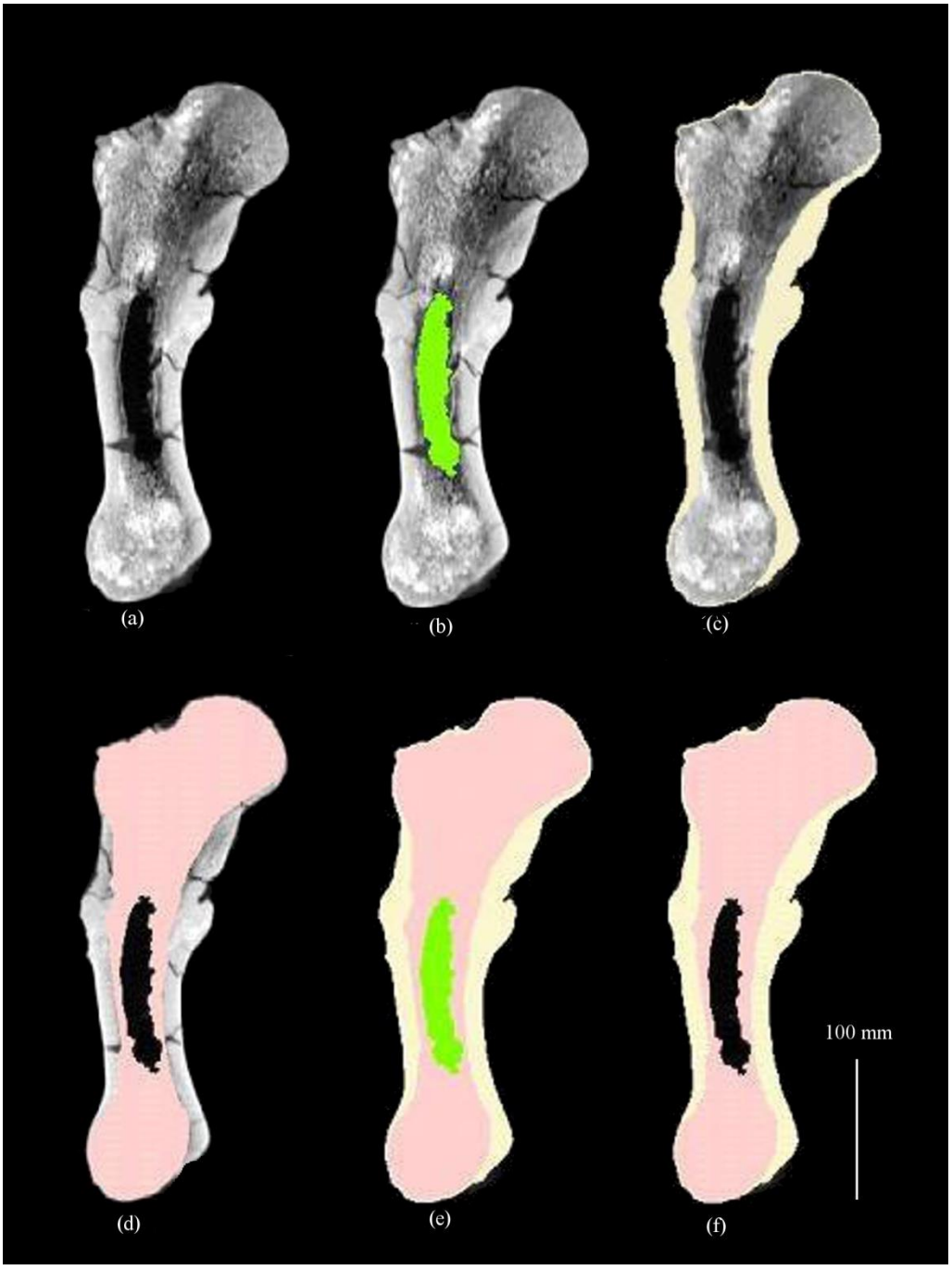

Figure 2. Image processing carried out before creating the finite element model of FMNH PR 2081. (a) The original image with diagenetic cracks of non-biological origin. (b) A mask of the region that would have occupied bone marrow or soft tissue. (c) A mask of the cortical bone with cracks removed. (d). A mask of the spongy bone with cracks removed after virtual repair. (e) Image fully segmented into three phases. (f) The result of a Boolean operation to remove the bone marrow phase from the image and the computer model (Scale bar is 100 mm).

Finite Element Modelling

The remaining two phases were converted into a finite element mesh comprising around 7,237,620 tetrahedral elements using the ScanFE software developed by Simpleware Ltd [26]. The mesh is shown in Figure 3.

Boundary conditions were applied such that a patch of nodes at the distal end of the bone was constrained from moving in any direction. A compressive load was applied to a patch on the most proximal end of the bone. This load was directed vertically through the long axis of the bone. The set-up was the "insilico" equivalent of an experimental set-up using an Instron machine [28].

The bone was modelled as a linear elastic solid using published bone property values [29-31]. Material properties for the bone were selected as follows. The cortical bone was given a value for Young's modulus of 20GPa [30]. The cancellous bone, which was treated as a solid in the modelling, was given a value for Young's modulus of 11GPa [20]. The latter value can be thought of as the effective property of a composite material containing trabeculae and voids that has been homogenized into an equivalent solid for modelling purposes [32]. The Poisson's ratio was set to 0.33 in both cases [31].

A simulation was carried out for a load of 4kN using Abaqus on a 16-core Dell workstation. As there is a linear relationship between load and displacement, the results of this analysis could be scaled up to provide results for loads of 26 kN, 52 kN and 78 kN. The load values were increased until the mises stress in the bone was ~130MPa, a conservative estimate for the stress at which the bone would start to fail [30, 33]

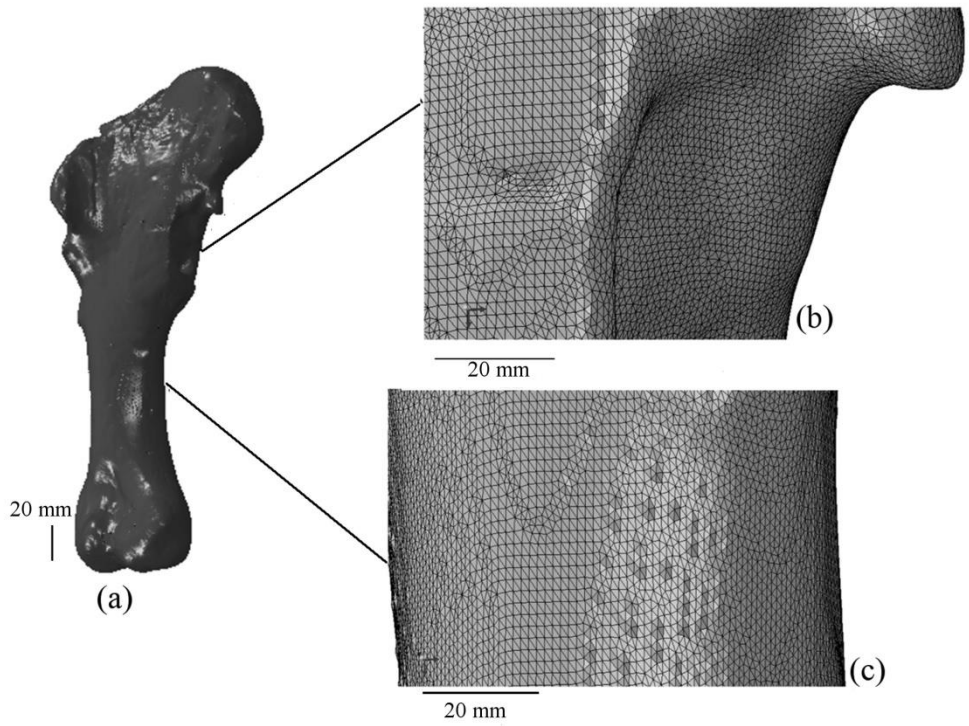

Figure 3 Finite element model with close-ups of the pathology (a, b) and the shaft (c).

Analytical Solution

The results of the finite element analysis were compared with an analytical solution for an idealised problem: an axial load applied to a right cylinder. This is an important verification and validation step in the computer modelling. The equation for change in length in a right cylinder due to the application of an axially applied load is given by:

$$dl = \sigma l_0 / E$$

Where dl is the change in length, σ is the stress, l_0 is the original length and E is the Young's modulus [34].

Stress is load divided by cross-sectional area. A solid cylinder has a larger cross-sectional area than a hollow cylinder and therefore the change in length of the former will be less than that of the latter. If the results of the finite element analysis are reliable, the finite element prediction of change in length should be of a similar order of magnitude, and may lie between these two extremes.

The values for the quantities required to evaluate the analytical solutions are given in

Quantity	**Value**	**Source**
Original length	385 (mm)	Measured by authors
Diameter of lower shaft	60 (mm)	Measured by authors
Lower shaft cortical thickness	18 (mm)	Measured by authors
Young's modulus	20 (GPa)	Reilly (Reilly and Burstein, 1974)
Applied load	4 (kN)	N/A

Table 1: Quantities used for the analytical solution

Interpretation of the X-ray Tomography Data

The XRCT data permitted interrogation not only of the deep pit and posterodistal process on the posterior surface of the humeral shaft (Fig. 4a), but also the relative thickness of the cortical bone around the site of trauma (Fig. 4). The humerus is 175 mm circumference in the circular part of shaft (Fig. 4c) and 265 mm circumference at mid pathology (Fig. 4h). The lower edge of the pit is 225 mm from distal end of humerus and the top edge of pit 115 mm for head of humerus, max depth of pit is 9 mm (Fig 4i). The pit is 45 mm wide by 55 mm long and the osteophyte that is proximal to the pit is 10 mm long at its maximum growth (Fig. 4g). The cortical bone thickness is maintained within the floor of the pit (Fig. 4h-j) relative to the cortical thickness in the rest of the humeral shaft. This shows that even after the trauma has resulted in a 9 mm deep pit in the cortical bone wall, that the adjacent bone has remodelled to compensate for the pathology. The remodelling and restoration of cortical wall thickness is marked around the trauma site, with cortical bone thickened relative to the surrounding non-injured bone (Fig. 4b), especially between the distal edge of the pathology (Fig. 4 d) to the mid-shaft of the humerus (Fig. 4c). The highly active remodelling process of bone provides an opportunity to map the biomechanical properties of bone tissue after remodelling, allowing for a better understanding of the mechanical strength of a bone, post trauma.

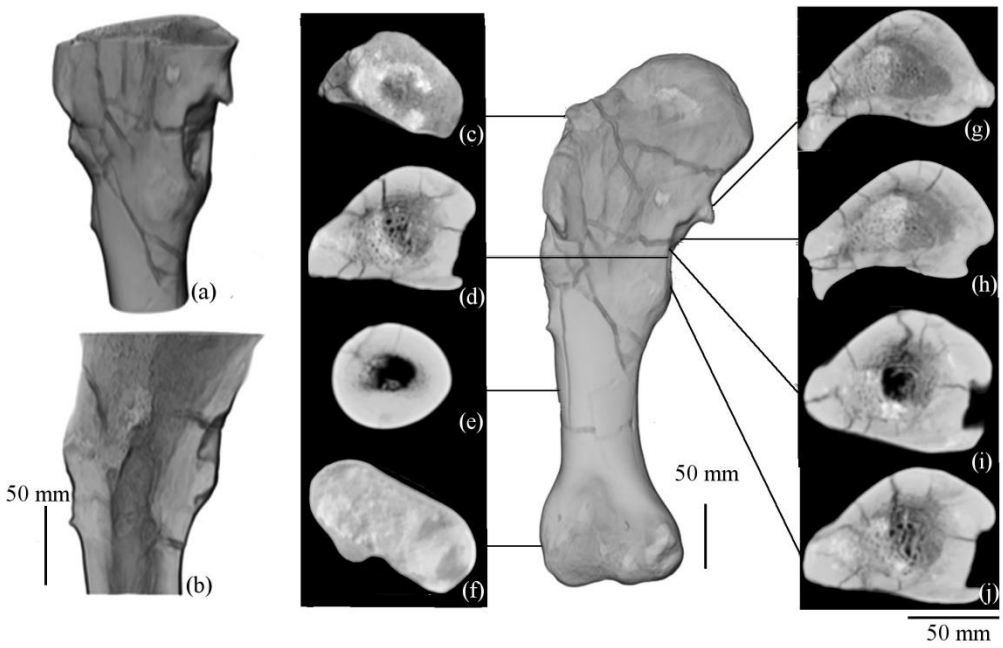

Figure 4. X-ray computed tomography data showing 3D volume reconstructions and 2D sections. The central image is of the full reconstructed bone. (a) shows a close-up of the pit. (b) is a cross section of the same section. Images (c) to (f) show multiple 2D sections through the humerus. (c) shows a section through head of the humerus, (d) shows a cross section through the middle of the pathology and (e) a section through the mid-shaft with no evidence of trauma. The distal condyle is seen in section in (f). Images (g) to (j) show relative cortical bone thickness relative to the pathology.

Structural Response to a Compressive Axial Load

The vertical displacement of the humerus, computed in line with the shaft, ranged from 0.021mm to 0.043mm for a load of 4kN, according to the finite element analysis. The range is due to the non-uniform shape of the humerus. This value compared well with the analytical solutions for a solid and hollow cylinder, with vertical displacements of 0.027mm and 0.053mm respectively. Therefore the authors are satisfied that the analytical solution verifies that the finite element results are reasonable.

A set of results are shown in Figure 4 for three different compressive loads applied along the axis of the humerus. The loads applied were 26kN, 52kN and 78kN. The plots show contours of Mises stress, a quantity used to gauge proximity to structural failure in elastic finite element analyses. A value of Mises stress close to the yield

stress of the material under study indicates that the bone may be close to breaking. The yield stress of bone is quite variable. Reported values in the literature range from 110MPa in bovine femur bone to 200 MPa in human subchondral bone [29-30, 35]. At 78kN, the Mises stress ranges from 90 MPa to 135 MPa (the red contour interval) in a broad region of the shaft, indicating that 78kN may have been close to the maximum load the bone may have supported.

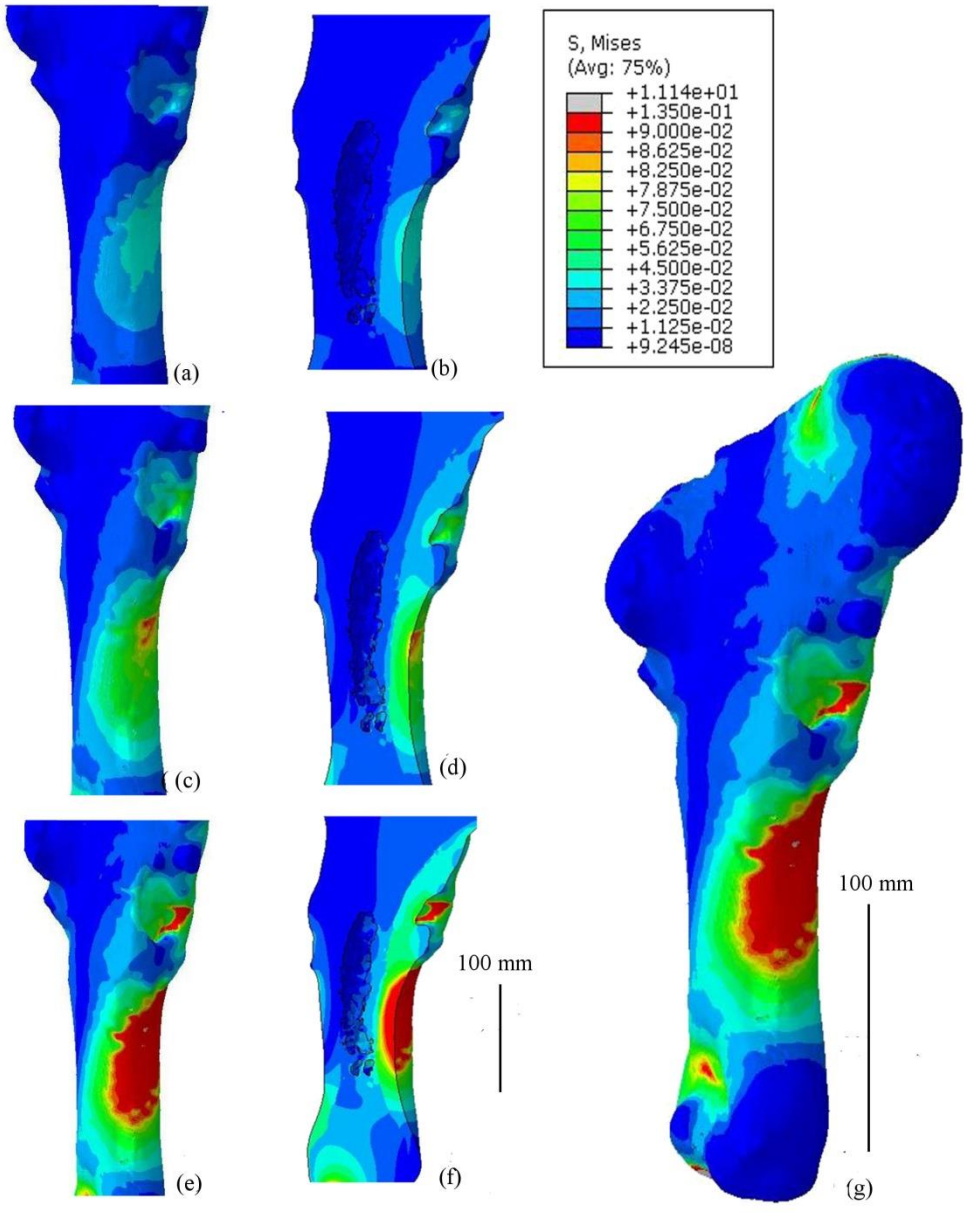

Figure 4: Mises stress computed using finite element analysis. Plots (a), (c) and (e) show Mises stress for the section of humerus containing the injury and a section of shaft for loads of 26 kN (a), 52kN (c) and 78kN (e). Plots (b), (d) and (f) show the corresponding cross-

sections of the plots (a), (c) and (e). Plot (g) shows response of the whole bone to a load of 78kN. The same contour intervals are used in all images. The units in the key are GPa.

Discussion

Throughout their lives, all vertebrates deal with the constant interplay between bone absorption and redeposition as part of growth and development [36]. This essential process assists mineral homeostasis, the maintenance of immune cells, but crucially the regulation of bone structure effects its mechanical properties [37]. Pathologic tissue is dependent on upon the same remodelling processes to mediate the repair of trauma to bone [38]. Two key cell types that regulate bone maintenance are osteoblasts (bone forming) and osteoclasts (bone resorption) [36]. The interplay between osteoblasts and osteoclasts regulate bone repair and healing post–trauma [36]. However, calculating the time it took for trauma on the humerus of FMNH PR2081 to remodel and heal is fraught with difficulties, given it is hard to constrain the exact physiology of *T. rex*. Studies of extant reptiles have shown that if the organism is able to maintain access to food whilst maintaining an optimal body temperature, they can heal remarkably fast, with fractures completely healing in 6-8 weeks. If indeed theropod dinosaurs maintained elevated body temperatures with a more avian physiology [7, 39], it is possible that the trauma seen in FMNH PR2081 could have healed in only 3-5 weeks, permitting *T. rex* to maintain its role as a top predator.

The finite element analyses suggest that the bone in the region around the deep pit and posterodistal process on the posterior surface of the humeral shaft had been remodelled to such an extent that, after healing, it was mechanically stronger than presumably healthy bone elsewhere in the humerus. In each load case, the stress in the (assumed) healthy shaft is higher than the remodelled bone around the trauma site. This observation is supported by the tomography data that shows the cortical bone is significantly thicker around the site of the pathology available than elsewhere on the shaft.

The author’s analyses are quite simple in that they assume the bone to be a linear elastic solid. Assumptions are also made about the material properties and bone strength as these can only be estimated. Soft tissues, such as muscle mass are also

ignored. Taking note of these sources of error, the finite element results suggest the bone could support an axial load of around 60 kN if the bone yield stress was 110 MPa. In layman's terms and applying a generous safety factor, this particular *T. rex* humerus could safely support a load of 1800kg if applied vertically along the axis of the bone. The potential maximum humeral load of 1800kg is significantly higher than previously predicted by Carpenter [6], who indicated the forelimb of *T. rex* might support a load of ~400 kg. This suggests the forelimb function of this huge predator has been previously misjudged and that it might have played a more significant role in *T. rex* ecology.

The position and geometry of the pathology suggests that a tendonous attachment might well have existed in *T. rex* for the medial head of the triceps that tore free from its origin resulting in the trauma and observed healing. The FEA result and XRCT data indicate that the injury was non-fatal. Our results backs-up previous studies that suggest a single trauma event gave rise to the distinct pathology in the humerus and maybe associated with additional skeletal trauma observed on FMNH PR2081 [38-40]. This study also provides a quantitative approach to the imaging of palaeopathologies coupled with the functional analysis of the humerus of *Tyrannosaurus rex*.

Ethics statement

The study uses a tomography scan of a fossilized humerus. No animal experimentation was involved.

Data accessibility statement

The datasets are available from the authors on request.

Competing interests statement

The authors have no competing interests.

Authors contributions statement

All authors made substantial contributions to the conception and design of the study, the acquisition of data, and analysis and interpretation of data. All authors were

involved in drafting the article, revising it critically for important intellectual content and giving final approval for this version to be published.

Acknowledgements

This work was funded by the Microsoft-BBSRC Dorothy Hodgkin Award, grant number FA01546. Access to computing facilities for image processing and the simulation was provided by IT Services for Research at the University of Manchester, UK and RCMS-NUST, Islamabad, Pakistan.

References

[1] Osborn., H.F. 1905 Tyrannosaurus, upper cretaceous carnivorous dinosaur.(Second communication). Bulletin of the American Museum of Natural History 21, 259-265.

[2] Owens, R. 1942 Report on British fossil reptiles, Part II. (pp. 60-294, Report of the British Association for the advancement of science.

[3] Brochu, A.C. 2003 Osteology of Tyrannosaurus rex:Insight from a nearly complete skeleton and high resolution computed tomography analysis of skull. Journal of vertebrate palaeontology 22, 1-138.

[4] Bates, K.T. & Falkingham, P.L. 2012 Estimating maximum bite performance in Tyrannosaurus rex using multi-body dynamics. Biology letters; The Royal Society. 8, 660-664.

[5] Rayfield, E.J. 2004 Cranial mechanics and feeding in Tyrannosaurus rex. Proceedings of the Royal Society of London Series B-Biological Sciences 271, 1451-1459.

[6] Carpenter, K. & Smith, M. 2001 Forelimbs Osteology and biomechanics of Tyrannosuarus rex. In Mesozoic vertebrate life (pp. 90-102, Indian University press.

[7] Anne, J., Edwards, N.P., Wogelius, R.A., Tumarkin-Deratzian, A.R., Veelen, v.A., Bergmann, U., Sokaras, D., Alonso-Mori, R., Ignatyev, K., Egerton, V.M., et

al. 2014 Synchrotron imaging reveals bone healing and remodelling strategies in extinct and extant vertebrates. Journal of The Royal Society Interface 11.

[8] Rothschild, M.B. & Martin, D.L. 1993 Palaeopathology: Disease in the fossil record. In The complete dinosaur (CRC press London.

[9] Rothschild, B.M. 1997 Dinosaurian Palaeopathology. In The Complete Dinosaur (pp. 426-448, Indiana University Press.

[10] Hudson, G. & Lanzilloti, P. 1955 Gross anatomy of the wng muscles in the family Corvidae. AM Nidl Mat 53, 1-44.

[11] Manning, P.L., Margetts, L., Johnson, M.R., Withers, P.J., Sellers, W.I., Falkingham, P.L., Mummery, P.M., Barrett, P.M. & Raymont, D.R. 2009 Biomechanics of Dromaeosaurid Dinosaur Claws: Application of X-Ray Microtomography, Nanoindentation, and Finite Element Analysis. The Anatomical Record: Advances in Integrative Anatomy and Evolutionary Biology 292, 1397-1405.

[12] Edwards, N.P., Manning, P.L. & Wogelius, R.A. 2014 Pigments through time. 27, 684–685,.

[13] Edwards, N.P., Barden, H.E., Dongen, v.B.E., Manning, P.L., Larson, P.L., Bergmann, U., Sellers, W.I. & Wogelius, R.A. 2011 Infrared mapping resolves soft tissue preservation in 50 million year-old reptile skin. Proceedings of the Royal Society B: Biological Sciences 3.

[14] Wogelius, R.A., Manning, P.L., Barden, H.E., Edwards, N.P., Webb, S.M., Sellers, W.I., Taylor, K.G., Larson, P.L., Dodson, P., You, H., et al. 2011 Trace metals as biomarkers for eumelanin pigment in the fossil record. Science 333, 1622-1626.

[15] Manning, P.L., Edwards, N.P., Wogelius, R.A., Bergmann, U., Barden, H.E., Larson, P.L., Schwarz-Wings, D., Egerton, V.M., Sokaras, D., Mori, R.A., et al. 2013 Synchrotron-based chemical imaging reveals plumage patterns in a 150 million year old early bird. J. Anal. At. Spectrom. 28, 1024-1030.

[16] Smith, I.M., Griffiths, V.D. & Margetts, L. 2013 Programming the Finite Element Method, 5th Edition .

[17] Margetts, L., Smith, I.M., Lever, L.M. & Griffiths, V.D. 6/2014 Parallel processing of excavation in soils with randomly generated material properties. In 8th European Conference on Numerical Methods in Geotechnical Engineering (Delft, Holland.

[18] Arregui-Mena, J., Margetts, L. & Mummery, P. 2014 Practical Application of the Stochastic Finite Element Method. Archives of Computational Methods in Engineering, 1-20. (doi:10.1007/s11831-014-9139-3).

[19] Brassey, C.A., Margetts, L., Kitchener, A.C., Philip, W.J., Phillip, M.L. & William, S.I. 2013 Finite element modelling versus classic beam theory: comparing methods for stress estimation in a morphologically diverse sample of vertebrate long bones. Journal of The Royal Society Interface 10.

[20] Falkingham, P.L., Bates, K.T., Margetts, L. & Manning, P.L. 2011 The 'Goldilocks' effect: preservation bias in vertebrate track assemblages. Journal of The Royal Society Interface 8, 1142-1154.

[21] Falkingham, P.L., Bates, K.T., Margetts, L. & Manning, P.L. 2011 Simulating sauropod manus-only trackway formation using finite-element analysis,. Biology letters 7, 142-145.

[22] Rayfield, E.J. 2007 Finite Element Analysis and Understanding the Biomechanics and Evolution of Living and Fossil Organisms. Annual Review of Earth and Planetary Sciences 35, 541–576.

[23] Rayfield, E.J. 2005 Using finite-element analysis to investigate suture morphology: A case study using large carnivorous dinosaurs. Anatomical Record Part a-Discoveries in Molecular Cellular and Evolutionary Biology 283A, 349-365.

[24] Bright, J.A. & Rayfield, E.J. 2011 The Response of Cranial Biomechanical Finite Element Models to Variations in Mesh Density. The Anatomical Record: Advances in Integrative Anatomy and Evolutionary Biology 294, 610-620.

[25] Witzel, U. & Preuschoft, H. 2005 Finite-Element Model Construction for the Virtual Synthesis of the Skulls in Vertebrates: Case Study of Diplodocus. The Anatomical Record Part A 283, 391–401.

[26] www.simpleware.com.

[27] Johnson, M.R., Manning, P.L., Margetts, L., Withers, P.J. & Mummery, P.M. 2010 Virtual repair of fossil scan data. The Geological Curators group 9 193-198.

[28] Petzing, N.J., Heras-palou, C., King, J. & Tyrer, R.J. 1997 The analysis of human femurs and prostheses using electronic speckle pattern interferometry. IEEE.

[29] Reilly, T.D. & Burstein, H.A. 1974 The Mechanical Properties of Cortical Bone. The Journal of Bone and Joint Surgery. 56, 1001-1022.

[30] Reilly, T.D. & Burstein, H.A. 1975 The elastic and ultimate properties of compact bone tissue. Journal of biomechanics 8.

[31] Reilly, T.D., Burstein, H.A. & Frankel, H.V. 1974 The elastic modulus of bone. Journal Biomechanics 7, 271–275.

[32] Hollister, S.J., Fyhrie, D.P., Jepson, J.K. & Goldstien, A.S. 1991 Composite material containing trabeculae and voids that has been homogenized into an equivalent solid for modelling purposes Journal of biomechanics 24, 825-839.

[33] Pavlatos, E. 2013 Finite Element Analysis of Radius and Ulna human.

[34] Young, W.C. & Budynas, R.G. 2002 Roark's Formulas for Stress and Strain. In 7th edition (7ed, McGraw-Hill: Chicago, USA.

[35] Razak, A.S.I., Fadzliana, N.S.a. & Aizan Wan, A.R. 2012 Biodegradable Polymers and their Bone Applications: A Review. International Journal of Basic & Applied Sciences 12.

[36] Currey, J.D. 2006 Bones: Structure and Mechanics. Princeton, N.J., Oxford: Princeton University Press.

[37] Wopenka, B. & Pasteris, J.D. 2005 A mineralogical perpective on the apatite in bone. Mater. Sci. Eng. C 25, 131-143.

[38] Cristin, F., Eytan, A., Theodore, M. & Jill, H. 1999 Does Fracture Repair Recapitulate Embryonic Skeletal Formation? Mechanisms of Development 87. 57–66.

[39] Redig, P. 1986. In M. Fowler (ed). Clinical review of orthopedic techniques used in the rehabilitation of raptors. 2nd Edn. In Zoo and Wild Animal Medicine (pp. 388-400 in, Saunders, Philadelphia, Pennsylvania.

[40] Waldron, T. 2009 Palaeopathology. In Cambridge Manuals in Archaeology. (pp. 10013-12473. USA, Cambridge ; New York, NY

6 The Stiffness of Bone

Mustansar Z[1] and Margetts L.[1, 2],

---

1 Interdisciplinary school for ancient life, School of Earth, Atmospheric and Environmental Science, University of Manchester, UK.

[2] Research Computing, University of Manchester, UK

A paper submitted in Journal of PLOS-One

The Stiffness of Bone

Mustansar Z[1] and Margetts L.[1, 2, 3]

[1] Interdisciplinary school for ancient life , School of Earth, Atmospheric and Environmental Science, University of Manchester, Williamson Building, Oxford Road, Manchester, M13 9PL, UK.

[2] Research Computing, University of Manchester, Devonshire House, Oxford Road, Manchester, M13 9PL, UK.

[3] Oxford eResearch Centre, University of Oxford, 7 Keble Road, Oxford, UK.

Abstract

The purpose of this paper is to critically review and address the factors and the type of methods used for determination of elastic modulus of bone. Finding exact material properties e.g. elastic modulus is a difficult process. The paper therefore raises an important scientific question as to what systemic methodology should be adapted to get a value of elastic modulus that is equally reliable and reasonable. Using different techniques and methods for the derivation elastic modulus give rise to different values of elastic modulus. This paper therefore addresses a review of factors affecting the derivation of elastic modulus using different methods and techniques. The study takes into account factors like aging, density, bone condition, bone thickness, specie type and type of mechanical environment, medication and bone architecture for this purpose.

KEYWORDS: Elastic modulus, bone, mechanical environment, bone architecture.

**Corresponding author*: Lee.margetts@manchester.ac.uk

Introduction

Young's/elastic modulus is one of the fundamental inputs in the constitutive analysis of bones using FEM. It is therefore important to get (at least) the linear part of the FE analysis correct. Elastic modulus can be obtained experimentally from a material that is subjected to a load, where the strain and stress can be determined respectively [1].

Bone, consist of combination of ingredients, details of which can be obtained from [2]. The shape of bone is determined by the arrangement of the HA crystals. The arrangement of the collagen fibrils and HA crystals enhances bone strength [3]. Due to a higher elastic modulus of HA crystals, bone is more stiffer to bear the external fractures. Bone has two distinct components. Cortical bone which constitutes the outer thick layer providing strength to the inner porous structure. Whereas the shape of trabeculae bone is related to porosity. Trabecular orientation is commonly studied nowadays mainly as a composite with anisotropic and open porous cellular solid from an engineering point of view [4-6].

Bones possesses specific material properties, fundamentally the most important factors which help determining an overall mechanical behaviour. The Young's modulus and the Poisson ratio are widely considered. The Young's modulus is already described above and the Poisson ratio (ν) is the negative ratio of transverse strain to the longitudinal strain [1]. When a specimen is loaded in compression, it will shorten in the direction of the load and will elongate in width. In other case if the specimen is loaded in tension it enlarges in the direction of the load but become narrower in width. The ratio of change of these quantities give rise to the Poisson ratio. In bones, it usually ranges from 0.1 – 0.33. A vast variation is seen in the results of the values of Young's modulus (from 1GPa – 20GPa) in different analytical bone models (Please see section methods).

This paper provides a systematic study of the values of the Young's modulus from literature and author's own experiments. Methods, where Young's modulus is used as an important factor and the issues associated with each method is also discussed. Another objective of this paper is to report an evaluation of the degree of refinement

of biomechanical experimental data. Despite the advances in technology and state-of-the-art methods in the field of computational mechanics and biology in general, there is a need to devise a standard method which could validate the predicted results from numerical methods. The fact that different experimental methods leads to variation in the ultimate results leads to the formulation of this paper.

Methodology

This section describes the rationale behind the survey in order to identify published literature for determination of bone's Young's modulus. Author points out how various biological, mechanical and experimental factors can affect the value elastic modulus of bone. We use two approaches here:

Search methods

Search methods includes the relevant articles retrieved from published literature. In order to maintain the originality, the paper is divided in two subsections in the results section; (i) Methods used in literature and (ii) Review of FE based methods using values of Young's modulus as an input.

Inclusion/exclusion

Any information with incomplete citation on the web is excluded. The discussion includes only peer-reviewed journals and conference papers, conference proceedings, books and edited book sections, high impact letters and internationally accepted reports. We report that the elastic modulus is related to following sensitivity factors:

Elasticity–aging, Elasticity–density, Elasticity–type of method, Elasticity–architecture, Elasticity–bone thickness, Elasticity–supplements/medication, Elasticity–specie type, Elasticity–mechanical-Environment.

Results

Methods in the literature

Compression, which determines the behaviour of materials under crushing loads is used in [7-11] and [12] in bones; in biomedical research [13]; in natural sciences [5, 14-16] and [17], it was also employed in complex biological behaviour under mechanical testing for localized deformation [13] and [18]; and to determine the material properties [19-21]. This method has some limitations including; (i) end artifact reported in [22-24] caused due to the anatomical sites and sometimes due to the length of specimen; (ii) Size limitation caused due to the limitation of physical resources' including capability of holding sample within the CT machine or resolution; (iii) technical faults in Instron machine.

Tension tests are typically pulling test to determine material response to the applied forces. This method is widely used method for testing bones seen in [16, 25-27]. It shares the same limitations as in compression test. Bending tests are used for the prediction of stress-strain response of the material. The gradient of the stress-strain curve gives the value of the Young's modulus. Examples seen in [28-30]. This method also encounters limitations associated with the sensitivity to the type of specimen, loading condition, geometry and strain rate.

Buckling which is defined as a mathematical instability leading to failure in a specific material is mostly seen in thin bones where they tend to break the structure into two. A kind of failure mode that causes incapability to the function of the bone can also be used to determine Young's modulus. Studies using buckling as a method of finding Young's modulus includes [31] and [31-32].

CT (Computed Tomography) can also be used for the determination of the elastic modulus. It is a non-destructive evaluation technique that allows the internal structure of an object to be imaged by reconstructing the spatial distribution of local linear X-ray absorption coefficients of the materials/phases contained within [33]. Example of deriving elastic modulus from bone using CT came from [34] coupled with voxel specific tissue density [34]. Other examples include [35-39] and [40]. The limitation of this method is based on computational, resolution, size and

experimental factors. Ultrasonic method which uses natural resonance frequencies for a single small sample of bone to measure the elastic modulus of material is seen in [41]. Briefly, wave propagation time is measures in specimen [42] to determine the Young's modulus. Some indirect examples includes [40, 42-43]. Limitations of this method includes the necessity of ensuring reliable acoustic mechanical contact of the sensor with specimen.

In another instance, multiscale modelling has also been used for derivation of elastic modulus using successive homogenization steps. Homogenization is the method of treating different scales/levels within the same specimen at individual phases. The method is described in [44]. Other relevant examples include [44-47]. Limitations of this method falls in correct assumptions between the mineral and collagen matrix, uncertainty in the material properties of collagen and usually restricted to linear models for precise definition.

Finite Element Method (FEM) can also be used By employing CT based data, and converting a digital model into a numerical model. The numerical model (FE- based model) is used to determine the Young's modulus by testing the specimen under compression, tension and/or bending. The constitutive models therefore obtained calculates the elastic modulus via stress-strain curves. Cantilever bending with finite element analysis is another method that uses cantilever beam type bone specimen followed by finite element modelling of specimen and boundary conditions. The actual material properties are obtained by initial input estimates of bone tissue material properties. This data is then used in finite element model. Difference between the calculated FE displacements and the experimentally observed displacements help in the determination of actual Young's modulus.

It is also possible to back-calculate Young's modulus from finite element model by using the deformation values i.e. change in length to the original length of samples, FEM models can be used to determine the elastic properties 'Young's modulus' of the materials. Some relevant examples include [4, 6, 19, 48-52]. Mente and Lewis [53] used cantilever bending with FEA for elastic properties determination and Williams and Lewis [54] used back-calculation from FE models. Acquiring a lower value than the original value in case of bones is one of the major drawback of this method. Another problem associated with this method, is the selection of right

material properties etc, access to the computing facilities for large scale problems. Micro hardness is another method which uses the static indentations made with loads not exceeding than 1 kg, e.g. [55]. This method requires a metallographic finish for the surface to be tested. Stochastic operators were used by Wille et al [56] to pool data cited in the literature based on the relationship between Young's modulus and bone density. All the experiments were pooled over time regarding the E-d (Young's modulus-density) relationship a stochastic relationship between them was developed. Nanoindentation calculates intrinsic elastic properties of individual micro structural bone components in various directions. This method has the ability to give a spatial resolution of around 1 μm [57] to determine bone's mechanical properties and to achieve bone's nearly accurate Young's modulus in several directions [58-59] because of the highly anisotropic [5, 51, 60-65] nature of trabecular bone. The method can successfully be applied on complex surfaces [66] as well based on depth sensing approach [67]. This method however, fails to measure the bulk modulus of specimen. Any polish or silica particles during the sample preparation may induce a high risk of uncertainty in the final results.

Digital volume correlation (DVC) is another approach in this regard. DVC is a measurement technique that quantifies strains throughout the interior of a specimen unlike traditional strain gauge methods where only few points on the surface of the materials are considered. It is possible to generate stress-strain curve, using a software suite e.g. Daviz. The gradient of stress-strain curve gives value of the Young's modulus. Limitation includes factors that contribute to the flawed results are DVC with low resolution data, sample noise and internal 'speckle'.

Review papers on FEM using values for Young's modulus from literature

Rayfield used FEM to find biting forces in T. rex's skull [68-70] and used estimated elastic modulus for skulls. Bates [71] investigated the amount of forces in the *T rex's* skull during the fight or combat in terrestrial vertebrates with an estimated value of elastic modulus. FEM was also to find bone strength in cortical and trabecular regions [19, 49], in the dinosaur study [38, 72-73], and for determination of elastic properties of bone [34, 44, 48, 51, 74-75]. In some studies, FEM was employed in

biomechanical analysis of biological structures [4, 76-77]. In each of these examples, the reliability of elastic modulus values was a matter of question.

Table. 1 show the author's own review collected from literature for the values and the source of Young's modulus of bone from FEM to determine stress-strain curves (value achieved from simulation). The table indicates the variations of the input of Young's modulus values used in FEA could, can affect overall results of bone modelling in terms of prediction of stress-strain.

Fig. 1 illustrates a scatter chart of author's own review on values of Young's modulus in bones. This fig includes values of elastic modulus obtained from FEM as a method of determination. The significant part of this review is, how these variations leads to faulty results in simulations of bone while applying FEM. FEM is a mathematical technique used to virtually predict the bone behaviour under specific circumstances. It uses the values from the user input and interprets the results using the input value. Any change in Young's modulus value yields a different simulation value [83]. In modelling, this is analyst who has to test whether the answer to the question is sensitive to the elastic properties or not.

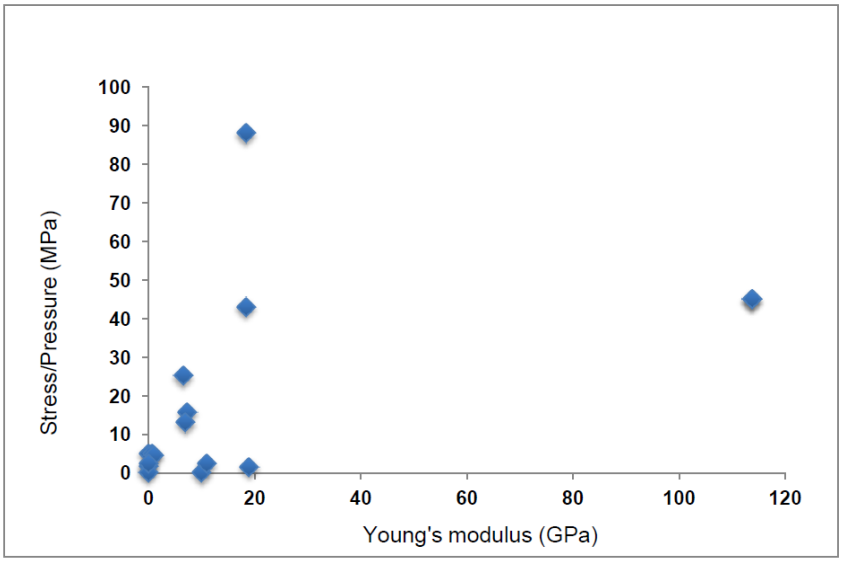

Fig. 1. Graph showing the scatter of values of Young's modulus (GPa) used in FEM against the value achieved from simulations in terms of pressure and/or stress (MPa).

Method used	Value of Young's modulus (GPa)	Source of Young's modulus	Value achieved from simulation. Stress/pressure (MPa)	Specimen used
FEM-Linear-Elastic	18.4	**[8]**	88–121	Bovine tibial trabecular bone- under compression
FEM-Linear-Elastic	18.4	**[8]**	35–43	Bovine tibial trabecular bone –under tension
FEM-Linear-Elastic	0.0142	**[78]**	1.67	L3 human vertebra
FEM-Linear-Elastic	0.04775	**[78]**	5.02	L5 vertebra cancellous bone
FEM-Linear-Elastic	0.00087	**[78]**	0.17	L4 human vertebra cancellous bone
FEM-Linear-Elastic	6.57	**[18]**	25.14	Trabecular bone from Bovine proximal tibia
FEM-Linear-Elastic	7.34	**[18]**	15.70	Trabecular bone from Bovine proximal tibia
FEM-Linear-Elastic	6.99	**[18]**	12.98	Trabecular bone from Bovine proximal tibia
Macro-scale FEM	0.7	**[47]**	5 (SCF) at MVF of 0.2	Human collagen matrix
Macro-scale FEM	1	**[47]**	4.5 (SCF) at MVF of 0.25	Human collagen matrix
FEM-Linear-Elastic	10	**[79]**	Length based results (in mm-N/A here)	Adult bovine distal femurs for cancellous bone cube
FEM-Linear-Elastic	19	**[80]**	1.5 (Max princ. Strain)	4 node tet elements for Elephant femur
FEM-Linear-Elastic	113.8	**[81]**	45 at 93.1°	Femoral component for hip flexion joint (TiAl6V4)
FEM-Linear-Elastic	113.8	**[81]**	45 at 93.1°	Tibial component hip flexion joint (TiAl6V4)
FEM-Linear-Elastic	11	**[81]**	2.42 and 1.61 (CP on femoral cartilage during HS)	Femur
FEM-Linear-Elastic	0.059	**[82]**	2.42 and 1.61 (CP on femoral cartilage during HS)	Articular cartilage

MVF=Mineral Volume fraction; SCF = Stress concentration factor; CP = contact pressure; HS = Heel strike.

Table. 1. Shows a review of methods used to determine young's modulus in bones; the values of Young's modulus obtained; source of Young's modulus; Value achieved for simulation and the type specimens used.

Based on fig. 1, authors propose a correlation study in the form of a guide-chart to select Young's modulus relevant to the methods of determination of elastic modulus and laboratory conditions. The chart also shows the spread of material properties (along vertical axis) compared to the results obtained (along horizontal axis). This fig also provides an evidence of how the input of various numbers for Young's modulus can change the value of stress in bones. It is also seen that that no specific behaviour/trend of the analysis is observed due to (i) Different value of Young's modulus for each input; (ii) Different methods; (iii) Different specimens. Fig. 2 shows authors review on trend of variation in the values of Young's modulus.

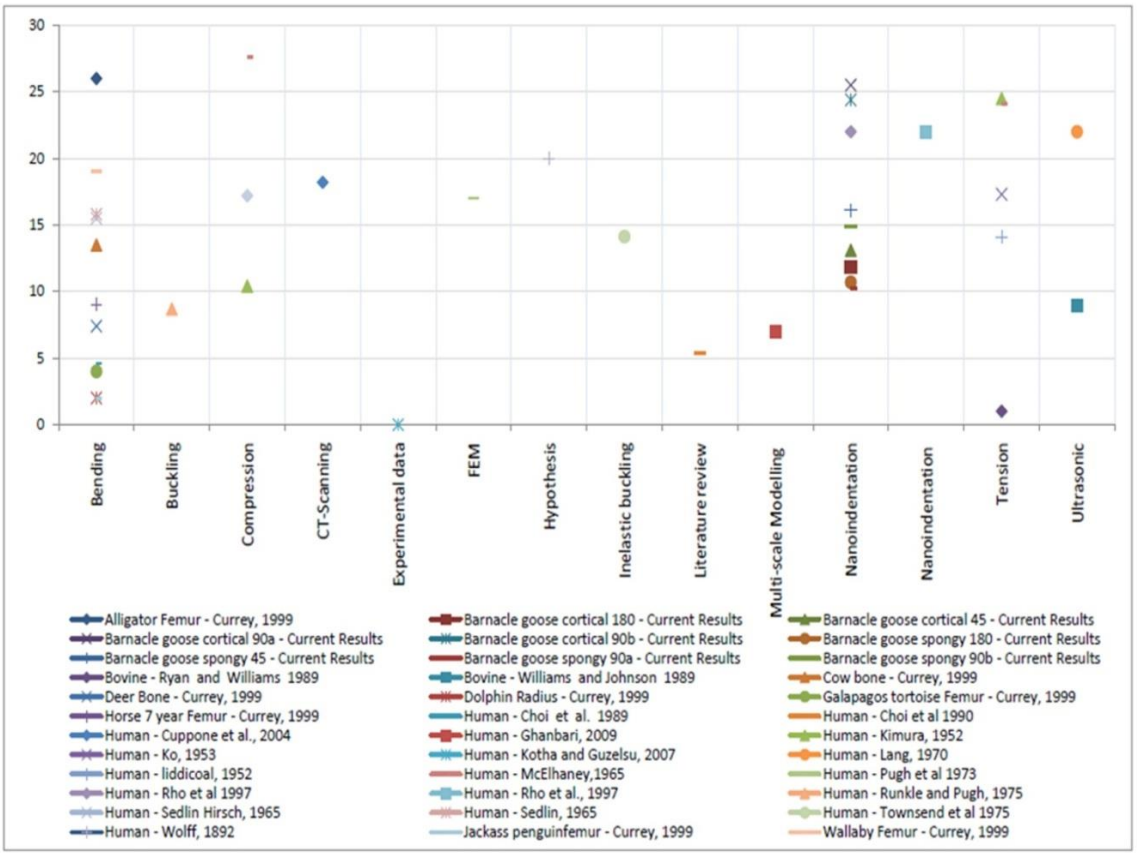

Fig. 2. Chart showing spread of material properties compared to results obtained from Barnacle goose *(Branta leucopsis)* specimen

It is clear from fig. 2 that the variation in the method of determination yields a large variation in the spread of elastic modulus values.

Discussions

Due to the complex geometry of bone it is not possible to measure the exact Young's modulus of bone. The way bone samples are prepared and the methods used for testing, equally contribute to the variation of the elastic modulus values achieved for bones. A correlation between methods used to determine Young's modulus with respect to the factors affecting E value is must required. By using similar methods and techniques to find an answer for material property can be helpful in maintaining a consistency and reliability among these values. Authors conclude that there is a need to hypothesize a 'generalized method' which can approximately give reasonable results under similar physical conditions.

That said, there are number of factors which affect the method of determining value of elastic modulus that may in turn affect elastic properties of bone. For example a healthy will function much better than a damaged bone whereas a damaged bone is likely to cause a functional disability. So if condition of specimen changes, its functionality also changes. The factors effecting value of E can be biological, mechanical or experimental. Among the biological factors, ageing [41, 84] is important. This can cause bone dysfunctioning due to loss of elasticity with age [85]. Increasing water loss from bones also initiate loss of elasticity due to breaking of bonds within the elastic trabeculae. This ultimately results into bone degeneration [40]. Bone elasticity also varies from species to specie under biological regime [86]. B

Among the experimental factors we have investigated that bone's elasticity can reduce with bone porosity [28, 78, 88-90], mineral content [88, 90] and vascular patterns. More porous bone tends to yield later than the less porous bone. Porosity at micro-level is the function of arrangement of the micro fibrils and collagen material in the bone [16]. It is seen [91] that vitamin E which is taken as a supplement across populations in the world could cause a serious problem in bone metabolism initiating independent fusion of osteoclast. These supplements are meant to decrease the

cardiovascular affects on large population instead the vitamin E doses can cause a danger to overall bone health. Intake of vitamin E decreases the bone mass by irregulating the remodelling process [92]. Process of remodelling is meant to maintain the bone homeostasis and vitamin E has a role to support this by stimulating the production of α-tocopherol in order to maintain the skeletal integrity. This compound initiates the process of fusion of osteoclast which disturbs bone metabolism and remodelling.

In terms of orientation a variation of elastic modulus is due to the different arrangement of trabeculae [93-94]. Mechanical environment also contribute to bone elastic modulus e.g. change of growth rate in different bones [95], the type of environment the bone is subjected to [96] and the habitat condition.

Different testing methods tend to yield different values of Young's modulus. For example, a bone in compression will yield a different value of Young's modulus compared to the bone tested in tension under the same physical conditions. Therefore, it is important to hypothesize a 'generalized method.

Recommendations on the paper

Few highlight are recommended by the authors including (i) Sample should be taken from the same species and type; (ii) They should be prepared in similar physical and experimental constraints e.g. elastic modulus obtained from bending method under one group, tension under another group and so on; (iii) Samples should be categorized in separate groups with different age; (iv) They should be prepared under similar conditions. For example, damaged bone, healthy bone, dry or wet in separate individual categories; (v) Treated samples should be excluded from the un-treated samples; (vi) Mechanical conditions should carefully be kept the same across species.

Ethic statement

No animal experimentation was involved.

Data accessibility statement

The datasets are available from the authors on request.

Conflict of interest statement

There is no potential conflict of interest. None of the authors received or will receive direct or indirect benefits from third parties for the performance of this study.

Authors contributions

1) Substantial contributions to conception and design: ZM LM

2) Acquisition of data, or analysis and interpretation of data: ZM, LM

3) Drafting the article or revising it critically for important intellectual content: LM, ZM

4) Final approval of the version to be published: LM, ZM.

Acknowledgements

School of Earth, Atmospheric and Environmental Sciences, The University of Manchester, UK, The Microsoft-Dorothy Hodgkin Postgraduate award (FA01546) and The university of Manchester

References

1. Sharir A, Barak MM, Shahar R. Whole bone mechanics and mechanical testing. The Veterinary Journal. 2008;177:8-17.

2. Currey JD. Bones: Structure and Mechanics.: Oxford, Princeton University Press; 2000.

3. Currey JD. Collagen and the Mechanical Properties of Bone and Calcified Cartilage. Collagen structure and mechanics: Springer US; 2000. p. 397-420.

4. Kolston PJ. Finite element modeling: a new tool for the biologist. Philosophical Transactions of the Royal Society (Series A: Mathematical, Physical and Engineering Sciences). 2000;358: 611-31.

5. Keaveny TM, Morgan EF, Niebur GL, Yeh OC. Biomechanics of trabecular bone. Annu Rev Biomed Eng. 2001;3:307–33.

6. Sobieszczyk S, Wojnicz W, Nowak B. FEM Approach to estimate the behaviour of Bio-Composite metal-surface coating systems. Advances in Materials Sciences. 2008;8(1):166-72.

7. Müller R, Gerber SC, Hayes WC. Micro-compression: a novel technique for the nondestructive assessment of local bone failure. Technology and Health Care. 1998;6:433-44.

8. Nagarajaa S, Couseb LT, Guldberg ER. Trabecular bone microdamage and microstructural stresses under uniaxial compression. Journal of biomechanics. 2005;38:707–16.

9. Thunrner. PJ, Blake E, Zachary S, John L, Jeff S, Maria Z, Et al. High-Speed Photography of Human Trabecular Bone during Compression. In: Material Research Society2005.

10. Das R, Cleary W, Paul. . Uniaxial compression test and stress wave propagation modelling using sph. CSIRO Mathematical and Information Sciences, Clayton, Victoria 3168, AUSTRALIA2006 15-16 December 2006.

11. Benoit A, Guerard S, Gillet B, Guillot G, Hild F, Mitton D, et al. 3D analysis from micro-MRI during in situ compression on cancellousbone. Journal of Biomechanics. 2009;42:2381–6.

12. Rodríguez-Martín R, Castro I, Ocaña JI, Martínez-Esnaola M. Use of electronic speckle pattern interferometry in the detection of fatigue failure in high strength steels. Engineering Failure Analysis. 2010;17(1):226–35.

13. Boyd S, Shrive N, Wohl G, Muller R, Zernicke R. Measurement of cancellous bone strain during mechanical tests using a new extensometer device. Medical Engineering & Physics. 2001;23:411–6.

14. Perilli E, Baleani M, Öhman V, Baruffaldi F, Viceconti M. Structural parameters and mechanical strength of cancellous bone in the femoral head in osteoarthritis do not depend on age. Official journal of the international bone and mineral society. 2007;41: 760-8.

15. Lee Gyh, Lim CT. Biomechanics approaches to studying human diseases. Trends in Biotechnology. 2007;25(3): 111-8.

16. Kotha SP, Guzelsu N. Tensile behavior of cortical bone: dependence of organic matrix material properties on bone mineral content. Journal of Biomechanics. 2007;40:36-45.

17. Deligianni DD, Apostolopoulos CA. Multilevel finite element modeling for the prediction of local cellular deformation in bone. Biomechanics and Modeling in Mechanobiology. 2008;7:151–9.

18. Verhulp E, Rietbergen VB, Müller R, Huiskes R. Indirect determination of trabecular bone effective tissue properties using micro-finite element simulations Journal of biomechanics. 2008;41:1479-85.

19. Boyda S, Macdonalda H, Hanley D. Measuring bone strength from in vivo micro-CT using the finite element method. International Conference on Osteoporosis and Bone Research 20082008. p. S59

20. Gupta HS, Zioupos P. Fracture of bone tissue: The 'hows' and the 'whys'. Medical Engineering & Physics. 2008;30:1209–26.

21. Warshaw J. Primate bone microstructural variability: relationships to life history, mechanical adaptation and phylogeny [Ph.D. dissertation]. New York: The City University of New York; 2007.

22. Allard RN, Ashman R, B. A comparison between cancellous bone compressive moduli determined from surface strain and total specimen deflection. . Transactions of orthopedic research society. 1991;16:151.

23. Zhu M, Keller S, T. , Spengler M, D. Effects of specimen load-bearing and free surface layers on the compressive mechanical properties of cellular materials. Journal of biomechanics 1994;27:57-66.

24. Keaveny. TM, Pinilla. TP, Paul R, Crawford., Kopperdahl. DL, Albert L. Systematic and Random Errors in Compression Testing of Trabecular Bone. Jouurnal of orthopaedic research. 1997;5:101-10.

25. Carter DR, Schwab GH, Spengler DM. Tensile fracture of cancellous bone. Acta Orthop Scand. 1980;51:733-41.

26. Kaplan SJ, Hayes WC, Stone JL, Beaupré GS. Tensile strength of bovine trabecular bone. Journal of biomechanics. 1985;18:723-7.

27. Ryan CB, Williams JL. Tensile testing of rodlike trabeculae excised from bovine femoral bone. . Journal of Biomechanics. 1989;22:351-5.

28. Currey JD. What determines the bending strength of the compact bone? The journal of experimental biology. 1999;202:2495-503.

29. Megan PW, Espinoza. NR, Sagar RS, Richard WB. Mechanical Properties of the Hindlimb Bones of Bullfrogs and Cane Toads in Bending and Torsion. The Anatomical Records. 2009;292:935–44.

30. Kuhn JL, Goldstein SA, Choi KW, London M, Feldkamp LA, Matthews LS. Comparison of the trabecular and cortical tissue moduli from human iliac crests. Journal of Orthopaedic Research. 1989;7:876-4.

31. Zheng X-P, Cao Y-P, Li B, Feng X-Q, Jiang H, Huang YY. Determining the elastic modulus of thin films using a buckling-based method: computational study. Journal of physics D: Appplied physics. 2009;42.

32. Townsend PR, Rose RM, Radin EL. Buckling studies of single human trabeculae. . Journal of Biomechanics. 1975;8:199-201.

33. Elliott JC, Dover SD. X-ray Microtomography. Journal of Microscopy-Oxford. 1982;126(211-213).

34. Wagner WD, Lindsey PD, Beaupre SG. Deriving tissue density and elastic modulus from microCT bone scans. BONE. 2011;49:931–8.

35. Hounsfield GN, Ambrose JA. Computerized Transverse Axial Scanning (Tomography). British Journal of Radiology. 1973;46:1016-22.

36. Marrow TJ, Buffiere JY, Withers PJ, Johnson G, Engelberg D. High resolution X-ray tomography of short fatigue crack nucleation in austempered ductile cast iron. International Journal of Fatigue. 2004;26:717-25.

37. Ebinger T, Steeb H, Diebels S, Ripplinger W, Tjardesy T. A biomechanical model based on a FE2 approach using data from computer tomography. In: VIII C, editor. VIII International Conference on Computational Plasticity. °c CIMNE, Barcelona2005.

38. Manning PL, Margetts L, Johnson MR, Withers PJ, Sellers WI, Falkingham PL, et al. Biomechanics of Dromaeosaurid Dinosaur Claws: Application of X-Ray Microtomography, Nanoindentation, and Finite Element Analysis. The Anatomical Record: Advances in Integrative Anatomy and Evolutionary Biology. 2009;292(9):1397-405.

39. Davis GR, Wong FS. X-ray microtomography of bones and teeth. Physiological Measurement. 1996;17:121-46.

40. Kokabi N, Bae W, Diaz E, Chung BC, Bydder MG, Du J. Ultrashort TE MR Imaging of Bovine Cortical Bone: The Effect of Water Loss on the T1 and T2 * Relaxation Times. Magnetic Resonance in Medicine. 2011.

41. Ashman RB, Rho JY. Elastic modulus of trabecular bone material. . Journal of Biomechanics. 1988;21(177-81).

42. Nìmcová H, Plachý T, Tesárek P, Hájková A, Polák M. Comparison of methods for dynamic young´s modulus determination in gypsum materials. The 4th International conference: MODELLING OF MECHANICAL AND MECHATRONIC SYSTEMS 2011; September 20-22, 2011; The 4th International conference: Faculty of Mechanical engineering, Technical university of Košice; 2011.

43. Langs SB. Ultrasonic Method for Measuring Elastic Coefficients of Bone and Results on Fresh and Dried Bovine Bone. IEEE transactions on biomedical engineering. 1970;17(2):101-5.

44. Hamed E, Jasiuk I, Yoo A, Lee Y, Liszka T. Multi-scale modelling of elastic moduli of trabecular bone. Journal of royal society interface. 2012;(in press).

45. Porter D. Pragmatic multiscale modelling of bone as a natural hybrid nanocomposite. Materials Science and Engineering. 2004;365:38-45.

46. Sansalone V, Lemaire T, Naili S. Multiscale modelling of mechanical properties of bone: study at the fibrillar scale. Comptes Rendus Mecanique 2007;335:436–42.

47. Ghanbari J, Naghdabadi R. Nonlinear hierarchical multiscale modeling of cortical bone considering its nanoscale microstructure. Journal of Biomechanics. 2009;42:1560–5.

48. Kowalczyk P. Elastic properties of cancellous bone derived from finite element models of parameterized microstructure cells. Journal of Biomechanics. 2003;36:961–72.

49. Bevill G, Keaveny MT. Trabecular bone strength predictions using finite element analysis of micro-scale images at limited spatial resolution. Bone. 2009;44:579-84.

50. Taylor M, Cotton J, Zioupos P. Finite Element Simulation of the Fatigue Behaviour of Cancellous Bone. Meccanica. 2002;37:419-29.

51. Zhang J, Niebur GL, Ovaert TC. Mechanical property determination of bone through nano- and micro-indentation testing and finite element simulation. Journal of Biomechanics. 2008;41:267–75.

52. Cuppone M, Seedhom BB, Berry E, Ostell AE. The Longitudinal Young's Modulus of Cortical Bone in the Midshaft of Human Femur and its Correlation with CT Scanning Data. Calcified Tissue International. 2004;74:302–9.

53. Mente PL, Lewis JL. Experimental method for the measurement of the elastic modulus of trabecular bone tissue. Journal of Orthopaedic Research. 1989;7(456-461).

54. Williams JL, Lewis JL. Properties and an anisotropic model of cancellous bone from the proximal tibial epiphysis. Journal of Biomechanics and Engineering. 1982;104:50-6.

55. Hodgskinson R, Currey JD, Evans GP. Hardness, an indicator of the mechanical competence of cancellous bone. Journal of Orthopaedic Research. 1989;7:754-8.

56. Wille H, Rank E, Yosibash Z. Prediction of the mechanical response of the femur with uncertain elastic properties. Journal of Biomechanics. 2012;45:1140–8.

57. Rho JY, Roy M, Tsui TY, Pharr GM, editors. Young's modulus and hardness of trabecular and cortical bone in various directions determined by nanoindentation. In: Transactions of the 43rd Annual Meetings of the Orthopaedic Research Society; 1997.

58. Rho J-Y, Roy ME, Tsui TY, Pharr GM. Elastic properties of microstructural components of human bone as measured by nanoindentation. Journal of Biomedical Materials Research 1999a;45: 48-54.

59. Rho J-Y, Zioupos P, Currey JD, Pharr GM. Variations in the individual thick lamellar properties within osteons by nanoindentation. Bone. 1999b;25:295-300.

60. Yang G, Kabel J, Van Rietbergen B, Odgaard A, Huiskes R, Cown SC. The anisotropic hooke's law for cancellous bone and wood. Journal of Elasticity. 1999;53:125-46.

61. Seto J, Gupta HS, Zaslansky P, Daniel Wagner H, Fratzl P. Tough Lessons From Bone: Extreme Mechanical Anisotropy at the Mesoscale. Advance Function Materials. 2008;18(13):1905-11.

62. Dendorfer S, Maier JH, Taylor D, Hammer J. Anisotropy of the fatigue behaviour of cancellous bone, Journal of Biomechanics. Journal of Biomechanics. 2008;41(3).

63. Fratzl P. Collagen and the Mechanical Properties of Bone and Calcified Cartilage. In: Currey JD, editor. Collagen structure and mechanics: Springer US; 2008. p. 397-420.

64. Rho JY, Spearing LK, Zioupos P. Mechanical properties and the hierarchical structure of bone. Medical Engineering and Physics. 1998;20:92–102.

65. Zysset PK, Guo XE, Hoffler CE, Moore KE, Goldstein SA. Elastic modulus and hardness of cortical and trabecular bone lamellae measured by nanoindentation in the human femur. Journal of Biomechanics. 1999;32:1005–12.

66. Randall XN, Vandamme M, Ulm F-J. Nanoindentation analysis as a 2-dimensional tool for mapping mechanical properties of complex surfaces. . Journal of Materials Research. 2009;24(3).

67. Oliver CW, Pharr GM. An improved technique for determining hardness and elastic modulus using load and displacement sensing indentation experiments. Journal of Materials Research. 1992;7(1564).

68. Rayfield EJ. Cranial mechanics and feeding in Tyrannosaurus rex. proceedings of Royal society of Biological Sciences. 2001;271:1451-9.

69. Rayfield EJ. Cranial mechanics and feeding in Tyrannosaurus rex. Proceedings of the Royal Society of London Series B-Biological Sciences. 2004;271(1547):1451-9.

70. Rayfield EJ. Using finite-element analysis to investigate suture morphology: A case study using large carnivorous dinosaurs. Anatomical Record Part a-Discoveries in Molecular Cellular and Evolutionary Biology. 2005;283A(2):349-65.

71. Bates KT, Falkingham PL. Estimating maximum bite performance in Tyrannosaurus rex using multi-body dynamics. Biology letters; The Royal Society 8 660-664. 2012.

72. Margetts L, Smith IM, Leng J, Manning PL. Parallel three-dimensional finite element analysis of dinosaur trackway formation. Numerical Methods in Geotechnical Engineering, In Press. 2006.

73. Falkingham PL, Manning PL, Margetts L. Finite Element Analysis of Dinosaur Tracks. 47th Meeting of the Society of Vertebrate Paleontology; Austin, Texas2007.

74. Kabel J, Rietbergen BV, Odgaard A, Huiskes R. Constitutive Relationships of Fabric, Density, and Elastic Properties in Cancellous Bone Architecture. 1999;25(4):481-6.

75. Natali AN, Carniel, E.L., Pavan, P.G. Constitutive modelling of inelastic behaviour of cortical bone. Medical Engineering & Phy. 2008.

76. Woo DG, Lee TW, Ko CY, Kim HS, Won Y-Y. Biomechanical Tests of Osteoporotic Vertebral Trabecular Bone using Finite Element Analysis Based on Micro-CT. Intl Conf on Biomedical and Pharmaceutical Engineering (ICBPE)2006.

77. Dunmout ER, Grosse IR, Slater GJ. Requirements for comparing the performance of finite element models of biological structures. Journal of theoretical biology 2009;256:96-103.

78. Teoh. SH, Chui. CK. Bone material properties and fracture analysis: Needle insertion for spinal surgery. Journal of the mechanical behaviour of biomedical Materials. 2008;I:115-39.

79. Lieversa B, W. , Waldmana D, V., Pilkey K, A. . Minimizing specimen length in elastic testing of end-constrained cancellous bone. Journal of the mechanical behaviour of biomedical materials. 2010;3:22-30.

80. Panagiotopoulou O, Wilshin DS, Rayfield JE, Shefelbine JS, Hutchinson RJ. What makes an accurate and reliable subject-specific finite element model? A case study of an elephant femur. (in press). 2011.

81. Zach L, Konvickova S, Ruzicka P, editors. Investigation of In-vivo Hinge Knee Behavior Using a Quasi-Static Finite Element Model of the Lower Limb. 5th European IFMBE Conference, IFMBE Proceedings; 2011.

82. Mamat N, Osman AAN, Oshkour A. Numerical measurement of contact pressure in the tibiofemoral joint during gait. International Conference on Biomedical Engineering (ICoBE); Penang2012. p. 27-8.

83. Mollison PL. Stress in the bones. British medical Journal. 1958;22(12-76).

84. Zioupos P. Ageing Human Bone: Factors Affecting Its Biomechanical Properties and the Role of Collagen. Journal of biomaterials application. 2001;15:187-229.

85. Parfitt AM. Relationships between surface, volume and thickness of iliac trabecular bone in aging and in osteoporosis. Implications for the microanatomic and cellular mechanisms of bone loss. Journal of Clinical Investigation. 1983;72:1396-409.

86. Biewener AA, editor. Biomechanics Structures and Systems. Chicago, USA: IRL Press; 1991.

87. Doube M, Kłosowski M, Michał., Wiktorowicz-Conroy M, Alexis., Hutchinson R, John., Shefelbine J, Sandra. Trabecular bone scales allometrically in mammals and birds. Proceedings of Royal society. 2011.

88. Currey JD. The effects of drying and re-wetting on some mechanical properties of cortical bone. Journal of Biomechanics. 1988;21(5):439-41.

89. Currey JD. Bones: Structure and Mechanics. Oxford: Princeton University Press; 2002.

90. Currey JD, Pitchford WJ, Baxter DP. Variability of the mechanical properties of bone, and its evolutionary consequences. Journal of royal society interface. 2007;4:127-35.

91. Wong W. Break a bone. Science Signal [serial on the Internet]. 2012; 5(126).

92. Fujita K, Iwasaki M, Ochi H, Fukuda T, Ma C, Miyamoto T, et al. Vitamin E decreases bone mass by stimulating osteoclast fusion. Nature, Medicine [serial on the Internet]. 2012; 18.

93. Gong H, Zhu D, Gao J, Lv L, Zhang X. An adaptation model for trabecular bone at different mechanical levels. BioMedical Engineering OnLine 2010. 2010;9:32.

94. Ishimoto T, Nakano T, Umakoshi Y, Tabata Y. Changes in bone microstructure and toughness during the healing process of long bones. Journal of Physics-Conference series. 2009;165:606–8507.

95. Wolff JD. Gesetz der Transformation der Knochen. Berlin: Hirschwald. 1982.

96. Donald HE. Wolff's law and the factor of architectonic circumstance. The American Journal of Orthodontics and Dentofacial Orthopedics. 1968;54:803-22.

Thesis own pagination starts

7 DISCUSSION

7.1 Research contributions

7.1.1 Contribution 1: Significance of the level of detail study

In level of detail study, the author has carried out static elastic finite element analyses only. The results show that the assumption of elastic behaviour greatly underestimates the expected maximum stress values in the axially loaded goose femur (and therefore overestimates ultimate strength), even when incorporating (i) a certain degree of complexity in the geometry and assuming generous values for (i) animal weight, (iii) safety factors and (iv) material properties.

The findings highlight that a working estimate of stress-strain response, needed for a quick 'yes' or 'no' decision in a computer program, probably requires undertaking finite element analyses that incorporate more realistic stress-strain responses described by nonlinear constitutive models incorporating anisotropic material properties. This needs to be addressed in the future and may be seen in future papers.

There is a tight time constraint in the stress analysis. As stated at the beginning of the thesis, there is a need to evaluate, in less than 1 second, whether a bone might break in a certain loading regime. The thesis shows that elastic analyses are not fit-for-purpose. So to do this, another strategy needs to be found. A possible approach (that is finding its way into engineering analysis) is to parameterize a more complicated analysis using emerging numerical techniques such as model order reduction (Margetts et al., 2011; Goury et al., 2011)

In a broader context (beyond the needs of gait simulation), this work is of major significance in research that uses computer simulation in studies of bone. Until now, there appear to be no journal papers or other scholarly work published where a ‘level of detail’ study has been carried out in the context of FEM based simulation of bone. In the field of palaeontology, Rayfield (2001, 2004, 2007, 2011) has been one of the most prolific authors, using FEM for bone mechanics to study dinosaurs. However, none of her papers takes this type of study into account. In most of the papers, bones are treated as solid objects that have small strain linear elastic material behaviour. As

this thesis has shown, assuming bones to be solid over-estimates their strength (as there is more material over which the load can be supported), which is further compounded by an over-estimation of strength due to the elastic assumption. These factors may lead to erroneous scientific interpretations, especially in palaeontology where living examples cannot be studied and therefore there is little opportunity for verification and validation of the analyses.

When the work in this thesis was being carried out, the author did wonder about the validity of the analyses reported in (Panagiotopoulou et al., 2011). This paper has recently been criticized by the scientific community and has been retracted (RetractionCall, 2014). The paper is a study of an elephant femur and the call for retraction questions both the methods of measurement used and the validity of the FE procedures followed.

The FEM modelling of bone as a solid, as in (Panagiotopoulou et al., 2011), seems to be a generally accepted "malpractice" in the literature. That is exactly why in the level of detail study undertaken in this thesis, the simulated results are compared for different levels of details. The conclusion of the elephant femur paper states that experimental models matched quite well with the simulation data. However, the comparison was carried out in a subjective manner where even the regions and the resolutions of the both the data sets (experimental and simulation) did not match well. Analyses that use the FEM are sensitive to resolution and this particular issue should be handled carefully.

The paper's last author, John Hutchinson, tells Retraction Watch:

"Between April and July 2014 the Royal Veterinary College held an investigation regarding the paper: J. R. Soc. Interface (2012) 9, 351–361, following a receipt of a complaint. This investigation included the involvement of an external expert to review all raw data and analysis, and an interview panel held with the authors on 15th July. The investigation found that the methods used to validate the theoretical models though experimental measurements were scientifically invalid, thus making the conclusions of the paper flawed. The panel recommended that this paper should therefore be retracted, a conclusion also reached by the authors of the paper after reviewing the findings from the external expert. The journal was kept informed

throughout the process and the authors asked the journal editors to retract the paper, which has been done on 20 August 2014."

Therefore, the work carried out in this thesis is particularly timely and the level 3 model (with a hollow bone and separate material properties for the cortical and cancellous bone), improved in future work with elasto-plastic material behaviour, may give reasonable predictions of the response to loading.

7.1.2 Contribution 2: Significance of the review of the derivation of elastic properties

When looking for typical values of material properties to put into the finite element analysis program, the author found that there was a huge range of values for the Young's modulus across species and individuals. An essay on the sources of this variation has been written up as a journal paper, *"The stiffness of bone"*, submitted to the Journal of PLoS-ONE. However, just to discuss some major shortcomings, in the literature to date, there appears to be no systematic study of the Young's modulus of bone. In finite element analyses, reported in the literature, "mean" values or "typical" values are used. These may not give the analyst the best insight into bone behaviour. Diseased bone, which is likely to be encountered in patients requiring hip replacements, is less stiff than healthy bone – but hip replacement simulations may use "typical" values. The author recommends that the community carries out a systematic review of the values of the Young's modulus present in the literature and designs a series of experiments to define a set of "guide charts" for material properties, so that users of the FEM can select values that are closest to the correct ones for their particular type of analysis. These charts would take into account variation due to experimental method (used to determine Young's modulus), biological factors and mechanical condition for a particular species.

The output of this proposed activity is especially useful for those working in the field of FEM as it may improve best practice in the simulation of bone using the FEM and therefore make the FEM technique more reliable.

7.1.3 Contribution 3: Significance of doing mechanical testing using digital image correlation

The study of the progression of strain in the *Branta leucopsis* bone has provided excellent examples of several deformation mechanisms that occur internally in the bone in response to the externally applied load. This is especially useful in the study of bones under locomotion, where forces from different directions (muscles, joints or bones themselves) can lead to internal bone damage that is not possible to observe otherwise.

This work is a significant contribution to research as there is no other example of this type of study in the literature, particularly for a whole long bone. Work by other authors focuses on the stress-strain response of cubes of trabecular bone to derive effective elastic properties. Furthermore, this work is particularly important as a verification and validation exercise for future high resolution (or micro-structurally faithful) FEM modelling of bone. An accurate numerical method needs to incorporate both brittle and ductile mechanisms as the experimental work shows that both these mechanisms operate at the same time to accommodate the applied load. Therefore, the output of this work is a very useful contribution to those using computers to simulate the stress-strain response of bone.

7.1.4 Contribution 4: Significance of Dinosaur experiment using *Tyrannosaurus rex's* humerus

The paper presented in chapter 5 is an example of the use of FE modelling in Palaeontology. The objective of the study was to seek insights into the pathology of *Tyrannosaur rex's* humerus and assess the strength of the bone after healing. The pathology is a purported tendon avulsion injury and this type of injury is one of the "failure" modes for bone that needs to be incorporated into the gait simulation program. It is therefore a key part of the research presented in this thesis. Using this example, I have highlighted the usefulness of advanced numerical methods (here FEM) in the traditional sciences (here Palaeontology). This work is of broad scientific and public interest because using computer modelling, it is possible to accurately study the life of extinct animals and demonstrate how they might have lived in the past.

7.2 Justification of assuming linear elastic bone behaviour

The main objective of this study was to investigate whether a linear elastic analysis is good enough to predict failure, as required in our gait simulations. To enhance the linear elastic modelling, a study of the effect of varying geometrical complexity and mesh resolution was carried out. It was determined that even varying three factors i.e. (i) geometrical complexity (ii) mesh resolution and (iii) separate material properties for each bone component (with homogenization for the cancellous bone), the elastic assumption still does not prove useful. This is because the finite element results predicted a safety factor of 18, which is far too high and therefore not realistic. Corresponding with this high safety factor, the stress values obtained using these elastic analyses, for a conservative estimate of applied load and material properties, were very low (64 MPa) compared to the ultimate compressive strength of the bone i.e. 200 MPa. The correlation between analysis results and the strength values reported in the literature is poor. A better estimation of failure strength may be obtained using a nonlinear elasto-plastic constitutive model, with anisotropic material properties. With more realistic material behaviour, it is expected that the predicted stress values will be closer to the ultimate failure stress values for bone reported in literature.

As well as the use of more realistic constitutive models, there is a need to test the response of bone to other loading regimes. For example, models of bone subject to 3-point or 4-point bending will have a different response to the same models subject to axial compression. Under 3-point or 4-point bending, the finite element models may experience larger displacements and higher stresses when smaller loads are applied, compared to compressive loads as in the *Branta leucopsis* study.

The purpose of the research has been to look at the incorporation of skeletal loading into the gait simulation software, GaitSym. Until now, skeletal loading is a factor that has not been considered. The genetic algorithm operates on populations of individuals which evolve as the simulation progresses forwards in time. In computing terms, each individual is evaluated using a single CPU (core in a multi-core processor) in less than 1 second. The researchers who develop GaitSym use highly parallel multi-processor systems for their work as the total run time for a

simulation becomes very large considering a population of individuals evolving over generations. Therefore, to evaluate whether bones will break, this needs to be done in as short a time as possible. For example, adding another 1 second of computation for each individual may double the run time of the analysis. It is for this reason (computational cost), that elastic analysis has been considered for incorporation into GaitSym. Elastic analyses can be carried out very quickly and it was believed that elastic analysis could be used in the program to obtain a 'yes' or 'no' answer (in less than a second) as to whether a bone would break due to skeletal loading.

In contrast, if more realistic, nonlinear constitutive models for bone are used in the stress analysis, the run times may increase by hours for each individual in a population. The run times of the gait simulation would then increase to such an extent that the methodology would no longer be practical. As a preliminary approach, the linear elastic assumption is justified. However, the research presented in this thesis clearly demonstrates that linear elastic analysis is not good enough for failure prediction in the GaitSym program. This in itself is a very useful result.

Another success of the study is the building a finite element model of a complete vertebrate long bone that includes all the internal microstructure. This is the first time that this has been achieved, but it was not possible to run the full analysis on the same workstation that was used to generate the model.

7.3 Assumptions of mode of failure

Fracture in this study is the most conservative criterion for the failure of bone, considering the stance phase of locomotion. At the point (just after the yield point) when the fracture is induced, the forces on the bone become too high and the bone can no longer support locomotion. As mentioned earlier, the purpose of this study is to quickly check if the bone breaks or not in response to the application of the external forces. The genetic algorithm therefore needs something really simple to understand. Simple fracture is an easy input to test solutions produced by the genetic algorithm. This is strongly dependent on the correct alignment and the application of load on bone. All other modes of failure, for example the greenstick fractures and comminuted fractures described in the background chapter, are too difficult to describe in a simple computer algorithm, so that the genetic algorithm can detect

whether or not these mechanisms occur. Furthermore, these modes of failure would need to be described by complex constitutive models (of failure and damage) in the finite element program.

This work could be extended to look at other failure modes, including various types of fracture, as well as a wider choice of loading scenarios for a range of vertebrates. This would serve as a verification and validation exercise for the "simple" scenarios that would need to be implemented in the gait simulator.

7.4 Assumption of static loading - sufficient for Gait study?

The aim of the evolutionary robotics program is to output a sensible set of gaits for a particular extinct or extant vertebrate. The objective of the thesis is to introduce stress analysis as a criterion in the genetic algorithm. Static loading may not be a good assumption for the tests in this thesis as the bones are subject to complex loading patterns generated by muscles and tendons attached to the skeleton. Static loading is only a starting point to evaluate whether linear elastic analyses can give a quick, approximate assessment as to the strength of a bone.

In a typical gait set, a long bone (femur, tibia or fibula) is oriented vertically such that the load of body is distributed across the whole bone anteriorly and/or posteriorly in a stance or swing phase e.g. the scenario as used in (Christen et al., 2014). In locomotion studies (Alexander, 2003), femur models used for locomotion are created in a way that they are sufficiently simple as to be understandable and tractable, but not so simple that they stray far from biological reality. Therefore, in order to achieve a biological reality in the bone models used in this thesis, there is a need to parameterize a more complicated analysis for complex loading scenarios. This may be achieved using emerging numerical techniques such as model order reduction (Goury et al., 2011).

In the finite element modelling of the *Branta leucopsis* femur carried out in this thesis, the possible influence of muscle mass is ignored. This assumption may have an influence on the results. However, in animals such as tortoises where speed is completely unimportant with very low muscles proves that it is economical of energy cost (Woledge et al., 1985). This may means, it is OK to avoid muscle mass

to some extent. Speed is a result of particular gait pattern, and gaits are chosen by nature. In walking animals, the speed is the biggest issue which can be alleviated by appropriate choice of gait pattern. For this there is need of pool of gaits generated in the stance, swing and heel-off phases of locomotion. Among which the ones with the lowest energy cost, and higher stability can be chosen as a good solution for the evolutionary algorithm.

Static loading does not provide a complete picture of the pattern of loading a bone experiences during a particular gait, but it does provide a reasonable starting point as set out in this thesis.

7.5 GaitSym then and now

GaitSym, the forward dynamics simulation program (explained in chapter 1 and chapter 2), only has the capacity to take as input 2D skeletons, which it uses to generate locomotion patterns. Regarding one of the future extensions of this program, the addition of stress analysis, the study undertaken in this thesis will prove useful. It shows that linear stress analysis is not appropriate for evaluating whether forces generated for particular gaits will damage the animal's own skeleton.

Even using different levels of detail (as described this study), it is not possible to estimate which forces are suitable for the bone in reference to the specific geometrical model. Solid models give rise to significant underestimates of bone stress in locomotion. Models that are even more complicated (but still linear elastic) do not give reasonable predictions of the response to loading, i.e. a hollow bone with separate properties for cortical and cancellous bone.

7.5.1 2D models and their simplicity

The use of 2D models is a simple way to deal with the complexity of the problems that we encounter in traditional biology and biomechanics. It is a good preliminary solution for a given problem but does not reflect the 3D anatomy of vertebrates, which is required for accuracy and reliability. Therefore, geometry in terms of anatomy and internal detail is a very important focus in the area of advanced sciences these days to map the problems to a virtual reality environment.

Regarding anatomy some biomechanical parameters e.g. muscle mass, moment arm, physiological cross sectional area are important variables to consider before doing any modelling. However the solid mass that occupies matter in the specimen is a significant pointer for accurate and reasonable estimation for segmentation. The biomechanical parameters are not very useful if the functional anatomy is not considered. For example, a hollow cylinder will move faster and quicker than a solid cylinder or a semisolid cylinder. Whereas a hollow cylinder is easier to break than a solid one under the same load. Similar is the case with the bone due to a cylindrical analogy. The mass inside the bone and that surrounds the bone are equally important as other biomechanical parameters.

7.5.2 Models of GaitSym so far and requirement of GA optimization

I. Evolutionary robotics employs numerical optimization methods as well as the use of principles of Newtonian physics.

II. 2D models are too simple for estimations.

III. Determining analytical solutions for locomotion is not possible, hence computer based numerical models are required.

IV. In the future, it will be possible to adapt the genetic algorithm in GaitSym to take into account whether the owner's skeleton will be damaged during locomotion.

7.6 Application of FEA in general on extinct vertebrates

During the fossilization process, there is a loss of information regarding the internal structure of ancient bones and the material properties due to burial and mineralization. However, the FEM as addressed in this thesis can still prove advantageous for such types of problems.

It is already inferred in this study that the assumption of solid linear elastic bones is not a good solution. There needs to be more complex modelling assumptions for bone in order to obtain reasonable answers. Therefore, in situations where it is difficult to determine the internal microstructure, as in extinct vertebrates, techniques like the FEM and scaling methods can be used in combination with one

another. Features observed in the living vertebrate relatives of dinosaurs can be scaled up or down according to the dimensions of the dinosaur bone. Moreover, in dinosaur biology, the biggest argument is about the absolute values of material properties of tissues and bones. This is again due to the fact that soft tissue is not preserved in the fossilization process. Computational approaches such as the FEM are advantageous, as it enables quantifiable and repeatable experiments to be carried out, whereby the unknowns, such as material properties, can be estimated. Computer models can easily be modified to test the sensitivity of the results (and therefore the insights they give) to assumptions made about geometry and material properties.

A mesh of a dinosaur bone, created from tomography data, may comprise millions of elements. Based upon the computational resources available; a model may be down sampled to adjust the memory requirements of the model.

In the future, the author looks forward to apply this technique on human bone in the study of human locomotion. The advantage of using human models is that material properties, bone stress-strain response and locomotion patterns are easier to study.

7.7 Problems encountered in this research

In this section, the author discusses some of the limitations and problems encountered in this thesis.

7.7.1 X-ray CT and suggested improvement

1. Hollowing affect due to rig artifact

The word, “hollowing” is from the shape of the cylinder. This arose because of the air space of the tube in which the bone was held during scanning. It has a grey scale value similar to the trabecular bone. This artifact was observed in the last few slices of the scanned images where there was no bone mass detected, therefore it was rectified by removing those slices using thresholding. This ultimately helped in the clean segmentation of *Branta leucopsis* bone for digital image correlation.

2. Particles from abrasive paper

In the mechanical testing experiment, when the load was increased, the bone was pressed against the abrasive paper. Abrasive paper particles were observed in the last few slices of the scan where no bone mass was detected. Such unwanted slices were hence removed for clean reconstruction of the image data to differentiate trabecular bone mass from the particles from abrasive paper.

3. Shadowing effect

While the CT scan of the *Branta leucopsis* femur was carried out, there was a possibility of a shadowing effect. This shadow would be cast by the steel platens, as steel platens are denser than bone. To overcome this, epoxy resin was used on the top of both platens, serving to reduce the possibility of the shadowing effect occurring.

7.7.2 FEA of *Branta leucopsis* and suggested improvements

There were some problems experienced in performing the FEA of the *Branta leucopsis* femur. Some of the improvements have already been introduced into the work carried out in this thesis and others are noted for the future.

1. Stripe affects in FEA of *Branta leucopsis*

In regards to the FEA of the extant bone (SF320), a peculiar pattern of striping was observed in the results of the first stress analyses carried out, as shown in the figure 7.1. This effect was thought to rule the FEA results as erroneous. The effect was thought to originate due to problems in the finite element mesh.

Later in the modelling work, through careful reviewing and using quick test runs on the smallest models, it was found that the stripe effect arises due to a specific "compound" coarseness of the mesh on some parts of bone. Compound coarseness in the Simpleware Ltd software is a measure of the overall aspect ratio of the target edge lengths of elements. The software, in response to a user defined target error, obtains a particular compound coarseness value during the meshing process. The effect was fixed (figure 7.2), achieving a reasonable value for compound coarseness, by manual experimentation with the meshing parameters.

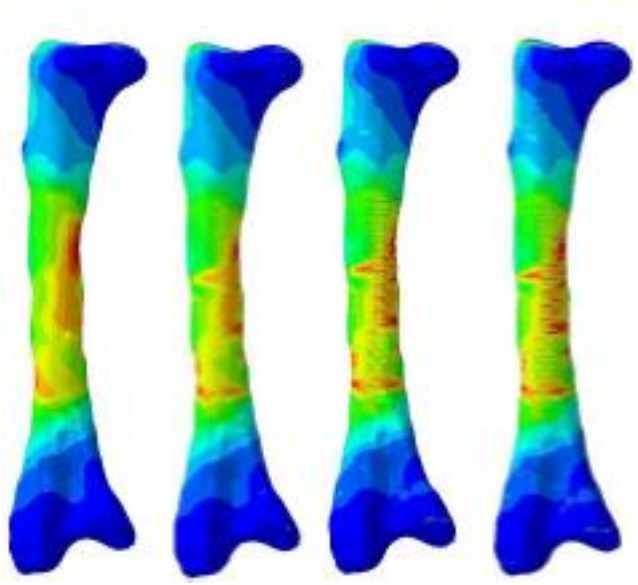

Figure 7-1 SF320' femora with stripe effect in the middle of the shaft (images from level 2, model 1-4).

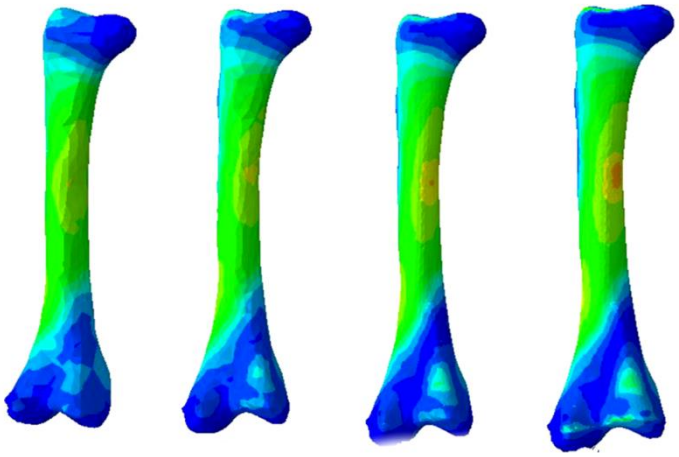

Figure 7-2: SF320 Femora after compound coarsening (images from level 2, model 1-4).

7.7.3 Mounting methods and suggested improvements.

It is well known that, in reality, the response of bone to loading, regardless of elasticity and inelasticity, depends on the direction of (applied) loads. Any misalignment of a bone during a test may therefore lead to the wrong results and/or interpretation. Before applying any load it should be considered that the load needs to sit on the head exactly in line with the neutral axis of the bone (Cristofolini et al., 2010). This attention to detail may help ensure that any experimental or modelling carried out is realistic. If the neutral axis is aligned with the direction of load, an ideal solution can be obtained. However, in nature a neutral axis is never fixed.

Usually, a neutral axis is considered such that it includes least mass of of the bone (in terms of mass) in order to comply with minimum weight analysis theory (Currey, 2002).

A careful analysis of the results obtained from the mechanical testing highlighted some limitations in the work carried out in this thesis. Therefore, it was proposed not to compare the results from the mechanical testing with the modelling experiments using FEM. These limitations include:

1. The bone slipped off the neutral axis when the first loading increments were applied. This was despite testing the mounting methodology using other samples.

2. Creep that arose due to the two following causes:

i. The time taken by the microCT scanner to capture data for each load step (i.e. 45 minutes generating 2100 projections).
ii. A technical fault in the Nikon 320kV Custom bay when the tungsten filament burned out. A delay in repairing the scanner lasted for 14 hours.

Another cause of uncertainty in the results came from the mechanical experiment due to a technical problem in the rig. It was suggested by the laboratory technician that the forces measured by the micro-compression test rig are half what is actually applied. At the time of writing, the validation of this measurement is still unknown. Instead of using results from the physical tests in the FEA of the *Branta leucopsis* femur, the work in this thesis applied the maximum weight of an adult goose multiplied by a maximum safety factor. The reason this load was used was to estimate the maximum possible weight can be applied to a goose bone before it will break. Therefore 540N (9kg x 10N/m2 x max safety factor (i.e. 6)) was applied to the bone in the simulations.

7.7.4 Mechanical test and suggested improvements

The reliability of the results obtained through the mechanical testing can be assessed by carrying out another test on some other material with a known analytical solution and comparing the force and displacement values of both (i.e. from MicroTension

compression and analytical solution). This will confirm if the laboratory technician's assessment of a technical problem is correct.

7.7.5 Modelling technique and suggested improvements

In the FEA of *Branta leucopsis*, results obtained from the physical testing were not used for correlation; instead several assumptions were used regarding material behaviour especially assuming bone, a linear elastic material with isotropic material properties. The purpose of the linear analysis to be used in this study was to know how bone behaves within the elastic regime because in locomotion study, the functional strength is very important to considered, in the plastic regime, bone deforms hence no locomotion. Another reason of using elastic analysis is to quickly check in yes or no if the bone will break or not under elastic analysis.

Results from the FEA can be validated with the mechanical testing experiment, after all the technical problems with the rig and testing protocols have been fixed as discussed earlier.

7.8 Challenges encountered

This section describes some of the challenges encountered during this research that were not overcome.

7.8.1 Boundary conditions in Level 4

Level 4 is the most challenging FEA model handled during this research. The model includes all the internal micro-structure and is the largest of all the models created. The model was generated using Simpleware's grid meshing algorithm. Boundary conditions for all the levels of detail were applied using Abaqus CAE. This was not possible for level 4, as the mesh was too large to open in the Abaqus CAE software, even using a workstation with 64GB RAM. This model could be run using ParaFEM, but only if new software is written to apply the boundary conditions first (Margetts, 2009).

In order to validate the results achieved from Abaqus CAE with the result obtained from ParaFEM, the '.inp' file of the simplest level of detail i.e. level 1-model 1 can

be chosen to run in ParaFEM in order to check if ParaFEM gives the same answer as Abaqus CAE. Due to time limitations, it has not been implemented yet.

7.8.2 Computational cost

Another significant parameter to consider is the ‘solution time’ of the finite element modeling, which has to be comparable with the solution time taken by GaitSym. At the moment, GaitSym takes less than a second to evaluate a proposed gait for each individual in a population. An outstanding objective of this project is to achieve a solution time of less than 1 second for the stress-analysis for each individual in the population.

8 Future work

The work undertaken in this research has been applied for a particular vertebrate model (i.e. *Branta leucopsis*) using one testing method (i.e. uniaxial compression) and assuming elastic bone behaviour in the finite element analysis. The results therefore obtained are specific to this model under the specific assumptions as detailed in the discussion section. These factors are some of the drawbacks of this study, which are well recognized by the author.

It has been stated earlier in the thesis and in the level of detail paper that the safety factor obtained from this study is too high (18) to be considered realistic. Furthermore, the predicted stress values are too low (64MPa) when compared with the ultimate failure stress (typically 180-200MPa) of bone. Therefore, further steps that can be taken in the future to improve this work are listed below:

1. FE analyses need to be carried out in order to investigate how bone behaves when a non-linear constitutive model of material behaviour is used. Furthermore, the effect of the soft tissues on the mechanical behaviour of bone need to be studied. For example, future models may incorporate muscle mass, soft tissues and tendons.

2. Different loading scenarios need to be studied – to see whether these are important regarding the "level of detail" of FEM simulations. For example the response of bone to bending tests, where small forces can induce larger displacements and higher stresses, would be of interest. Different bone alignment/configuration tests need to be carried out in terms of mechanical testing (experimental work), as well as future FEM simulation, as a verification and validation exercise.

3. The work needs to be greatly expanded to look at bones in a wide range of living vertebrates. Experiments on one specimen of one vertebrate is not good enough to derive any general insight about the response of bones to loading in locomotion across all vertebrates.

4. In future work, bone must be modelled as a non-linear material. The requirement to carry out the simulation in less than 1 second will remain, so

incorporating non-linear behaviour needs to be done in some smart way. This could involve the use of better homogenization methods e.g. one used in (Makowski and Kuś, 2014) may be applied by adding a buffer zone that surrounds the trabecular bone. Moreover, methods such as model order eduction where numerical complexity can possibly be reduced, may be a good choice as well in future.

5. In this thesis, it was not possible to run an analysis for the full FE model (that meshed all the trabecular bone as micro-structure) due to difficulties in pre-processing. That said, these difficulties may be overcome in the future so that the full FE model can be run using elastic and elasto-plastic finite element analysis. The results of this model can be compared with the CT data of the incremental axial loading test, thus validating the FE modelling.

6. The major outstanding piece of work is the incorporation of FEA into the gait simulation program, Gaitsym. This needs to carried out, keeping in view the preliminary questions that have been addressed and answered in this research.

7. In life sciences, especially, one of the most studied vertebrates are human beings (*Homosapions*). It is suggested that human models are used in future work for verification and validation of the incorporation of FEA into the gait analysis software. The gait of humans, from the point of view of speed, energy consumption and forces on the skeleton is well known.

8. The combined FEA and gait analysis program needs to be tested to ensure that suitable gaits are accepted or rejected on the basis of skeletal loading and the probability of failure of bones in the skeleton.

9. At the time of writing, a full skeleton of a *Branta leucopsis* has not been created for use in the gait simulation program. Therefore, this project can be extended by developing the *Branta leucopsis* (SF320) skeleton for GaitSym.

By carrying out the future work outlined above, the original objectives of this research project will be completed, contributing to studies in animal locomotion science and the further use of the finite element method in biomechanics research.

REFERENCES

Adleman, L. & Huang., M. (Year) Recognizing primes in random polynomial time. *In:* In Proceedings of the 19th ACM Symposium on the Theory of Computing,, 1987. ACM, New York, 462-469.

Alexander, R. M. (1981) Factors of safety in the structure of animals. *Science Progress (Oxf.),* 67**,** 109–130.

Alexander, R. M. (1984) Optimum strengths for bones liable to fatigue and accidental fracture. *Journal of theoretical biology,* (4)**,** 621-36.

Alexander, R. M. (1989) *Dynamics of Dinosaurs & other extinct giants.*: Columbia University Press, Chichester, .

Alexander, R. M. (2003) *Principles of Animal Locomotion*. New Jersey.: Princeton University Press.

Allaire, G. & Brizzi, R. (2005) A multiscale finite element method for numerical homegization. *Multiscale modelling and simulation,* 4**,** 790-812.

Alotta, G., Failla, G. & Zingales, M. (2014) Finite element method for a nonlocal Timoshenko beam model. *Finite Elem. Anal. Des.,* 89**,** 77-92.

Ara, N., John, M., David, Z., Ralph, M. l. & Brian, D. S. (2007) Densitometric, morphometric and mechanical distributions in the human proximal femur. *Journal Biomechanics*, 40**,** 2573–2579.

Arbenz , P. & Müller, R. (July, 2008) Microstructural Finite Element Analysis of Human Bone Structures. *ERCIM, Special edition: Supercomputing at Work.* Zurich, Switzerland.

Ascenzi, A., Bonucci, E. & Bocciare, D. S. (1967) An electron microscope study on primary periosteal bone. *Journal of Ultrastructure Research, ,* 18**,** 605-618.

Bauchau, O. A. & Craig, J. I. (2009) Euler-Bernoulli beam theory. *Structural Analysis, Solid Mechanics and Its Applications* 163**,** 173-221.

Beaupr´e, G. S., Orr, T. E. & Carter, D. R. (1990) An approach for time-dependent bone modelling and remodeling - application: a preliminary remodelling simulation. *Journal of Orthopaedic Research* 8**,** 662-70.

Belill, K. A., Settle, T. L., Angel, C. R., Kim, S.-W. & Rothwell, S. W. (2014) Femoral Strength after Induced Lesions in Rats (Rattus norvegicus). *Comparative Medicine,* 64(3)**,** 186-192.

Benoit, A., Guerard, S., Gillet, B., Guillot, G., Hild, F., Mitton, D., Pierie, J.-N. & Roux, S. (2009) 3D analysis from micro-MRI during in situ compression on cancellousbone. *Journal of Biomechanics,* 42**,** 2381–2386.

Berkelmans, W. M., Schreurs, P. G. & de Vree, J. P. (1992) Continuum damage mechanics for softening of brittle materials. *Acta Mechanica,* 93**,** 133–143.

Bevill, G. & Keaveny, M. T. (2009) Trabecular bone strength predictions using finite element analysis of micro-scale images at limited spatial resolution. *Bone,* 44**,** 579-584.

Biewener, A. A. (ed.) (1991) *Biomechanics Structures and Systems,* Chicago, USA: IRL Press.

Biewener, A. A. (1993) Safety Factors in Bone Strength. *Calcified tissue international,* 53**,** S68-S74.

Blob, R. W. & Biewener, A. A. (1999) In vivo locomotor strain in the hindlimb bones of alligator mississippiensis and iguana iguana: implications for the evolution of limb bone safety factor and non-sprawling limb posture. *Journal of Experimental Biology,* 202(9)**,** 1023-1046.

Boyce, T. M., Fyhrie, D. P., Glotkowski, M. C., Radin, E. L. & Schaffler, M. B. (1998) Damage type and strain mode associations in human compact bone bending fatigue. *Journal of Orthopaedic Research,* 16(3)**,** 322-329.

Boyda, S., Macdonalda, H. & Hanley, D. (2008) Measuring bone strength from in vivo micro-CT using the finite element method. *International Conference on Osteoporosis and Bone Research 2008.*

Brassey, A. C., Margetts, L., Kitchener, C. A., Withers, J. P., Manning, L. P. & Sellers, I., William. (2013 (in press)) Finite element modelling versus classic beam theory: comparing methods for stress estimation in a morphologically diverse sample of vertebrate long bones. *Journal of royal society interface,* 10**,** 79.

Brassey, C. A., Kitchener, A. C., Withers, P. J., Manning, P. L. & Sellers., W. I. (2013a) The Role of Cross-Sectional Geometry, Curvature, and Limb

Posture in Maintaining Equal Safety Factors: A Computed Tomography Study. *The Anatomical Records,* 296**,** 395-413.

Brassey, C. A., Margetts, L., Kitchener, A. C., Withers, P. J., Manning, P. L. & Sellers, W. I. (2013b) *Finite element modelling versus classic beam theory: comparing methods for stress estimation in a morphologically diverse sample of vertebrate long bones*. *Journal of The Royal Society Interface,* **10** (79).

Breder, C. M. (1926) The locomotion of fishes. *Zoologica-New York* 4**,** 159-297.

Breder, C. M. & Edgerton, H. E. (1942) An analysis of the locomotion of the seahorse, Hippocampus hudsonius, by means by of high speed cinematography, . *Annals of the New York Academy Sciences,* 43**,** 145-172.

Brekelmans, W., Poort, H. & Slooff, T. (1972) A new method to analyse the mechanical behaviour of skeletal parts. *Acta Orthopaedica Scandinavica.* , 43(5)**,** 301-17.

Brown, D. T. (2004) Finite Element Modeling in Musculoskeletal Biomechanics. *Journal of applied biomechanics,* 20**,** 336-366.

Callum, F. R. (2005) Finite Element Analysis in Vertebrate Biomechanics. *Anatomical Record Part A* 283A**,** 253-258.

Carpenter, K. & Smith, M. (2001) Forelimbs Osteology and biomechanics of Tyrannosuarus rex. *Mesozoic vertebrate life.* Indian University press.

Carter, D. R., Vasu, R. & Harris, W. H. (1982) Stress distributions in the acetabular region-II. *Journal of Biomechanics,* 15(3)**,** 165-70.

Chabanas, M., Payan, Y., Mar´ecaux, C., Swider, P. & Boutault, F. (Year) Comparison of Linear and Non-linear Soft Tissue Models with Post-operative CT Scan in Maxillofacial Surgery. *In:* ISMS, LNCS., 2004. 19–27.

Chiang, C. K. & Wang, J. L. (2006) Strain energy density variations of osteoporotic spine column after bone segment augmentation - An in vitro porcine biomechanical model. *Journal Biomechanics,* 39**,** 16.

Chinsamy-Turan, A. (2005) Deciphering Biology with Fine-scale Techniques. *The Microstructure of Dinosaur Bone.* Baltimore and London: The John Hopkins University Press.

Christen, P., Ito, K., Ellouz, R., Boutroy, S., Sornay-Rendu, E., Chapurlat, R. D. & van Rietbergen, B. (2014) Bone remodelling in humans is load-driven but not lazy. *Nat Commun,* 5.

Cooper, J. (2006) *Improving Performance of Genetic Algorithms by Using Novel Fitness Functions.* PhD, Loughborough University.

Cristofolini, L., Schileo, E., Juszczyk, M., Taddei, F., Martelli, S. & Viceconti, M. (2010) Mechanical testing of bones: the positive synergy of finite -element models and in vitro experiments. *Philosophical transactions of Royal Society.,* 308**,** 2725-2763.

Crowninshield, R. D., Brand, R. A., Johnston, R. C. & Milroy, J. C. (1980) An analysis of femoral component stem design in total hip arthroplasty. *Journal of bone and joint surgeory,* 62**,** 68–78.

Currey, D. J. (1962) Stress concentrations in bone. *Journal of microscopical Science,* 103**,** 111-133.

Currey, J. D. (1999) What determines the bending strength of the compact bone? *The journal of experimental biology,* 202**,** 2495-2503.

Currey, J. D. (2002) *Bones: Structure and Mechanics*. Oxford: Princeton University Press.

Das, R. & Cleary, W., Paul. . (2006) Uniaxial compression test and stress wave propagation modelling using sph. *Fifth International Conference on CFD in the Process Industries.* CSIRO Mathematical and Information Sciences, Clayton, Victoria 3168, AUSTRALIA.

Deng, H.-w., Liu, Y.-z. & Guo, C.-Y. (eds.). (2005) *Current topics in bone biology,* Singapore/SG: World Scientific Publishing Co Pte Ltd.

Doube, M., Kłosowski, M., Michał., Wiktorowicz-Conroy, M., Alexis., Hutchinson, R., John. & Shefelbine, J., Sandra. (2011) Trabecular bone scales allometrically in mammals and birds. *Proceedings of Royal society*.

Ebinger, T., Steeb, H., Diebels, S., Ripplinger, W. & Tjardesy, T. (2005) A biomechanical model based on a FE^2 approach using data from computer tomography. *In:* VIII, C. (ed.) *VIII International Conference on Computational Plasticity.*

Elizabeth, A. Z., Bernd, G., Eric, S., Björn, B. & Robert, O. R. (2014) Fracture resistance of human cortical bone across multiple length-scales at physiological strain rates. *Biomaterials,* 35**,** 5472-5481.

Fagin, R. (1973) *Contributions to the model theory of finite structures.* Ph.D thesis., U.C. Berkeley.

Farlow, J. O., Gatesy, S. M., Holtz, T. R., R., H. J. J. & Robinson, J. M. (2000) Therapod Locomotion. *American Zoologist,* 40**,** 640-663.

Gao, H. & Ji, B. (2004) Mechanical properties of nanostructure of biological materials. *Journal of the Mechanics and Physics of Solids,* 52**,** 1963-1990.

Gao, H. J., Ji, B. H., Jager, I. L., Arzt, E. & Fratzl, P. (Year) Materials become insensitive to flaws at nanoscale: lessons from nature. *In:* Proc. Natl. Acad. Sci. USA 2003 USA. 5597–600.

Gauthier, J. (1986) Saurischian Monophyly and the Origin of Birds. *Memoires of the California Academy of Sciences* 8(1-55)**,** 145.

Gebhardt, W. (1906) Uber funktionell wichtinordnungsweisen der feineren und groberen Bauelemente des Weibeltierknochen. II. Spezieller Tiel. Der Bau der Haversschen Lamellensysteme und seine funktionelle Bedeutung. *Arch Engtwickl Mech Org,,* 20**,** 187.

Genuth, S. M. (ed.) (1998) *The Endocrine System In: Berne, Physiology.*: Mosby, St. Louis.

Georgeanu, V., Atasiei, T. & Gruionu, L. (2014) Periprosthetic Bone Remodelling in Total Knee Arthroplasty. *Mædica,* 9(1)**,** 56-61.

Gercek, H. (2007) Poisson's ratio values for rocks. *International Journal of Rock Mechanics and Mining Sciences,* 44(1)**,** 1-13.

Goury, O., Kerfriden, P. & Margetts, L. (2011) Rationalised computational time in fracture simulation: adaptive model reduction and domain decomposition. *International Conference on Extended Finite Element Methods* Cardiff, UK.

Guilherme, G. J. M. & da Silva, K. L. J. (2004) On the scaling of mammalian long bones. *The Journal of Experimental Biology,* 207**,** 1577-1584.

Guillet, A., DOYLE, W. S. & RÜTHER, H. (1985) The combination of photogrammetry and finite elements for a fine grained functional analysis of anatomical structures. *Zoomorphology,* 105**,** p51-59.

Gulati, S. T., Westbrook, J., Carley, S., Vepakomma, H. & Ono, T. (2011) 45.2: Two Point Bending of Thin Glass Substrate. *SID Symposium Digest of Technical Papers,* 42(1)**,** 652-654.

Gupta , H. S. & Zioupos, P. (2008) Fracture of bone tissue: The 'hows' and the 'whys'. *Medical Engineering & Physics,* 30**,** 1209–1226.

Harrison, N., McDonnell, P., Mullins, L., Wilson, N., O'Mahoney, D. & McHugh, P. (2013) Failure modelling of trabecular bone using a non-linear combined damage and fracture voxel finite element approach. *Biomechanics and Modeling in Mechanobiology,* 12(2)**,** 225-241.

http://www.animalsimulation.org/.

Huiskes, R. & Chao, E. Y. S. (1983) A Survey of Finite Element Analysis in Orthopedic Biomechanics: The First Decade. *journal of biomechanics,* 16**,** 385-409.

Huiskes, R. & Hollister, S. J. (1993) From Structure to Process, From Organ to Cell: Recent Developments of FE-Analysis in Orthopaedic Biomechanics. *Journal of biomechanics,* 115(4B)**,** 520-527.

Hutchinson, J. R. & Gatesy, S. M. (2006) Dinosaur locomotion beyond bones. *Nature,* 440**,** 292-294

Ijspeert, J. A. & Kodjabachian, J. (1991) *Artificial life: Evolution and Development of a Central Pattern Generator for the Swimming of a Lamprey* (Vol. 5): MIT press.

Jennings, A. & de Boer, P. (1999) Should we operate on nonagenarians with hip fractures? *Injury,* 30**,** 169-72. .

Jules, M., Étienne. (1888) The Mechanism of the Flight of Birds. *Nature,* 37**,** 369-374.

Kabel, J., Rietbergen, B. V., Odgaard, A. & Huiskes, R. (1999) Constitutive Relationships of Fabric, Density, and Elastic Properties in Cancellous Bone Architecture. 25(4)**,** 481-486.

Kazuo Tanne, Mamoru Sakuda & Burstone., C. J. (1987) Three dimensional finite analyses for stress distribution in the periodontal tissue by orthodontic forces. *Am J Orthod Dentofacial Orthop,* 92(6)**,** 499-505.

Keaveny, T. M., Morgan, E. F., Niebur, G. L. & Yeh, O. C. (2001) Biomechanics of trabecular bone. *Annu. Rev. Biomed. Eng.,* 3**,** 307–33.

Kemp, T. J., Bachus, K. N., Nairn, J. A. & Carrier, D. R. (2005) Functional trade-offs in the limb bones of dogs selected for running versus fighting. *J Exp Biol.,* 208(Pt 18)**,** 3475-82.

Kim, M. S. & Uther, W. (Year) Automatic gait optimisation for quadruped robots. *In:* Roberts, J. & Wyeth, G., eds. Proceedings of the 2003 Australasian Conference on Robotics and Automation, Brisbane, Australia, 2003.

Kolston, P. J. (2000) Finite element modeling: a new tool for the biologist. *Philosophical Transactions of the Royal Society (Series A: Mathematical, Physical and Engineering Sciences),* 358**,** 611-631.

Lakes, R. (2008) *What is Poisson ratio?* [Online]. Available: http://silver.neep.wisc.edu/~lakes/Poisson.html [Accessed].

Lance, F. (July 7-10, 2003) The Computational Complexity Column. *In:* Dirk van Dalen, John Dawson & Kanamori., A. (eds.) *18th Annual Conference on Computational Complexity* Denmark NEC Laboratories America 4 Independence Way, Princeton, NJ 08540, USA fortnow@nec-labs.com.

Lanir, Y. (1983) Constitutive equations for fibrous connective tissues. *Journal of Biomechanics,* 16(1)**,** 1-12.

Launey, M. E., Buehler, M. J. & Ritchie, O. R. (2010) On the mechanistic origins of toughness in bone. . *The Annual Review of Materials Research.,,* 40**,** 24-53.

Lenaerts, L. & Lenthe, G. H. v. (2008) Multi-level patient-specific modelling of the proximal femur. A promising tool to quantify the effect of osteoporosis treatment. *Philosophical transactions of the royal society,* 367**,** 2079-2093.

Lieversa, B., W. , , WALDMANA, D., V. & PILKEY, K., A. . (2010) Minimizing specimen length in elastic testing of end-constrained cancellous bone. *Journal of the mechanical behaviour of biomedical materials,* 3**,** 22-30.

Long, C. & Siegel, R. E. (1975) The Muyerbridge / Animal locmotion collection at the national museum of American history *Topics in Photographic Preservation, Volume 8,* 8**,** 1-10.

Loong, C.-K., Rey, C., Kuhn, L. T., Combes, C., Wu, Y., Chen, S.-H. & Glimcher, M. J. (2000) Evidence of hydroxyl-ion deficiency in bone apatites: an inelastic neutron-scattering study. *Bone,* 26**,** 599–602.

Lotz, J. C., Cheal, E. J. & Hayes, W. C. (1991) Fracture Prediction for the Proximal Femur Using Finite Element Models: Part I—Linear Analysis. *Journal of Biomechanical Engineering,* 113(4)**,** 353-360.

Main, R. P. & Biewener, A. A. (2007) Skeletal strain patterns and growth in the emu hindlimb during ontogeny. *The Journal of Experimental Biology,* 210**,** 2676-2690.

Makowski, P. & Kuś, W. (2014) Trabecular bone numerical homogenization with the use of buffer zone. *CAMES,* 21(2)**,** 113-121.

Manning, P. L., Margetts, L., Johnson, M. R., Withers, P. J., Sellers, W. I., Falkingham, P. L., Mummery, P. M., Barrett, P. M. & Raymont, D. R. (2009) Biomechanics of Dromaeosaurid Dinosaur Claws: Application of X-Ray Microtomography, Nanoindentation, and Finite Element Analysis. *The Anatomical Record: Advances in Integrative Anatomy and Evolutionary Biology,* 292(9)**,** 1397-1405.

Margetts, L. (2009) *parafem.org.uk* [Online]. [Accessed].

Margetts, L., Ford, R. & Riley, G. (2011) Integration of Scalable Interactive FEA into the Design Process. *5th Autosim Workshop.* Bilbao, Spain.

Margetts, L., Smith, I. M., Leng, J. & Manning, P. L. (2006) Parallel three-dimensional finite element analysis of dinosaur trackway formation. *Numerical Methods in Geotechnical Engineering, In Press*.

Martin, R. B. & Burr, D. B. (eds.). (1989) *The structure, function and adaptation of cortical bone.*: Raven Press, New York.

McCalden R. W., McGeough J. A. & Court, B. C. (1997) Age-related changes in the compressive strength of cancellous bone. The relative importance of changes in density and trabecular architecture. *The Journal of Bone and Joint Surgery,* 79**,** 421–27.

McCalden, R. W., McGeough, J. A. & Court, B. C. (1997) Age-related changes in the compressive strength of cancellous bone. The relative importance of changes in density and trabecular architecture. *The Journal of Bone and Joint Surgery,* 79**,** 421–27.

McElhaney, J. H. (1965) Dynamic response of bone and muscle tissue. *Journal of applied physiology,* 21(4)**,** 1231-1236.

McElhaney, J. H. & Byarse. (1965) *Dynamic Response of Biological Materials*.

McMahon, T. A. (1973) Size and shape in biology. *Journal of Science,* 179**,** 1201-1204.

McMahon, T. A. (1975a) Using body size to understand the structural design of animals: quadrupedal locomotion. *Journal of applied physiology,* 39**,** 619-627.

McMahon, T. A., Valiant, G. & Frederick, E. C. (1987) Groucho running. *Journal of Applied Physiology,* 62**,** 2326-2337.

Mellon, S. J. & Tanner, K. E. (2012) Bone and its adaptation to mechanical loading: a review. *International Materials Reviews,* 57(5)**,** 235-255.

Müller, M., Sachse, F. & Meyer-Waarden, C. (2005) Creation of Finite Element Models of Human Body based upon Tissue Classified Voxel Representations.

Müller, R., Gerber, S. C. & Hayes, W. C. (1998) Micro-compression: a novel technique for the nondestructive assessment of local bone failure. *Technology and Health Care,* 6**,** 433-444.

Muybridge. (1878) Cover of Scientific American. *In:* New York Public Library, A., Lenox, and Tilden Foundations (ed.).

Natali, A. N., Carniel, E.L., Pavan, P.G. (2008) Constitutive modelling of inelastic behaviour of cortical bone. *Medical Engineering & Phy*.

Newman, B. H. (1970) Stance and gait in the flesh-eating dinosaur Tyrannosuurus. *Biological Journal of the Linnean Society,* 2**,** 119-123.

Nikishkov, G. P. (2004) Introduction to the finite element method. [Accessed www.u-aizu.ac.jp/~niki/feminstr/introfem/introfem.html].

Nolfi, S. & Floreano, D. (2000) *Evolutionary Robotics: The Biology, Intelligence, and Technology of Self-Organizing Machines*: MIT press.

Ofer, R. T. (2005) LNIC: Evolutionary Gait-Optimization Using a Fitness Function Based on Proprioception Springer-Verlag BerlinHeidelberg.

Osborn, H., Fairfield . & Brown, B. (1906) Tyrannosaurus, Upper Cretaceous carnivorous dinosaur : (second communication). Bulletin of the AMNH ; v. 22, article 16. *Bulletin of the American Museum of Natural History ; v. 22, article 16.*

Osborn., H. F. (1905) Tyrannosaurus, upper cretaceous carnivorous dinosaur.(Second communication). *Bulletin of the American Museum of Natural History,* 21**,** 259-265.

Ostrom, J. H. (1990) The Dinosauria. University of California Press, Berkley.

Author. (1969) Osteology of Deinonychus antirrhopus, an unusual theropod from the Lower Cretaceous of Montana. *Peabody Museum of Natural History, Bulletin*.

Padian, K. & Oslen, P. E. (1989a) Dinosaur tracks and traces. *In:* Gillette, D. D. & Lockley, M. G. e. (eds.). Cambridge Univ. Press.

Padian, K. & Oslen, P. E. (1989b) Ratite footprints and the stance and gait of Mesozoic theropods. *In:* Gillette, D. D. a. L., M.G. (ed.) *Dinosaur tracks and traces.*

Panagiotopoulou, O., Wilshin, S. D., Rayfield, E. J., Shefelbine, S. J. & Hutchinson, J. R. (2011) What makes an accurate and reliable subject-specific finite element model? A case study of an elephant femur. *Journal of Royal Society interface.,* 9**,** 351–361.

Parfitt, A. M. (2003) Letters to the editor ; What is bone mineralization. *The Journal of Clinical Endocrinology & Metabolism,* 88(10)**,** 5043–5044.

Pedersen, D. R., Crowninshield, R. D., Brand, R. A. & Johnston, R. C. (1982) An axisymmetric model of acetabular components in total hip arthroplasty. *Journal Biomechanics,* 15**,** 305-315.

Pedersen, P. & Bendsøe, M. P. (Year). *In:* IUTAM Symposium on Synthesis in Bio Solid Mechanics, Chemistry and Materials Science, 1999. 33-42.

Pithioux, M., Chabrand, P. & Jean, M. (2002) Constitutive Laws and Failure Models for Compact Bones Subjected to Dynamic Loading. *Computer Methods in Biomechanics and Biomedical Engineering,* 5(5)**,** 351–359.

Porro, L. (2006) Cranial biomechanics of basal ornithischians using finiteelement analysis. . *Journal of Vertebrate Paleontology,* 26**,** 112A.

Porro, L. (2007) Feeding and Jaw Mechanism in Heterrodontosaurus tucki Using Finite Element Analysis. *Journal of Vertebrate Paleontology,* 27(3)**,** 131A.

Ratner, B. D. (2004) *Biomaterials Science* Elsevier academic press.

Rayfield, E. J. (2001) Cranial mechanics and feeding in Tyrannosaurus rex. *proceedings of Royal society of Biological Sciences,* 271**,** 1451-1459.

Rayfield, E. J. (2004) Cranial mechanics and feeding in Tyrannosaurus rex. *Proceedings of the Royal Society of London Series B-Biological Sciences,* 271(1547)**,** 1451-1459.

Rayfield, E. J. (2005) Using finite-element analysis to investigate suture morphology: A case study using large carnivorous dinosaurs. *Anatomical Record Part a-Discoveries in Molecular Cellular and Evolutionary Biology,* 283A(2)**,** 349-365.

Rayfield, E. J. (2007) Finite Element Analysis and Understanding the Biomechanics and Evolution of Living and Fossil Organisms. *Annual Review of Earth and Planetary Sciences,* 35**,** 541–76.

Reilly, T. D. & Burstein, H. A. (1974) The Mechanical Properties of Cortical Bone. *The Journal of Bone and Joint Surgery.,* 56**,** 1001-1022.

Reilly, T. D. & Burstein, H. A. (1975) The elastic and ultimate properties of compact bone tissue. *Journal of biomechanics,* 8(6).

Reilly, T. D., Burstein, H. A. & Frankel, H. V. (1974) The elastic modulus of bone. *Journal Biomechanics,* 7**,** 271–275.

RetractionCall. (2014) *Elephant femur paper subject to expression of concern retracted following investigation by Elephant femur paper by Panagiotopoulou et al 2011* [Online]. Available: http://retractionwatch.com/2014/08/20/elephant-femur-paper-subject-to-expression-of-concern-retracted-following-investigation/ [Accessed 2/27/2015].

Rey, C., Miquel, J. L., Facchini, L., Legrand, A. P. & Glimcher, M. J. (1995) Hydroxyl Groups in Bone Mineral, . *Bone,* 16(583-586).

Ritchie, R. O., Kinney, J. H., Kruzic, J. J. & Nalla, R. K. (2005) A fracture mechanics and mechanistic approach to the failure of cortical bone. *Fatigue & Fracture of Engineering Materials & Structures,* 28(4)**,** 345-371.

Rodríguez-Martín, R., Castro, I., Ocaña, J. I. & Martínez-Esnaola, M. (2010) Use of electronic speckle pattern interferometry in the detection of fatigue failure in high strength steels. *Engineering Failure Analysis,* 17(1)**,** 226–235.

Rubin, T. C. (1984) Skeletal Strain and the Functional Significance of Bone Architecture. *Calcified Tissue International,* 36**,** S11-S18.

Rybicki, E. F., Simonen, F. A. & Weis Jr, E. B. (1972) On the mathematical analysis of stress in the human femur. *Journal Biomechanics,* 5**,** 203-215.

Said, R., Chang, J., Young, P., Tabor, G. & Coward, S. (2008) Image-based meshing of patient-specific data: Converting medical scans into highly accurate computational models. *The 2nd International Conference on bioinformatics and biomedical engineering by IEEE*

Sellers, W. I. & Manning, P. L. (2007) Estimating dinosaur maximum running speeds using evolutionary robotics. *Proceedings of Royal society,* 274**,** 2711-2716.

Sellers, W. I., Manning, P. L., Lyson, T., Stevens, K. & Margetts, L. (2009) Vrtual palaeontology: Gait constructuction of extinct vertebrate using high performance computing. *Palaeontologea electronica,* 12(3).

Seto, J., Gupta, H. S., Zaslansky, P., Daniel Wagner, H. & Fratzl, P. (2008) Tough Lessons From Bone: Extreme Mechanical Anisotropy at the Mesoscale. *Advance Function Materials,* 18(13)**,** 1905-1911.

Sharir, A., Barak, M. M. & Shahar, R. (2008) Whole bone mechanics and mechanical testing. *The Veterinary Journal,* 177**,** 8-17.

Sideridis, E. & Papadopoulos, G. A. (2004) Short-beam and three-point-bending tests for the study of shear and flexural properties in unidirectional-fiber-reinforced epoxy composites. *Journal of Applied Polymer Science,* 93(1)**,** 63-74.

Siedlecki, W. & Sklansky, J. (1989) A note on genetic algorithms for large-scale feature selection., 10, 335-347. *Pattern Recognition Letters,* 10**,** 335-347.

Singh, A. V., Nagalingam, J., Saad, M. & Pailoor, J. (2010) Which is the best method of sterilization of tumour bone for reimplantation? a biomechanical and histopathological study. *Biomedical engineering online (BME),* 9**,** 48.

Skedros, J. G., Dayton, M. R., Sybrosky, C. L., Bloebaum, R. D. & Bachus, K. N. (2003) Are uniform regional safety factors an objective of adaptive modeling/remodeling in cortical bone? *The Journal of Experimental Biology,* 206**,** 2431-2439.

Sroga, G. E. & Vashishth, D. (2012) Effects of bone matrix proteins on fracture and fragility in osteoporosis. *Current osteoporosis reports,* 10(2)**,** 141-150.

Svesnsson, L. N., Valliappan, S. & Wood, D. R. (1977) Stress analysis of human femur with implanted Charnley prosthesis. *Journal of Biomechanics*.

Szaroletta, W. K. & Denton, N. L. (Year) Four Point Bending: A New Look. *In:* Proceedings of the 2002 American Society for Engineering Education Annual Conference & Exposition., 2002 Purdue University, West Lafayette, Indiana. American Society for Engineering Education.

Tang, S. Y., Zeenath, U. & Vashishth, D. (2007) Effects of non-enzymatic glycation on cancellous bone fragility. *Bone,* 40**,** 1144–1151.

Taylor, T. (October 2012) *The inner body* [Online]. HowToMedia, Inc) http://www.innerbody.com/. Available: http://www.innerbody.com/ [Accessed].

Thulborn, R. A. (1990) *Dinosaur Tracks*: Chapman & Hall, London.

Torcasio, A., Zhang, X., Duyck, J., van Lenthe & Harry, G. (2011) 3D characterization of bone strains in the rat tibia loading model. *Biomech Model Mechanobiol*.

Ulrich, D. (1998) Finite element analysis of Trabecular bone structure: a comparison of imagebased meshing techniques. *Journal of Biomechanics,* 31**,** 1187-1192.

Ural, A. & Vashishth, D. (2014) Hierarchical perspective of bone toughness – from molecules to fracture. *International Materials Reviews,* 59(5)**,** 245-263.

Verhulp, E., Rietbergen, V. B., Müller, R. & Huiskes, R. (2008) Indirect determination of trabecular bone effective tissue properties using micro-finite element simulations *Journal of biomechanics,* 41**,** 1479-1485.

Vicecont, M. (2012) *Multiscale Modeling of the Skeletal System*. Cambridge: Cambridge University Press.

Wang, X., Shen, X., Li, X. & Agrawal, C. M. (2002) Age-related changes in the collagen network and toughness of bone. *Bone.*, 31(1)**,** 1-7.

Warshaw, J. (2007) *Primate bone microstructural variability: relationships to life history, mechanical adaptation and phylogeny.* Ph.D. dissertation, The City University of New York.

Warwick, R. (1973) *Gray's anatomy* (Published 35th British ed.): Philadelphia : Saunders, .

Weiner, S. & Wagner, H. D. (1998) The material bone: Structure-mechanical function relations. *Annual Reviews Materials Science,* 28**,** 271-298.

Wille, H., Rank, E. & Yosibash, Z. (2012) Prediction of the mechanical response of the femur with uncertain elastic properties. *Journal of Biomechanics*, 45**,** 1140–1148.

Witzel, U. & Preuschoft, H. (2005) Finite-Element Model Construction for the Virtual Synthesis of the Skulls in Vertebrates: Case Study of Diplodocus. *The Anatomical Records Part A*, 283**,** 391–401.

Woledge, R. C., Curtin, N. A. & Homsher, E. (1985) *Energetic Aspects of Muscle Contraction.* : London: Academic Press.

Wolff, J. D. (1892) *Gesetz der Transformation der Knochen. Berlin: Hirschwald*.

Woo, D. G., Lee, T. W., Ko, C. Y., Kim, H. S. & Won, Y.-Y. (2006) Biomechanical Tests of Osteoporotic Vertebral Trabecular Bone using Finite Element Analysis Based on Micro-CT. *Intl. Conf. on Biomedical and Pharmaceutical Engineering (ICBPE).*

Yang, B., Tse, K.-M., Chen, N., Tan, L.-B., Zheng, Q.-Q., Yang, H.-M., Hu, M., Pan, G. & Lee, H.-P. (2014) Development of a Finite Element Head Model for the Study of Impact Head Injury. *BioMed Research International*, 2014**,** 14.

Young, P. G., Beresford-West, T. B., Coward, S. R., Notarberardino, B., Walker, B. & Abdul-Aziz, A. (2008) An efficient approach to converting three-dimensional image data into highly accurate computational models. *Philosophical Transactions of Royal Society*, 366**,** 3155-3173.

Zienkiewicz, O. C. & Cheung, Y. K. (1967) *The finite element method in structural and continuum mechanics: numerical solution of problems in structural and continuum mechanics*. London; New York: McGraw-Hill.

Zioupos, P. & Currey, J. D. (1994) The extent of microcracking and the morphology of microcracks in damaged bone. *Journal of Materials Science*, 29**,** 978-986.